Receptivity of the boundary layer in transonic flow past an aircraft wing

The report presented for partial fulfilment of
the requirements for the degree of
Doctor of Philosophy of Imperial College London
and the Diploma of Imperial College
by

Tomass Bernots

Department of Mathematics
Imperial College London

August, 2014

Declaration of Originality

I certify that this thesis, and the research to which it refers, are the product of my own work, and that any ideas or quotations from the work of other people, published or otherwise, are fully acknowledged in accordance with the standard referencing practices of the discipline.

Tomass Bernots

August 28, 2014

Copyright Declaration

Acknowledgements

First and foremost I offer my sincerest gratitude to my supervisor, Prof. Anatoly I. Ruban, who has supported me throughout my thesis with his patience and immense knowledge whilst allowing me the room to work in my own way. One simply could not wish for a better or friendlier supervisor.

This research was performed in the Laminar Flow Control Centre (LFC-UK) at Imperial College London. The centre is supported by EPSRC, Airbus UK and EADS Innovation Works.

Abstract

This thesis presents a theoretical analysis of the generation of Tollmien-Schlichting waves in a boundary layer on the wing surface due to external acoustic disturbances and elastic vibrations of the wing itself. An asymptotic approach based on the assumption that the Reynolds number, Re, is large is adopted here. In addition, it is assumed that in the spectrum of these disturbances there are harmonics, which come in resonance with the Tollmien-Schlichting wave on the lower branch of the stability curve. This work is restricted to the cases when the Stokes layer interacts with an isolated roughness, and the flow near the roughness is described by the triple-deck theory. The solution of the triple-deck problem is found in an analytic form and the main concern is with the flow behaviour downstream of the roughness. Further, it is found that there are Tollmien-Schlichting waves forming in the boundary layer behind the roughness, and their amplitudes have been expressed in terms of the receptivity coefficients, which represent the efficiency of the Tollmien-Schlichting wave generation process.

The analysis of the boundary layer receptivity to the acoustic disturbances is conducted with an assumption that the flow in the free-stream is in the transonic regime. It is shown that in this situation there are two plane acoustic waves with distinctively different characteristics. One wave always travels downstream in the streamwise direction and has $O(1)$ phase velocity. The second wave phase velocity is an order $Re^{-1/9}$ quantity and it changes the direction of propagation depending on the Mach number. The analysis has shown that the receptivity coefficient depends on the initial frequency of the perturbations and on the free-stream Mach number. It has been shown that the absolute value of the receptivity coefficient is achieved when the Mach number is one. For the negative values of the parameter, the subsonic behaviour of the receptivity coefficient is recovered.

The study of the "slow" moving wave shows that the receptivity coefficient now depends on the shape of the roughness itself as well as acoustic wave parameters and the free-stream Mach number.

The third problem considered is a receptivity of the boundary layer on the wing surface due to an elastic vibration of the wing itself. It is found that, when the frequency of the wing surface vibrations is high, the perturbations produced by wing surface vibrations can be described in the framework of "piston" theory. In the flow considered there are two physical mechanisms through which an oscillatory motion of the fluid in the Stokes layer is excited. The first one is the same as for the acoustic problem where the pressure gradient forces the fluid to oscillate in the direction along the wing surface. The second mechanism can only be observed in compressible flows.

It was found that there are two Tollmien-Schlichting waves forming in the boundary layer behind the roughness. The first receptivity process is similar to the one studied earlier with the difference that now the flow is considered to be in the subsonic regime. The second receptivity process does not have an analogue in the literature, and it was found that it is large as compared with the first receptivity. This suggests that the receptivity to the wing surface vibrations has to play a major role in the laminar-turbulent transition in the boundary layer.

Contents

List of Figures

1 Introduction

One of the most active areas of current research in fluid dynamics is study of the transition of laminar to turbulent flows. It is a problem of a practical importance to a broad range of applications, such as the aerospace and motor industries. Turbulent flow over an aircraft causes an increase in the drag and thus higher fuel consumption, so an optimisation of the aircraft design to delay transition can achieve a decrease in drag and consequently in fuel consumption. In addition in hypersonic flows knowledge of transition is essential in the accurate prediction of the heating of the surface of the flying vehicle. That allows to minimise the weight of the necessary heat shield requirements and a design for the nose of the vehicle to be determined.

In spite of its fundamental importance in science and practical relevance in engineering and technology, transition to turbulence is still not fully understood. From a theoretical point of view this is due to the difficulty inherent in the mathematical problem of transition. It is known that there exist several intermediate stages between laminar and turbulent flow. Whereas laminar flow is highly ordered spatially and temporally, turbulent flow is irregular, nonlinear and three-dimensional and is characterised by the presence of numerous instability modes with different length-scales and frequencies.

1.1 Linear stability theory

Hydrodynamic stability theory is concerned with the important question of how a laminar flow undergoes transition to a turbulent state. Reynolds (1883) was the first to perform careful experimental investigation of the laminar-turbulent transition process in the Hagen-Poiseuille flow in a circular tube. In his experiments the tube was placed horizontally inside a large glass tank filled with water. One end of the tube was connected through a tab to a sink which allowed to regulate the amount of water passing through the tube. The other end of the tube was open to the surrounding water allowing the water to enter the tube once the tab was opened. In order to reduce the disturbances at the tube inlet the open end was fitted with a trumpet mouthpiece. The flow visualisation was performed with coloured water added to the flow in front of the trumpet. It was supplied through a thin tube connected to a reservoir on the top of the water tank.

As a result of his observations Reynolds arrived at the following conclusions. Firstly, when the fluid velocity was sufficiently low, the streak of colour extended in a perfectly straight line through the tube. This means that the flow stays steady with the trajectories of the fluid particles being straight lines parallel to the tube axis. Secondly, as the velocity was increased by small steps, the flow would suddenly develop unsteadiness. This happens when the dimensionless parameter called the Reynolds number, Re, which is the ratio of inertial forces to viscous forces, reaches the critical value.

As the transition from laminar flow regime to turbulent takes place, the fluid motion becomes significantly more complicated. In addition to the primary flow parallel to the tube axis, the fluid particles are now involved in a secondary motion in the planes perpendicular to the axis. This leads to a mixing of the fluid and exchange of the momentum between the fluid particles. As a consequence, instead of the parabolic velocity profile characteristic of the laminar flow a more uniform distribution of the velocity is observed in the core of flow near the tube axis. Assuming that the fluid flux through the tube remains unchanged, the velocity has then to show steeper rise from zero near the tube wall. This explains why the resistance of the tube to the flow appears to increase in the turbulent flow regime.

The Hagen-Poiseuille flow is not the only form of the fluid motion that is subject to the laminar-turbulent transition. Following the Reynolds' discovery various other flows were investigated. In particular, the transition in the boundary-layer flow on a flat plate was in detail studied by Schubauer & Klebanoff (1956) and Klebanoff *et al.* (1962). They found that, near the leading edge, the flow is always laminar, and may be describes by the Blasius solution. However, at a certain distance from the leading edge the unsteadiness starts to develop in the flow in the form of so called Tollmien-Schlichting waves that are superimposed on the steady Blasius flow. The typical situation is that the initial amplitude of these waves is too small to cause noticeable changes in the velocity field, but they grow downstream, and there exists a second critical point near which the laminar-turbulent transition takes place (Schubauer & Skramstad, 1948). As a result of the transition the thickness of the boundary layer increases significantly, which is accomplished by an increase of the shear stress on the plate surface.

The hydrodynamic stability theory is aimed at predicting if, and when, the transition should be expected for a particular flow, and how the flow changes through the transition region. The earliest attempt to explain the stability of the flow between two parallel boundaries was performed by Lord Rayleigh (1880). In the analysis he considered only linear inviscid and incompressible flow, which resulted in derivation of the ordinary differential equation, the Rayleigh equation. Using this equation Rayleigh showed that for an inviscid parallel flow to be unstable it must have a point of inflexion in the basic velocity profile. This result was consequence of the assumption that viscous effects have a stabilising effect due to the diffusion. However, Prandtl (1921) deduced that the instability in non-inflectional share flows, such as plane Poiseuille flow, is caused by viscosity.

The viscous analogous of Rayleigh's equation was derived by Orr (1907) and Sommerfeld (1908). In their analysis disturbance components were superimposed on a basic laminar flow and the solutions to the Navier-Stokes equations were represented as superpositions of the parallel unidirectional base flow and small disturbances. Substitution into the Navier-Stokes equations led to the equations governing the evolution of the perturbed quantities, which in the first approximation are linear. Using further mathematical tools, such as the Fourier and Laplace transforms, this reduces to the Orr-Sommerfeld equation

$$\frac{1}{ikRe}\left(\frac{d^2}{dy^2}+k^2\right)^2 v(y)=(U-c)\left(\frac{d^2}{dy^2}-k^2\right)v(y)-v\frac{d^2U}{dy^2}$$

with $k^2=\alpha^2+\beta^2$, where α and β are wavenumbers in the streamwise and the wall-normal directions respectively. In addition, U is the base flow and is the function of the wall-normal coordinate, y, only, and c is the phase velocity. In the limit of $Re\to\infty$ this equation reduces to the Rayleigh equation, which becomes singular if $U(y_c)=c$, giving what is termed a critical layer at $y=y_c$.

With appropriate homogenous boundary conditions the Orr-Sommerfeld equation constitutes an eigenvalue problem, which, despite the Orr-Sommerfeld equation being much simpler than the original set of the Navier-Stokes equations for linear perturbation functions, cannot be solved analytically even for simple basic flows. Instead it has to be tackled using numerical or asymptotic methods. In general, the spectrum of the equation is discrete and infinite for a bounded flow, while for unbounded flows, the spectrum contains both continuous and discrete parts (Schmid & Henningson, 2001).

In 1933 Squire (Squire, 1933) proved the so called the Squire theorem, which states that if a growing three dimensional disturbance can be found at a given Reynolds number, then a growing two-dimensional disturbance exists at a lower Reynolds number. This theorem allows to transform certain three dimensional problems into two dimensions, which simplifies the flow analysis and allows the study of more complicated flows.

1.2 Nonparallel flow

In real applications the flow is often nonparallel, that is the base flow has two or more velocity components which depend on more than one coordinate. The typical nonparallel flows are boundary layers (Blasius flow), jets and wakes. In these cases the stability analysis leads to partial differential equations and cannot be reduced further using normal mode approach.

However, Tollmien and Schlichting for the Blasius flow stated that in a weakly nonparallel flow, the ratio of wall-normal and streamwise velocities and variations of the mean flow in the streamwise direction may be disregarded as $O(Re^{-1})$ effects, for the Reynolds number based on the displacement thickness and free steam velocity (see, for example Drazin & Reid, 2004). This reduces the partial differential equation problem to the Orr-Sommerfeld equation. They demonstrated that the boundary layer is unstable and yielded a good agreement with experiment by Schubauer & Skramstad (1948). The viscous share instability then became known as the Tollmien-Schlichting instability.

The eigenvalue problem obtained for the Blasius flow was solved numerically by various researchers and produced the neutral curve, which consists of two branches. These solutions had a noticeable difference near the nose of the neutral curve for the Blasius boundary layer compared to experimental measurements. To correct the discrepancy Bouthier (1972), Gaster (1974) used composite approximation method and (Saric & Nayfeh, 1975) used multiple-scale method to include the nonparallel influence of the boundary layer growth. Thought based on similar concepts the formulations are different and so as results.

The alternative method was proposed by Lin (1944) who used large Reynolds number asymptotic expansions to provide a consistent mathematical theory. His analysis showed that at the leading order, the instability near the lower branch is governed by the triple-deck structure (discussed in detail in section 1.3) with the wavelength of $O(Re^{1/4})$ times the boundary-layer thickness. As a result nonparallel effects appear as a $O(Re^{-3/4})$ correction to the growth rate Smith (1979*b*). Later this analysis was extended to the upper branch of the neutral curve, Bodonyi & Smith (1981).

Uses of the multiple-scale and the composite approximation methods by Saric & Nayfeh and Bouthier, Gaster, respectively, provided at intermediate steps a partial differential equation similar to the parabolised Navier-Stokes equations, except for additional terms containing frequency and wavenumbers. However these analyses proceeded further to simplify the problem, to more manageable ordinary differential equations.

These last steps are not only unnecessary but also restrict the scope and validity of the resulting equations. The intermediate partial differential equations obtained during the analyses are named parabolised stability equations (PSE). This is an alternative to previous methods, which was proposed by Herbert & Bertolotti (1987), Bertolotti *et al.* (1992). They used appropriate approximations to suppress any upstream propagation of the disturbance waves, which are expected to have negligible influence on transition in share flows. In this way a parabolised stability equations are obtained, which may be solved by marching in the downstream direction (Herbert, 1997). The use of the marching procedure for solving the PSE is only permitted if the stability problem is governed by downstream propagating information. According to the characteristics of the full PDEs governing the stability for a particular problem one can distinguish absolute and convective instabilities, and in view of these ideas PSE is valid for convectively unstable flows. The PSE may therefore be applied to many different flows. Furthermore, the derivation places no requirement on the amplitude of the disturbance so nonlinear terms can be consistently incorporated into the PSE.

1.3 Triple-deck theory

The triple-deck model is a large Reynolds number asymptotic approximation to the Navier-Stokes equations. The physical ideas for the triple-deck theory were established by Lighthill (1953). He described interactions mathematically by perturbing a parallel flow and linearising the Navier-Stokes equations around it, which allowed him to produce a self-consistent theory. It divides the region of interest into three parts: the inviscid flow outside the boundary layer, the displaced boundary layer, and an inner part close to the wall. Using this theory Lighthill described how spontaneous changes in the boundary layer could be set up and how these changes eventually may lead to a separation. In addition he assumed that the length of the interaction is of $O(Re^{-3/8})$, where Reynolds number is based on the location of the disturbance and free steam velocity, but a streamwise length scale is of the same order as the boundary-layer thickness, $O(Re^{-1/2})$.

Later Stewartson & Williams (1969) extended Lighthill's theory to nonlinear interactions. The most noticeable difference in the analysis was that they assumed interaction length and scaling factor in the streamwise direction is of $O(Re^{-3/8})$, instead of $O(Re^{-1/2})$ used by Lighthill. In the work they also assumed that the flow is described by three decks. The upper deck has a thickness of the order $Re^{-3/8}$ and is characterised by inviscid and irrotational disturbances. The governing equation of the perturbations in the deck is the Prandtl-Glauert equation. It is followed by middle deck or the displaced Prandtl boundary layer, which thickness is of the order $Re^{-1/2}$ and is characterised by inviscid and rotational disturbances. The main perturbation in this deck is bending of the streamlines without any pressure gradient. The lower deck is of the order $Re^{-5/8}$ thick and is characterised by viscous and rotational disturbances. This layer is incompressible and the governing equations in this layer satisfy the wall boundary conditions.

Neiland (1969) arrived at the same scalings and the triple-deck structure studying the interaction between a hypersonic flow and a boundary layer, and the upstream propagating disturbances. Messiter (1970) also arrived to the same scalings and the structure by looked at the problem of the boundary-layer flow near the trailing edge of the flat plate. The triple-deck structure arose from the problem of the occurring singularities in boundary-layer solutions at point of the separation.

The physics of the triple-deck can be explained as follows. If perturbations disturb the lower deck, the latter produces a displacement of the streamlines. This deflection of the streamlines is transmitted through the passive main deck to the upper deck where the displacement induces inviscid pressure perturbations which is transmitted back to the lower deck promoting the velocity disturbances. The asymptotic matching requirement between the three decks produces an interactive relationship between the pressure and displacement thickness (Sychev *et al.*, 1998).

1.4 Receptivity

In different flows the transition from laminar to turbulent state may take different routes and is influenced by external disturbances: free-stream turbulence, acoustic noise, wall roughnesses, wall vibrations etc. Depending on the characteristics of these disturbances, transition may proceed along different routs, see Figure 1.1 (Fedorov, 2011), before turning into the boundary-layer instability modes: Tollmien-Schlichting waves, Cross-Flow vortices or Taylor-Görtler vortices.

When the free-stream disturbance level is relatively low, the path **a** is followed. The initial growth of these disturbances is described by linear stability theory of primary modes of the Orr-Sommerfeld equation (Saric *et al.*, 2002). Here external disturbances excite the Tollmien-Schlichting waves and the growth of the waves is exponential in the streamwise direction. As the amplitude of the waves becomes large enough, nonlinear interaction and secondary instability occurs, and with the further growth of amplitude the breakdown and eventual transition to turbulence occurs. It was observed that

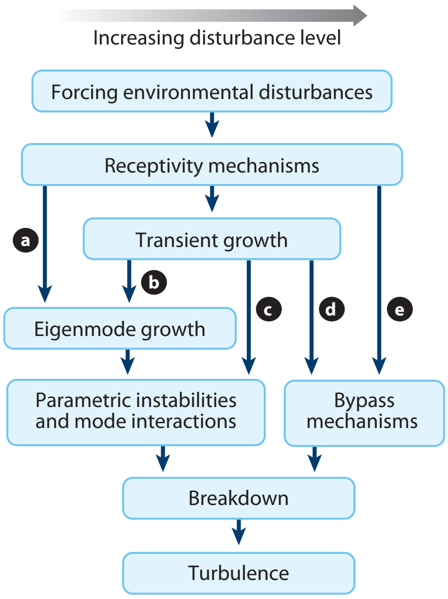

Figure 1.1: The paths to turbulence.

the location of the transition position changes significantly with the change in level of the free-stream disturbances and body surface roughnesses. This is explained by the receptivity process, where different initial disturbances excite different amplitudes of Tollmien-Schlichting waves, which clearly shows that the transition process cannot be predicted without studying receptivity.

In the case of a high level of free-stream disturbances the transition occurs without excitation of Tollmien-Schlichting waves and is referred as bypass transition (path **e**). The intermediate paths **b, c** and **d** have been identified, but in spite of significant progress, an overall theory remains incomplete.

The importance of the receptivity was recognised long before the term "receptivity" was proposed. Indeed, starting with Schubauer & Skramstad (1948), experimental investigations of the laminar-turbulent transition have been conducted in specially designed wind tunnels which have a significantly lower level of turbulence in the test section. Reduction of the free-stream turbulence makes the flow in the boundary-layer remain laminar well beyond the position where the boundary-layer becomes unstable. The instability modes may then be generated in the boundary-layer artificially. There are various ways of doing this; for example, using a vibrating ribbon installed a small distance above the plate surface, or with acoustic waves penetrating the boundary-layer.

In real flight conditions the external perturbations are typically very weak, in fact, significantly weaker compared to low turbulence wind tunnels. Therefore, the initial amplitude of the instability modes generated in the boundary-layer are small. However, they amplify further downstream, and when the amplitude reaches a certain level nonlinear effects come into play, and then a rapid transition to a turbulent state is observed. This means that the e^N method currently adopted by the aerospace industry is insufficient for accurate prediction of the transition. This semiempirical method uses linear stability theory to determine the values of N by measuring disturbance amplitude relative to the lower neutral stability point, which correlates with experimentally measured transition locations. Typical values of N in the literature range from 7 to 9, depending on flow geometry and external disturbances. This method only provides information relating to the growth rate of the disturbance, while the key aspect of receptivity studies is to determine an initial amplitude for the problem at hand. In mathematical terms receptivity manifests itself as a boundary value problem, rather than an eigenvalue problem which is found in linear stability analyses.

Traditionally there have been two distinct approaches to tackle the receptivity problem: High Reynolds number asymptotic theories and finite Reynolds number calculations. When dealing with transition caused by the growth of Tollmien-Schlichting waves, finite Reynolds number calculations revolve around solving inhomogeneous Orr-Sommerfeld type equations (see, for example, Choudhari & Streett, 1992), while asymptotic theory is based on the triple-deck model, which has been shown to describe Tollmien-Schlichting waves near the lower branch of the stability curve; see Smith (1979*a*,*b*). In this work the asymptotic approach is adopted.

The receptivity mechanisms previously developed can generally be classified in two distinct groups: localised receptivity and distributed receptivity. For both types effective generation of Tollmien-Schlichting waves is only possible if the external perturbations are in resonance with the natural flow oscillations in the boundary-layer. The resonance conditions require not only the frequency but also the wavelength of external perturbations be in tune with those of the Tollmien-Schlichting wave.

The first paper where triple-deck theory was used to study the receptivity of the boundary-layer was published by Terent'ev (1981). This study considered an incompressible fluid flow past a flat plate with the basic steady flow given by the Blasius solution. It was assumed that a short section of the plate surface performs periodic vibrations in the direction perpendicular to the wall. In order to ensure that the flow is described by triple-deck theory, the frequency of the vibrations was chosen to be $\omega = O(Re^{1/4})$ and the length of the vibrating section $\Delta x = O(Re^{-3/8})$. Terent'ev's formulation represents a simplified mathematical model of the classical experiments by

Schubauer & Skramstad (1948) where the Tollmien-Schlichting waves were generated by a vibrating ribbon. Terent'ev was able to determine the amplitude of the generated Tollmien-Schlichting as a function of the amplitude and the shape of the vibrating part of the wall.

The effect of acoustic noise on the boundary-layer was first considered by Goldstein (1983) who studied the Blasius boundary-layer flow on the flat plate surface and used the fact that this flow is highly non-parallel at the leading edge of the plate. He showed that when an acoustic wave interacts with the flow in the leading edge region the Lam-Rott eigensolutions are generated. However they decay exponentially before becoming Tollmien-Schlichting waves further downstream.

When identifying possible receptivity mechanisms that involve acoustic noise one has to keep in mind the following. If the boundary-layer in a subsonic flow is exposed to acoustic noise, then the harmonic whose frequency coincides with the frequency of the Tollmien-Schlichting wave has to be extracted from the entire acoustic spectrum. Since on the lower branch of the stability curve the frequency is an order $O(Re^{1/4})$ quantity, the chosen acoustic wave will have the wavelength of $O(Re^{-1/4})$, which is much larger than the wavelength of the Tollmien-Schlichting wave; the latter is an $O(Re^{-3/8})$ quantity. This means that in subsonic flows the acoustic wave alone is insufficient for Tollmien-Schlichting wave generation. In order to achieve resonance with respect to the wave number the acoustic wave has to come into interaction with possible irregularities in the steady boundary-layer flow produced, for example, by wall roughness.

The asymptotic theory for this form of receptivity was developed by Ruban (1984) and Goldstein (1985). They assumed that the streamwise length scale of the roughness element is of the order of the wavelength of the Tollmien-Schlichting wave, i.e. has streamwise magnitude of the order $Re^{-3/8}$. In this case the flow around the roughness is described by triple-deck theory. The generation of the Tollmien-Schlichting wave was found to be due to the interaction between the acoustic wave and steady flow perturbations in the lower tier of the triple-deck structure. It was shown that the receptivity process extracts from the spectrum of the steady flow perturbations the harmonic which is in resonance with the generated Tollmien-Schlichting wave. The amplitude of the wave was found to be proportional to the amplitude of the acoustic wave and the Fourier transform of the roughness shape calculated for the value of the wave number which coincides with the wave number of the Tollmien-Schlichting wave.

It is known from experimental observations that free-stream turbulence also has a significant influence on the laminar-turbulent transition in the boundary-layer. The asymptotic theory of the receptivity of the boundary-layer to free-stream turbulence was developed by Duck *et al.* (1996). They adopted a uniform turbulence model for the oncoming flow, where the disturbance field is represented as a superposition of vorticity waves, known as convective gusts. There is a significant difference in the way the boundary-layer interacts with acoustic waves and vorticity waves. The acoustic waves carry pressure perturbations which easily penetrate into the boundary-layer and lead to a formation of a Stokes layer near the body surface. The situation with the vorticity waves is somewhat different. They do not carry pressure perturbations and therefore are unable to penetrate into the boundary-layer. However, a wall roughness produces perturbations not only inside the boundary-layer but also in the upper tier of the triple-deck structure, which lies in the flow outside the boundary-layer. Non-linear interaction of the steady perturbations in the upper tier with vorticity waves creates the forcing necessary for Tollmien-Schlichting wave production.

Recently Ruban *et al.* (2013) studied the effect of wing surface vibrations on the generation of the Tollmien-Schlichting waves. They found that the wing vibrations produce the pressure waves in the flow outside the boundary-layer, which may be described in the framework of piston theory. As the pressure perturbations penetrate into the boundary-layer, a Stokes layer forms on the wing surface. It was shown that there are two physical mechanisms to excite flow oscillations in the Stokes layer: time oscillations of the pressure gradient and the oscillations of the pressure itself; the latter can only be observed in compressible flows only. Both mechanisms are equally important when the wavelength of the wing surface vibrations is an $O(Re^{-1/8})$ quantity. If the wavelength is smaller than the critical wavelength, then the first mechanism prevails; if the wavelength is larger, then the second mechanism is more important. As usual, the Stokes layer on its own is incapable of producing Tollmien-Schlichting waves, therefore a wall roughness is needed for the Tollmien-Schlichting waves to be produced.

The above receptivity mechanisms rely on a roughness element to achieve the desired wavelength shortening. An alternative way to achieve the resonance was studied by Wu (1999) who showed that a combination of a convective gust and an acoustic wave can produce the required conditions for a Tollmien-Schlichting wave to be generated. As there is now no roughness, the analysis centres on the neutral stability point and a so-called resonance region which occupies an $O(Re^{-3/16})$ vicinity of the neutral stability point. In this vicinity, the non-parallel flow effects appear at leading order. The receptivity analysis in this case is performed using a multi-scale asymptotic procedure with the "fast" longitudinal coordinate being comparable with the Tollmien-Schlichting wavelength and the "long" coordinate with the length of the resonance region. As a result an amplitude equation has been deduced, showing how the Tollmien-Schlichting wave grows over the resonance region.

Later Wu (2001) extended his approach to study the receptivity of the boundary-layer to both acoustic waves and convected gusts interacting with distributed wall roughness. Again the analysis centres around a resonance region and the amplitude is found to be the same as that derived in Wu (1999). The analysis also includes higher order effects, and a good agreement is found with the experiments of Dietz (1999). An extension of Wu's theory to a simple case of the Tollmien-Schlichting wave generation on an extended section of the body surface performing wave like vibrations were later presented by Kerimbekov & Ruban (2005).

1.5 Transonic flow

The receptivity mechanism put forward in this work is different to the others described previously in one distinct respect. The flow outside the boundary layer is now assumed to be transonic, rather than subsonic. A flow is called transonic when the local velocity of the flow is close to the speed of sound. Consequently transonic flow exhibits both subsonic and supersonic flow characteristics.

From the review paper by Bendiksen (2011), the theoretical study of transonic flow problems associated with aircraft applications started with von Kármán's research on transonic similarity principles, which continued further by theoretical and experimental work by Cole, Guderley, Landhal, Ferrari and Tricomi. By the second half of the 20th century, a relatively good mathematical and physical understanding of steady transonic flow had been developed for two-dimensional inviscid flow. The difficulties of the transonic flow analysis are related to the mixed subsonic and supersonic flow patterns. As an example, when the free-stream Mach number of subsonic flow past an airfoil is close to but not exactly unity, pockets of supersonic flow form around the airfoil. The supersonic flow terminates by a nearly normal shock-wave which reduces the flow velocity back to subsonic. Increasing the free-stream Mach number further, the shock moves aft and its strength increases. Further increase in the Mach number leads to separation of the boundary-layer.

Mathematically this change, from subsonic to supersonic flow, results in the partial differential equation that should change from locally elliptic in the subsonic region to the locally hyperbolic in the supersonic region. An additional difficulty is that the spatial extent of the local supersonic or subsonic region is not known in advance but must be determined as part of the solution. Further this equation should be able to model moving shock wave and to obtain the correct time-varying Rankine-Hugoniot shock jump conditions. These arguments suggest that to describe the physics of the transonic flow a nonlinear equation is required.

Considering a two-dimensional steady potential fluid flow and assuming that velocity perturbations are small, the Kármán-Guderley equation is obtained (Cole & Cook, 1986), whereas for the unsteady case, external flow is described by the Transonic Small Perturbation (TSP) equation. In both situations the governing equations involve the Kármán-Guderley parameter which measures the rate at which M_∞ tends to unity.

Triple-deck theory in steady transonic flow was studied by Messiter *et al.* (1971), who derived the scaling for transonic flow velocity to be $M^2 - 1 = O(Re^{-1/5})$ and the corresponding streamwise size of the region of interaction was found to be $O(Re^{-3/10})$. They showed that this flow regime is nonlinear and therefore is capable of incorporating the effects of the shock and boundary-layer separation. Using this triple-deck formulation Adamson (1974) investigated the interaction between a shock wave and a boundary-layer, and Bodonyi & Kluwick (1982, 1998) looked at the transonic trailing-edge flow. In recently years, the boundary-layer separation in a steady transonic flow was treated in detail by Ruban & Türkylmaz (2000); Buldakov & Ruban (2002) and Ruban *et al.* (2006).

The study of the boundary-layer stability in unsteady transonic flow was conducted by Timoshin (1990); Bowles & Smith (1993) and recently by Bogdanov *et al.* (2010). They showed that if $M^2 - 1$ is $O(Re^{-\frac{1}{9}})$ then the viscous-inviscid interaction system consists of unsteady boundary-layer equations coupled with the unsteady Transonic small perturbation equation, in the upper deck. They also showed the existence of unstable Tollmien-Schlichting modes when the Mach number is less but close to one.

1.6 Layout of thesis

This thesis is consists of two main parts. The first part, comprising of Chapters 2 and 3, deals with calculations of receptivity coefficients in transonic flows. Chapter 2 follows the earlier work by Ruban (1984) where the receptivity of the boundary layer to a downstream propagating acoustic wave was studied in subsonic flow. The current work is presented for the case when the flow is in the transonic regime. Chapter 3 studies the influence of the upstream propagating acoustic wave and its interaction with the steady perturbations due to surface irregularity.

The second part of the thesis, Chapter 4, is devoted to the calculations of the receptivity coefficient of the boundary layer on a vibrating wing in subsonic flow. It is followed by Chapter 5 with concluding remarks and discussion.

2 Receptivity of the Boundary Layer to a Downstream Propagating Acoustic Wave in Transonic flow

2.1 Introduction

In this chapter we study the generation of Tollmien-Schlichting waves in the boundary-layer on a flat plate due to external acoustic disturbances in the transonic flow regime. These disturbances induce a viscous-inviscid interaction between the boundary-layer and the outer region. The interaction region can be modelled by a triple-deck structure, in which the characteristic features of an unsteady transonic flow outside the boundary layer have been taken into account. In the present investigation, we shall employ the transonic regime corresponding to $M^2 - 1 = O(Re^{-\frac{1}{9}})$, as this scaling permits description to the Tollmien-Schlichting wave (Bowles & Smith, 1993).

The layout of the chapter is as follows. The mathematical formulation of the problem is given in section 2.2, which is followed by the flow analysis ahead of the wall roughness. In this region resonance conditions can not be satisfied, therefore the the wall roughness on the surface is introduced. The flow in vicinity of the wall roughness is described by triple-deck theory and presented in section 2.4. It is followed by formulation of the viscous-inviscid interaction problem, which is split into steady and unsteady problems, section 2.5. Section 2.6 concludes the analysis of the problem by showing that in the vicinity of the roughness the flow perturbation field is composed of discrete and continuous spectrums. It is shown that the continuous spectrum perturbations decay downstream of the roughness uniformly with respect to the frequency of oscillations, and so do all the perturbations of the discrete spectrum except the one which represents the Tollmien-Schlichting wave. The amplitude of the latter is found in an analytic form.

2.2 Problem Formulation

Consider a flat plate placed in a uniform unidirectional flow of a perfect gas parallel to the free-stream velocity with a plane acoustic wave travelling parallel to the plate as shown in Figure 2.1. The Cartesian coordinate system is used with $\hat{x}$ measured along

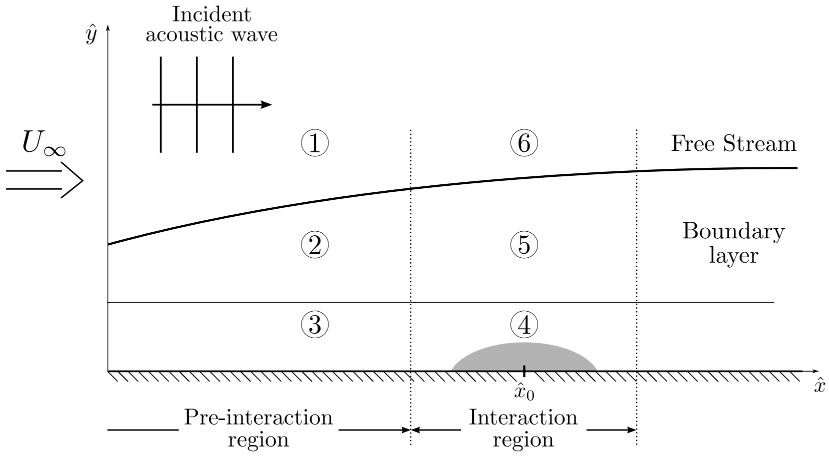

Figure 2.1: Illustration of the flow structure for the acoustic wave receptivity.

the plate surface from its leading edge, and $\hat{y}$ in the perpendicular direction. The dimensional velocity components are denoted as $(\hat{u}, \hat{v})$ and time by $\hat{t}$. The gas density is $\hat{\rho}$, the pressure $\hat{p}$, the enthalpy $\hat{h}$ and the dynamic viscosity coefficient $\hat{\mu}$.

In order to non-dimensionalise variables, we denote the distance from the leading edge of the plate to the roughness by L. The velocity, density, pressure and viscosity in the unperturbed flow upstream of the plate are U_∞, ρ_∞, p_∞ and μ_∞, respectively. Here M_∞ is the free-stream Mach number and Re is the Reynolds number, which are defined as

$$M_\infty = \frac{U_\infty}{a_\infty}, \qquad a_\infty = \sqrt{\gamma \frac{p_\infty}{\rho_\infty}}, \qquad Re = \frac{\rho_\infty U_\infty L}{\mu_\infty}. \tag{2.1a-c}$$

The flow analysis will be conducted using the non-dimensional compressible Navier-Stokes equations, see Appendix A.1. In addition, it will be assumed that the Mach number is close to one, and the Reynolds number is large, that is, we will conduct the asymptotic analysis of the Navier-Stokes equations (A.3) using the limit

$$Re \to \infty, \qquad Q_\infty = \frac{M_\infty^2 - 1}{Re^{-1/9}} = O(1), \tag{2.2a,b}$$

where Q_∞ is the Kármán-Guderley parameter.

2.3 Flow ahead of the wall roughness

As the first step in the analysis of the receptivity of the boundary layer to an acoustic wave one has to look at the acoustic wave propagation in the potential flow and its interaction with a boundary layer ahead of the wall roughness. Therefore the unsteady flow analysis begins with the study of the flow in the region 1 (Figure 2.1).

2.3.1 Potential flow analysis

The flow in the region 1 is far from the surface where the viscosity terms in the Navier-Stokes equations (A.3) may be neglected. It is also assumed that the acoustic perturbation in the free-stream propagate only in streamwise direction, x_*, thus allowing the derivatives with respect to y_* to be disregarded in the Navier-Stokes equations. As the result the flow governing equations outside the boundary-layer are represented by unsteady one-dimensional Euler's equations

$$\rho_* \frac{\partial u_*}{\partial t_*} + \rho_* u_* \frac{\partial u_*}{\partial x_*} = -\frac{\partial p_*}{\partial x_*}, \tag{2.3a}$$

$$\rho_* \frac{\partial h_*}{\partial t_*} + \rho_* u_* \frac{\partial h_*}{\partial x_*} = \frac{\partial p_*}{\partial t_*} + u_* \frac{\partial p_*}{\partial x_*}, \tag{2.3b}$$

$$\frac{\partial \rho_*}{\partial t_*} + \frac{\partial(\rho_* u_*)}{\partial x_*} = 0, \tag{2.3c}$$

$$h_* = \frac{\gamma}{\gamma - 1}\frac{p_*}{\rho_*} + \frac{1}{(\gamma - 1)M_\infty^2 \rho_*}. \tag{2.3d}$$

here γ is the specific heat ratio.

Setting the frequency of the acoustic perturbation to coincide with the frequency of the Tollmien-Schlichting waves in transonic flows, we shall introduce independent variables $(\bar{x}, \tilde{t})$ thought the scalings

$$x_* = Re^{-\frac{2}{9}}\bar{x}, \qquad t_* = Re^{-\frac{2}{9}}\tilde{t}. \tag{2.4a,b}$$

The solution of (2.3) is sought in the form

$$u_* = 1 + u_1(\tilde{t}, \bar{x}) + \dots, \tag{2.5a}$$

$$\rho_* = 1 + \rho_1(\tilde{t}, \bar{x}) + \dots, \tag{2.5b}$$

$$p_* = p_1(\tilde{t}, \bar{x}) + \dots . \tag{2.5c}$$

where the first terms represent the uniform undisturbed flow and terms with the subscripts represent small flow perturbations. Substituting (2.4), (2.5) into (2.3) and combining equations (2.3b) and (2.3d) we obtain at the leading order linearised Euler's

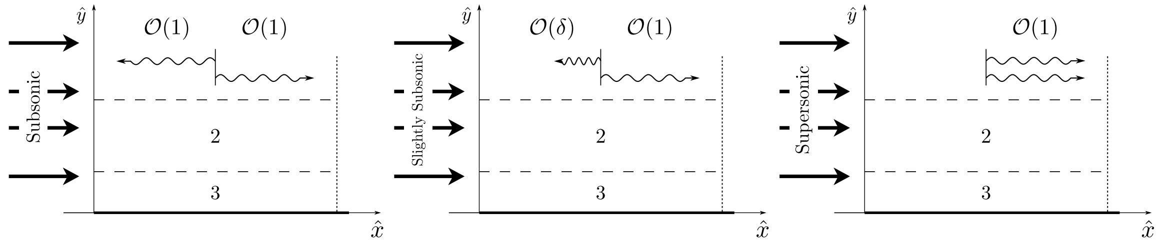

(a) Subsonic (b) Transonic (c) Supersonic

Figure 2.2: Schematic comparison of wave velocities and directions in different flow regimes.

equations

$$\frac{\partial u_1}{\partial \tilde{t}} + \frac{\partial u_1}{\partial \bar{x}} = -\frac{\partial p_1}{\partial \bar{x}}, \tag{2.6a}$$

$$\frac{\partial \rho_1}{\partial \tilde{t}} + \frac{\partial \rho_1}{\partial \bar{x}} = M_\infty^2 \left(\frac{\partial p_1}{\partial \tilde{t}} + \frac{\partial p_1}{\partial \bar{x}} \right), \tag{2.6b}$$

$$\frac{\partial \rho_1}{\partial \tilde{t}} + \frac{\partial \rho_1}{\partial \bar{x}} + \frac{\partial u_1}{\partial \bar{x}} = 0. \tag{2.6c}$$

To solve these equations we eliminate all the unknowns variables except the pressure perturbations, p_1, which leads us to the equations describing the propagation of one-dimensional acoustic wave in a moving gas

$$M_\infty^2 \frac{\partial^2 p_1}{\partial \tilde{t}^2} + \left(M_\infty^2 - 1\right) \frac{\partial^2 p_1}{\partial \bar{x}^2} + 2M_\infty^2 \frac{\partial^2 p_1}{\partial \bar{x} \partial \tilde{t}} = 0. \tag{2.7}$$

Equation (2.7) has two linearly independent wave-like solutions

$$p_1 = \bar{\alpha} e^{i\tilde{\omega}\left(\tilde{t} - \frac{M_\infty}{M_\infty + 1}\bar{x}\right)} + \bar{\alpha} e^{i\tilde{\omega}\left(\tilde{t} - \frac{M_\infty}{M_\infty - 1}\bar{x}\right)} + c.c., \tag{2.8}$$

where $\bar{\alpha}$ and $\tilde{\omega}$ are characteristic amplitude and frequency of the acoustic disturbance respectively; c.c. here denotes complex conjugate.

The solution (2.8) describes two waves with phase velocities $c_1 = -1 - 1/M_\infty$ and $c_2 = -1 + 1/M_\infty$, which will be referred to as "fast" and "slow" waves, respectively. Here negative phase velocity corresponds to a downstream propagating disturbance and the positive velocity corresponds to an upstream propagating disturbance. Note that the "fast" wave always travels downstream with $O(1)$ velocity independently of the free-stream flow velocity whereas "slow" wave propagation depends on the free-stream velocity. In subsonic flow ($M_\infty < 1$) the "slow" wave propagates upstream with

$O(1)$ velocity, see Figure 2.2. For the case when $M_\infty > 1$, that is the flow is supersonic, both waves are practically indistinguishable and both are propagating downstream with $O(1)$ velocities. In the case when the free-stream Mach number is close but less than one, the "slow" wave propagates upstream but with much smaller velocity than in the subsonic flow. Its propagation velocity reduces further, as the free-stream Mach number tends to one, when the "slow" wave becomes stationary. Further increase in the Mach number turns the "slow" wave so that now it propagates downstream as the "fast" wave, but with a small velocity.

The proposed receptivity mechanism is similar to the mechanism described by Ruban (1984) and Goldstein (1985) for subsonic flow. In this case for resonance to occur it is necessary to have a roughness on the surface of the plate which adjusts the acoustic wave wavenumber to be in resonance with the wavenumber of the Tollmien-Schlichting wave.

In this chapter we shall deal with the "fast" wave, which we write as

$$p_a(\tilde{t}, \bar{x}) = \bar{\alpha} e^{i\left(\tilde{\omega}\tilde{t} + \bar{k}\bar{x}\right)} + c.c., \tag{2.9}$$

where $\bar{k} = -\frac{M_\infty}{M_\infty + 1}\tilde{\omega}$ is the wavenumber of the "fast" wave.

2.3.2 Unsteady boundary-layer

A flat plate placed in a uniform flow of gas disturbs the flow only in the immediate vicinity of the plate surface. Thus the steady flow past the plate is uniform with the exception of the wall boundary-layer. This layer thickness tends to zero as the Reynolds number increases in accordance with $y_* = O(Re^{-1/2})$. The analysis of the steady compressible boundary layer flow is presented in Appendix A.2 and the appropriate asymptotic representation of the solution is given by (A.7). For the unsteady boundary-layer flow the asymptotic expansions are written in the form

$$u_* = U_0\left(\bar{Y}\right) + Re^{-\frac{1}{9}} M_\infty u_2(\bar{Y}) p_a(\tilde{t}, \bar{x}) + \dots, \tag{2.10a}$$

$$v_* = Re^{-\frac{7}{18}} i\bar{k} M_\infty v_2(\bar{Y}) p_a(\tilde{t}, \bar{x}) + Re^{-\frac{1}{2}} V_0\left(\bar{Y}\right) + \dots, \tag{2.10b}$$

$$p_* = Re^{-\frac{1}{9}} p_2(\bar{Y}) p_a(\tilde{t}, \bar{x}) + \dots, \tag{2.10c}$$

$$h_* = H_0\left(\bar{Y}\right) + Re^{-\frac{1}{9}} h_2(\bar{Y}) p_a(\tilde{t}, \bar{x}) + \dots, \tag{2.10d}$$

$$\rho_* = R_0\left(\bar{Y}\right) + Re^{-\frac{1}{9}} M_\infty^2 \rho_2(\bar{Y}) p_a(\tilde{t}, \bar{x}) + \dots, \tag{2.10e}$$

$$\mu_* = \mu_0\left(\bar{Y}\right) + Re^{-\frac{1}{9}} \mu_2(\bar{Y}) p_a(\tilde{t}, \bar{x}) + \dots, \tag{2.10f}$$

where the independent variables are scaled as

$$t_* = Re^{-\frac{2}{9}}\tilde{t}, \qquad x_* = Re^{-\frac{2}{9}}\bar{x}, \qquad y_* = Re^{-\frac{1}{2}}\bar{Y}. \tag{2.11a-c}$$

Substituting these expansions into (A.3) and retaining leading order terms, we deduce

$$R_0\left[\left(\frac{\tilde{\omega}}{\bar{k}} + U_0\right)u_2 + v_2\frac{\partial U_0}{\partial \bar{Y}}\right] = -\frac{p_2}{M_\infty}, \tag{2.12a}$$

$$\frac{\partial p_2}{\partial \bar{Y}} = 0, \tag{2.12b}$$

$$R_0\left[\left(\frac{\tilde{\omega}}{\bar{k}} + U_0\right)h_2 + M_\infty v_2\frac{\partial H_0}{\partial \bar{Y}}\right] = \left(\frac{\tilde{\omega}}{\bar{k}} + U_0\right)p_2, \tag{2.12c}$$

$$M_\infty\left(\frac{\tilde{\omega}}{\bar{k}} + U_0\right)\rho_2 + R_0 u_2 + \frac{\partial(v_2 R_0)}{\partial \bar{Y}} = 0, \tag{2.12d}$$

$$(\gamma - 1)\left(h_2 R_0 + M_\infty^2\rho_2 H_0\right) = \gamma p_2. \tag{2.12e}$$

It can be seen that these equations do not contain viscosity terms, thus instead of imposing the no-slip condition on plate's surface, the impermeability condition, $v_2 = 0$, on the surface should be applied. In addition, the matching condition when $\bar{Y} \to \infty$ is such that $u_2 = \rho_2 = h_2 = p_2 = 1$. Therefore solving (2.12) we obtain

$$u_2 = \frac{1}{R_0(0)\left(M_\infty + 1\right)}, \quad \rho_2 = \frac{1}{\left(M_\infty + 1\right)^2}, \quad h_2 = \frac{1}{R_0(0)} \quad \text{at} \quad \bar{Y} = 0. \tag{2.13a-c}$$

where $R_0(0)$ is a gas density on the surface of the plate in the unperturbed steady flow.

The solution (2.13) shows that the no-slip condition is not satisfied, thus the introduction of a Stokes layer near the wall is needed.

2.3.3 Stokes layer

As the pressure perturbation (2.9) penetrates into the boundary-layer, it causes the Stokes layer to form near the surface. The thickness of this layer is easily found by comparing the instantaneous acceleration term with the viscous forces in the longitudinal momentum equation (A.1a)

$$\hat{\rho}\frac{\partial \hat{u}}{\partial \hat{t}} \sim \frac{\partial}{\partial \hat{y}}\left(\hat{\mu}\frac{\partial \hat{u}}{\partial \hat{y}}\right). \tag{2.14}$$

Taking into account that density and viscosity are $O(1)$ and time is $O(Re^{-\frac{2}{9}})$ quantities, we find that the thickness of this sublayer should be $O(Re^{-\frac{11}{18}})$ quantity. From this it follows that in the viscous sublayer, region 3, the independent variables are scaled as

$$t_* = Re^{-\frac{2}{9}}\tilde{t}, \qquad x_* = Re^{-\frac{2}{9}}\bar{x}, \qquad y_* = Re^{-\frac{11}{18}}\bar{y}. \tag{2.15a-c}$$

and solutions are sought in the form

$$u_* = Re^{-\frac{1}{9}}u_3(\tilde{t}, \bar{x}, \bar{y}) + \dots, \tag{2.16a}$$
$$v_* = Re^{-\frac{1}{2}}v_3(\tilde{t}, \bar{x}, \bar{y}) + \dots, \tag{2.16b}$$
$$p_* = Re^{-\frac{1}{9}}p_3(\tilde{t}, \bar{x}, \bar{y}) + \dots, \tag{2.16c}$$
$$\rho_* = \rho_w + Re^{-\frac{1}{9}}\rho_3(\tilde{t}, \bar{x}, \bar{y}) + \dots, \tag{2.16d}$$
$$h_* = h_w + Re^{-\frac{1}{9}}h_3(\tilde{t}, \bar{x}, \bar{y}) + \dots, \tag{2.16e}$$
$$\mu_* = \mu_w + Re^{-\frac{1}{9}}\mu_3(\tilde{t}, \bar{x}, \bar{y}) + \dots. \tag{2.16f}$$

where h_w, μ_w and ρ_w are values of enthalpy, viscosity and density on the surface of the plate, respectively.

Substituting these solution into the Navier-Stokes equations and retaining leading order terms yields

$$\rho_w \frac{\partial u_3}{\partial \tilde{t}} = -\frac{\partial p_3}{\partial \bar{x}} + \mu_w \frac{\partial^2 u_3}{\partial \bar{y}^2}, \tag{2.17a}$$
$$\frac{\partial p_3}{\partial \bar{y}} = 0, \tag{2.17b}$$
$$\rho_w \frac{\partial h_3}{\partial \tilde{t}} = \frac{\partial p_3}{\partial \tilde{t}} + \frac{\mu_w}{Pr}\frac{\partial^2 h_3}{\partial \bar{y}^2}, \tag{2.17c}$$
$$\frac{\partial \rho_3}{\partial \tilde{t}} + \rho_w \frac{\partial u_3}{\partial \bar{x}} + \rho_w \frac{\partial v_3}{\partial \bar{y}} = 0, \tag{2.17d}$$
$$(\gamma - 1)\left(h_w \rho_3 + \rho_w h_3\right) = \gamma p_3. \tag{2.17e}$$

The boundary conditions for (2.17) are: the no-slip condition on the plate's surface and the matching condition with the solution in region 2:

$$u_3 = 0 \qquad \text{at} \qquad \bar{y} = 0, \tag{2.18a}$$
$$u_3 = \frac{\partial U_0}{\partial \bar{Y}}\bar{y} - \frac{\bar{k}}{\tilde{\omega}}\frac{p_a}{\rho_w} + c.c. \qquad \text{as} \qquad \bar{y} \to \infty. \tag{2.18b}$$

Solving (2.17a) with the boundary conditions (2.18) we deduce the solution for the

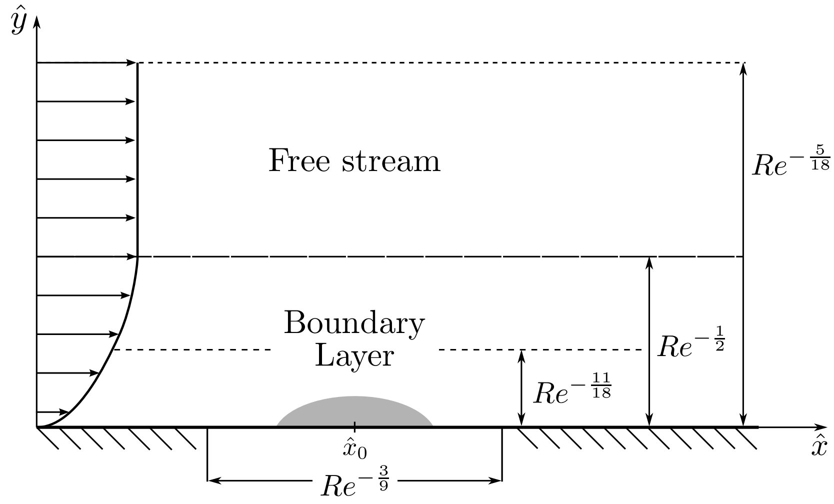

Figure 2.3: Triple-deck structure in transonic flow.

Stokes layer to be

$$u_3 = \frac{\partial U_0}{\partial \bar{Y}}\bar{y} + \frac{\bar{k}}{\tilde{\omega}}\frac{p_a}{\rho_w}\left[e^{-(1+i)\sqrt{\frac{\tilde{\omega}\rho_w}{2\mu_w}}\bar{y}} - 1\right] + c.c.. \tag{2.19}$$

2.4 Flow in the region of interaction

As mentioned in previous sections, in order to achieve resonance, both the frequency and the wavenumber of the acoustic perturbation should coincide with the frequency and the wavenumber of the Tollmien-Schlichting wave. In the transonic flow considered the frequency of the perturbations is set to be of the required order, $O(Re^{-2/9})$, in advance, which makes the wavelength of the acoustic wave to be $O(Re^{2/9})$ quantity. In order to adjust the wavenumber to coincide with the Tollmien-Schlichting wavenumber order, $O(Re^{3/9})$, it is necessary to introduce a wall roughness, which longitudinal extent is $O(Re^{-3/9})$ quantity. We shall assume that it is centred at point $\hat{x}_0$ and has the shape

$$y_* = Re^{-\frac{11}{18}}\bar{G}\left(\frac{x_* - x_0}{Re^{-3/9}}\right). \tag{2.20}$$

The region of interaction is located in the vicinity of the roughness and it is described by triple-deck theory, with structure and appropriate scalings as shown in Figure 2.3. In this region the external acoustic perturbation may be expanded using the Taylor series around the centre of the roughness

$$p_a(\tilde{t},\tilde{x}) = p_0(\tilde{t},\tilde{x}_0) + Re^{-\frac{1}{9}} i\bar{k}\tilde{x}p_0(\tilde{t},\tilde{x}_0) - \frac{1}{2}Re^{-\frac{2}{9}}\bar{k}^2\tilde{x}^2 p_0(\tilde{t},\tilde{x}_0) + \cdots + c.c., \tag{2.21}$$

where $p_0(\tilde{t},\tilde{x}_0) = \bar{a}e^{i\left(\tilde{\omega}\tilde{t}+\bar{k}\tilde{x}_0\right)}$.

2.4.1 Lower deck

An analysis of the flow in the interaction region begins with consideration of the viscous wall layer, region 4 (Figure 2.1), where the characteristic thickness of this layer is equal to the thickness of the Stokes layer (region 3). Therefore solutions to the Navier-Stokes equations are sought in the form

$$u_* = Re^{-\frac{1}{9}} u_4(\tilde{t},\tilde{x},\bar{y}) + \dots, \tag{2.22a}$$
$$v_* = Re^{-\frac{7}{18}} v_4(\tilde{t},\tilde{x},\bar{y}) + \dots, \tag{2.22b}$$
$$p_* = Re^{-\frac{1}{9}} p_0(\tilde{t},\tilde{x}_0) + Re^{-\frac{2}{9}}\left\{p_4(\tilde{t},\tilde{x},\bar{y}) + i\bar{k}\tilde{x}p_0(\tilde{t},\tilde{x}_0)\right\} + \dots, \tag{2.22c}$$
$$\rho_* = \rho_w(\tilde{x}_0) + \dots, \tag{2.22d}$$
$$\mu_* = \mu_w(\tilde{x}_0) + \dots, \tag{2.22e}$$
$$h_* = h_w(\tilde{x}_0) + \dots, \tag{2.22f}$$

with independent variables scaled as

$$t_* = Re^{-\frac{2}{9}}\tilde{t}, \qquad x_* = Re^{-\frac{2}{9}}\tilde{x}_0 + Re^{-\frac{3}{9}}\tilde{x}, \qquad y_* = Re^{-\frac{11}{18}}\bar{y}. \tag{2.23a-c}$$

Substituting expansions (2.22), (2.23) into (A.3) shows that the pressure, p_4 does not change across the region, and the momentum and continuity equations decouple from the other equations, thus allowing us to write them in the form

$$\rho_w\left(\frac{\partial u_4}{\partial \tilde{t}} + u_4\frac{\partial u_4}{\partial \tilde{x}} + v_4\frac{\partial u_4}{\partial \bar{y}}\right) = -i\bar{k}p_0 - \frac{\partial p_4}{\partial \tilde{x}} + \mu_w\frac{\partial^2 u_4}{\partial \bar{y}^2}, \tag{2.24a}$$
$$\frac{\partial u_4}{\partial \tilde{x}} + \frac{\partial v_4}{\partial \bar{y}} = 0, \tag{2.24b}$$

which are subject to the no-slip condition on the body surface

$$u_4 = v_4 = 0 \qquad \text{at} \qquad \bar{y} = \bar{G}(\tilde{x}), \tag{2.25a}$$

where $\bar{G}(\tilde{x})$ is a shape of the roughness on the surface of the plate.

The second boundary condition is obtained from the matching with the solution in region 3

$$u_4 = \frac{\partial U_0}{\partial \bar{Y}}\bar{y} + \frac{\bar{k}}{\tilde{\omega}}\frac{p_0}{\rho_w}\left[e^{-(1+i)\sqrt{\frac{\tilde{\omega}\rho_w}{2\mu_w}}\bar{y}} - 1\right] + c.c. \qquad \text{as} \qquad \tilde{x} \to -\infty, \tag{2.25b}$$

2.4.2 Main deck

The main deck (region 5) includes the main part of the streamlines belonging to the boundary-layer in front of the roughness and is a continuation of region 2 into the region of interaction. Asymptotic expansions, satisfying the matching conditions with (2.10) in region 2, assumes the form

$$u_* = U_0\left(\bar{Y}\right) + Re^{-\frac{1}{9}}\left\{M_\infty u_2(\bar{Y})p_0(\tilde{t}) + A_*(\tilde{t},\tilde{x})\frac{\partial U_0}{\partial \bar{Y}}\right\} + \dots, \tag{2.26a}$$

$$v_* = -Re^{-\frac{5}{18}}U_0(\bar{Y})\frac{\partial A_*}{\partial \tilde{x}}(\tilde{t},\tilde{x}) + \dots, \tag{2.26b}$$

$$p_* = Re^{-\frac{1}{9}}p_0(\tilde{t},\tilde{x}_0) + Re^{-\frac{2}{9}}\left\{p_5(\tilde{t},\tilde{x},\bar{Y}) + i\bar{k}\tilde{x}p_0(\tilde{t},\tilde{x}_0)\right\} + \dots, \tag{2.26c}$$

$$\rho_* = R_0\left(\bar{Y}\right) + Re^{-\frac{1}{9}}\left\{M_\infty^2\rho_2(\bar{Y})p_0(\tilde{t}) + A_*(\tilde{t},\tilde{x})\frac{\partial R_0}{\partial \bar{Y}}\right\} + \dots, \tag{2.26d}$$

where $A_*(\tilde{t},\tilde{x})$ is unknown displacement function. The pressure p_5 does not change across this region and is identical to p_4.

Matching solutions in region 4 to the solutions in region 5 we obtain the third boundary condition for the lower deck

$$u_4 = \frac{\partial U_0}{\partial \bar{Y}}\left[\bar{y} + A_*(\tilde{t},\tilde{x})\right] - \frac{\bar{k}}{\tilde{\omega}}\frac{p_0}{\rho_w} + c.c. \qquad \text{as} \qquad \bar{y} \to \infty, \tag{2.27}$$

and from (2.26b) we deduce that at the upper boundary of the main deck the vertical velocity component is

$$v_* = -Re^{-\frac{5}{18}}\frac{\partial A_*}{\partial \tilde{x}}, \tag{2.28}$$

which tends to zero as the Reynolds number increases. Thus the linearised small perturbation theory can be applied in region 6.

2.4.3 Upper deck

The upper deck (region 6) is the continuation of region 1, and making use of the unsteady linearised small perturbation theory, the solution in region 6 is sought in the form

$$p_* = Re^{-\frac{1}{9}} p_0(\tilde{t}, \tilde{x}_0) + Re^{-\frac{2}{9}} \left\{ p_6(\tilde{t}, \tilde{x}, \tilde{y}) + i\bar{k}\tilde{x} p_0(\tilde{t}, \tilde{x}_0) \right\} + \ldots, \tag{2.29}$$

with the independent variables being scaled as

$$t_* = Re^{-\frac{2}{9}} \tilde{t}, \qquad x_* = Re^{-\frac{2}{9}} \tilde{x}_0 + Re^{-\frac{3}{9}} \tilde{x}, \qquad y_* = Re^{-\frac{5}{18}} \tilde{y}. \tag{2.30a-c}$$

Substituting this expansions into the equation and retaining leading order terms we deduce the transonic small perturbation equation

$$2\frac{\partial^2 p_6}{\partial \tilde{x} \partial \tilde{t}} + Q_\infty \frac{\partial^2 p_6}{\partial \tilde{x}^2} - \frac{\partial^2 p_6}{\partial \tilde{y}^2} = 0. \tag{2.31}$$

Note that in contrast to the subsonic and supersonic cases equations (2.31) retains the time derivative and is hyperbolic if $Q_\infty > 0$ and elliptic otherwise.

Boundary conditions for this region are: matching condition with the lower deck

$$\frac{\partial p_6}{\partial \tilde{y}} = \frac{\partial^2 A_*}{\partial \tilde{x}^2} \quad \text{at} \quad \tilde{y} = 0, \tag{2.32a}$$

and the far field boundary condition, which states that all perturbations decay to zero sufficiently far away from the body surface, hence

$$p_6 \to 0 \qquad \text{as} \qquad \tilde{y} \to \infty. \tag{2.32b}$$

2.5 The viscous-inviscid interaction problem

In order to describe the flow past a wall roughness the flow governing equations in the viscous sublayer (2.24 , 2.25 and 2.27), have to be solved together with the upper deck equations (2.31, 2.32).

To decrease the number of parameters in the lower and upper deck equations we apply the following affine transformations and the Prandtl transposition theorem to the variables

$$\tilde{t} = \frac{t}{(2^2\rho_w^{-1}\mu_w^5\lambda^{14})^{\frac{1}{9}}} - \frac{\bar{k}}{\tilde{\omega}}\tilde{x}_0, \quad \tilde{x} = \frac{x}{(2^3\rho_w^3\mu_w^3\lambda^{12})^{\frac{1}{9}}}, \quad \bar{y} = \frac{y+g(x)}{(2\rho_w^4\mu_w^{-2}\lambda^7)^{\frac{1}{9}}}, \tag{2.33a-c}$$

$$v_4 = \frac{v + u\frac{dg}{dx}}{(2^{-1}\rho_w^5\mu_w^{-7}\lambda^{-7})^{\frac{1}{9}}}, \qquad u_4 = \frac{u}{(2\rho_w^4\mu_w^{-2}\lambda^{-2})^{\frac{1}{9}}}, \quad \tilde{y} = \frac{Y}{(2^7\rho_w\mu_w^4\lambda^{13})^{\frac{1}{9}}}, \tag{2.33d-f}$$

$$Q_\infty = \frac{K_\infty}{(2^{-8}\rho_w^4\mu_w^{-2}\lambda^{-2})^{\frac{1}{9}}}, \qquad A_* = \frac{A-g(x)}{(2\rho_w^4\mu_w^{-2}\lambda^7)^{\frac{1}{9}}}, \quad \bar{G} = \frac{g(x)}{(2\rho_w^4\mu_w^{-2}\lambda^7)^{\frac{1}{9}}}, \tag{2.33g-i}$$

$$(p_4,\, p_6) = \frac{(p,\, P)}{(2^2\rho_w^{-1}\mu_w^{-4}\lambda^{-4})^{\frac{1}{9}}}. \tag{2.33j}$$

In addition the frequency, wavenumber and amplitude of the acoustic perturbation are scaled as

$$\tilde{\omega} = \frac{\omega}{(2^{-2}\rho_w\mu_w^{-5}\lambda^{-14})^{\frac{1}{9}}}, \qquad \tilde{k}\bar{\alpha} = \frac{i\alpha}{(2^{-1}\rho_w^{-4}\mu_w^{-7}\lambda^{-16})^{\frac{1}{9}}}. \tag{2.33k,l}$$

As a result the lower deck equations (2.24) assume the form

$$\frac{\partial u}{\partial x} + \frac{\partial v}{\partial y} = 0, \tag{2.34a}$$

$$\frac{\partial u}{\partial t} + u\frac{\partial u}{\partial x} + v\frac{\partial u}{\partial y} = \alpha e^{i\omega t} - \frac{\partial p}{\partial x} + \frac{\partial^2 u}{\partial y^2}, \tag{2.34b}$$

with the boundary conditions (2.25) and (2.27) becoming

$$u = v = 0 \qquad \text{at} \quad y = 0, \tag{2.35a}$$

$$u = y + \frac{i\alpha}{\omega}\left[e^{-(1+i)\sqrt{\frac{\omega}{2}}y} - 1\right]e^{i\omega t} + c.c. \qquad \text{as} \quad x \to -\infty, \tag{2.35b}$$

$$u = y + A - \frac{i\alpha}{\omega}e^{i\omega t} + c.c. \qquad \text{as} \quad y \to \infty. \tag{2.35c}$$

The upper deck equation (2.31) now is written as

$$\frac{\partial^2 P}{\partial x \partial t} + K_\infty\frac{\partial^2 P}{\partial x^2} - \frac{\partial^2 P}{\partial Y^2} = 0. \tag{2.36}$$

This has to be solved subject to the boundary conditions

$$P = p \qquad \text{and} \qquad \frac{\partial P}{\partial Y} = \frac{\partial^2 A}{\partial x^2} - \frac{\partial^2 g}{\partial x^2} \qquad \text{at} \quad Y = 0, \tag{2.37a,b}$$

$$P \to 0 \qquad \text{as} \quad Y \to \infty. \tag{2.37c}$$

Here displacement function, A, is still undetermined whereas the shape of the roughness, g, is prescribed by (2.20).

In order to solve the problem at hand we assume that the amplitude of the acoustic wave, α, and the height of the wall roughness, h, are small. This allows us to write the equation of the roughness as $g(x) = hF(x)$, and seek the solution in the lower deck in the form

$$u = y + \alpha U_s(x, y) + hu_r(x, y) + \alpha hu'(t, x, y) + ..., \tag{2.38a}$$

$$v = hv_r(x, y) + \alpha hv'(t, x, y) + ..., \tag{2.38b}$$

$$p = \alpha e^{i\omega t} + hp_r(x, y) + \alpha hp'(t, x, y) + ..., \tag{2.38c}$$

$$A = hA_r(x, y) + \alpha hA'(t, x, y) + ..., \tag{2.38d}$$

$$P = \alpha e^{i\omega t} + hP_r(x, Y) + \alpha hP'(t, x, Y) + ..., \tag{2.38e}$$

where $U_s(x, y) = \frac{i}{\omega}\left[e^{-(1+i)\sqrt{\frac{\omega}{2}}y} - 1\right] e^{i\omega t}$+c.c. is the velocity profile in the Stokes layer.

The structure of the solution (2.38) may be explained as follows. As an example we look at the asymptotic expansion for the longitudinal velocity component, u, where the leading order term, y, represents the unperturbed steady boundary-layer, and would be the only term if neither the Stokes layer nor roughness were present. The next two terms, $\alpha U_s(x, y)$ and $hu_r(x, y)$ represent the perturbations produced by the Stokes layer and the roughness, respectively. The fourth term, $\alpha hu'(t, x, y)$, represents the perturbations produced in the boundary-layer due to the interaction of the Stokes layer with the steady flow field around the roughness.

Substitution of (2.38) into (2.34-2.37) lead to steady problem for $O(h)$ terms, and unsteady problem for $O(\alpha h)$ terms.

2.5.1 Steady problem

In the lower deck we obtain the following set of equations

$$\frac{\partial u_r}{\partial x} + \frac{\partial v_r}{\partial y} = 0, \tag{2.39a}$$

$$y\frac{\partial u_r}{\partial x} + v_r = -\frac{\partial p_r}{\partial x} + \frac{\partial^2 u_r}{\partial y^2}, \tag{2.39b}$$

which are subject to the boundary conditions

$$u_r = v_r = 0 \qquad \text{at} \qquad y = 0, \tag{2.40a}$$
$$u_r = A_r \qquad \text{as} \qquad y \to \infty, \tag{2.40b}$$
$$u_r = 0 \qquad \text{as} \qquad x \to -\infty. \tag{2.40c}$$

For the upper deck equation (2.36) we deduce

$$K_\infty \frac{\partial^2 P_r}{\partial x^2} - \frac{\partial^2 P_r}{\partial Y^2} = 0, \tag{2.41}$$

with the boundary conditions

$$P_r = p_r \quad \text{and} \quad \frac{\partial P_r}{\partial Y} = \frac{\partial^2 A_r}{\partial x^2} - \frac{\partial^2 F}{\partial x^2} \quad \text{at} \quad Y = 0, \tag{2.42a,b}$$
$$P_r \to 0 \qquad \text{as} \quad Y \to \infty. \tag{2.42c}$$

Solution of the steady problem

To solve the steady problem (2.39-2.42), we introduce the Fourier transform, which for the pressure, p_r, is defined as follows

$$\bar{p}_r(k, y) = \int_{-\infty}^{\infty} p_r(x, y) e^{-ikx} \, dx. \tag{2.43}$$

Applying the Fourier transform to (2.39, 2.40), reduces it to

$$ik\bar{u}_r + \frac{d\bar{v}_r}{\partial y} = 0, \tag{2.44a}$$
$$iky\bar{u}_r + \bar{v}_r = -ik\bar{p}_r + \frac{d^2\bar{u}_r}{dy^2}, \tag{2.44b}$$

and

$$\bar{u}_r = \bar{v}_r = 0 \qquad \text{at} \qquad y = 0, \tag{2.45a}$$
$$\bar{u}_r = \bar{A}_r \qquad \text{as} \qquad y \to \infty. \tag{2.45b}$$

In the upper deck we distinguish between two cases depending on the sign of the Kármán-Guderley parameter, K_∞, which has a plus sign if the flow is supersonic or aminus sign if it is subsonic. Thus the equations (2.41) and (2.42) in Fourier space are written as

$$k^2|K_\infty|\bar{P}_r - \frac{d^2\bar{P}_r}{dY^2} = 0 \qquad \text{if} \qquad K_\infty < 0, \tag{2.46a}$$

$$k^2|K_\infty|\bar{P}_r + \frac{d^2\bar{P}_r}{dY^2} = 0 \qquad \text{if} \qquad K_\infty > 0, \tag{2.46b}$$

with

$$\bar{P}_r = \bar{p}_r \qquad \text{at} \quad Y = 0, \tag{2.47a}$$

$$\frac{d\bar{P}_r}{dY} = -k^2(\bar{A}_r - \bar{F}) \quad \text{at} \quad Y = 0, \tag{2.47b}$$

$$\bar{P}_r \to 0 \qquad \text{as} \quad Y \to \infty. \tag{2.47c}$$

For simplification of the analysis we introduce a new quantity

$$\varkappa = \begin{cases} i & \text{if} \quad K_\infty < 0, \\ 1 & \text{if} \quad K_\infty > 0, \end{cases} \tag{2.48}$$

which allows us to write the solution for (2.46) with the boundary conditions (2.47b, 2.47c) in the form

$$\bar{P}_r = i|k|(\bar{A}_r - \bar{F})\varkappa^{-1}|K_\infty|^{-\frac{1}{2}}e^{i|k|\varkappa\sqrt{|K_\infty|}Y}. \tag{2.49}$$

Using (2.47a), and returning back to the equations in the lower deck, where setting $y = 0$ in (2.44b), and with the help of boundary condition (2.45a), we deduce an additional boundary condition for u_r

$$\frac{d^2\bar{u}_r}{dy^2} = i|k|(\bar{A}_r - \bar{F})\varkappa^{-1}|K_\infty|^{-\frac{1}{2}}. \tag{2.50}$$

Differentiating the momentum equation (2.44b) with respect to y and subtracting the continuity equation (2.44a) we obtain

$$\frac{d^3\bar{u}_r}{dy^3} - iky\frac{d\bar{u}_r}{dy} = 0. \tag{2.51}$$

Performing the variable change $z = \theta y$, where $\theta = (ik)^{\frac{1}{3}}$, reduces (2.51) to the Airy equation

$$\frac{d^3\bar{u}_r}{dz^3} - z\frac{d\bar{u}_r}{dz} = 0, \tag{2.52}$$

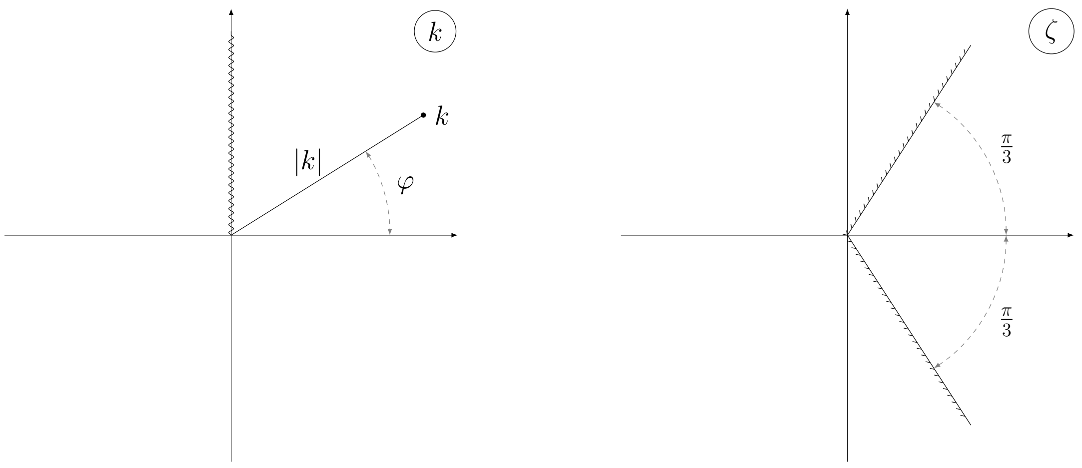

(a) k-plane

(b) ζ-plane

Figure 2.4: Choice of the analytical branch.

with boundary conditions becoming

$$\bar{u}_r = 0 \qquad \text{at} \qquad z = 0, \tag{2.53a}$$

$$\frac{d^2\bar{u}_r}{dz^2} = i(ik)^{\frac{1}{3}}|k|(\bar{A}_r - \bar{F})\varkappa^{-1}|K_\infty|^{-\frac{1}{2}} \qquad \text{at} \qquad z = 0, \tag{2.53b}$$

$$\bar{u}_r = \bar{A}_r \qquad \text{as} \qquad z \to \infty. \tag{2.53c}$$

The general solution of the Airy equation consists of the sum of two linearly independent solutions $Ai(z)$ and $Bi(z)$, namely,

$$\frac{\partial \bar{u}_r}{\partial z} = C_1 Ai(z) + C_2 Bi(z). \tag{2.54}$$

From (2.53c) we see that at large values of z the function u_r should stay finite, which suggests that $\partial\bar{u}_r/\partial z$ should approach zero as z tends to infinity. The behaviour of Ai(z) and Bi(z) at large z depends on the direction along which z tends to infinity in the complex plane. The latter is defined by a choice of analytical branch of $\theta = (ik)^{\frac{1}{3}}$. For our purposes it is convenient to make the branch cut in the complex k-plane along positive imaginary semi-axis (Figure 2.4) and define

$$\theta = (ik)^{\frac{1}{3}} = \left(e^{\frac{i\pi}{2}} k e^{i\phi}\right)^{\frac{1}{3}} = k^{\frac{1}{3}} e^{i\left(\frac{\pi}{6}+\frac{\phi}{3}\right)}. \tag{2.55}$$

Then for real positive y the argument of $z = \theta y$ will lie within the interval

$$\arg z \in \left(-\frac{\pi}{3}, \frac{\pi}{3}\right). \tag{2.56}$$

Within this sector the Airy function, $Ai(z)$ decays exponentially as

$$Ai(z) = \frac{1}{2}\pi^{-\frac{1}{2}} z^{-\frac{1}{4}} e^{-\frac{2}{3}z^{3/2}} + ... \qquad \text{as} \qquad z \to \infty, \tag{2.57}$$

but $Bi(z)$ is exponentially large

$$Bi(z) = \pi^{-\frac{1}{2}} z^{-\frac{1}{4}} e^{\frac{2}{3}z^{3/2}} + ... \qquad \text{as} \qquad z \to \infty, \tag{2.58}$$

see Abramowitz & Stegun (1965). Therefore we set C_2 to zero and the solution (2.54) becomes

$$\frac{d\bar{u}_r}{dz} = CAi(z). \tag{2.59}$$

Applying the boundary conditions (2.53a, 2.53c) to the solution above, we obtain a set of equations relating the constant C and the displacement function $\bar{A}_r$

$$CAi'(0) = i(ik)^{\frac{1}{3}}|k|(\bar{A}_r - \bar{F})\varkappa^{-1}|K_\infty|^{-\frac{1}{2}} \qquad \text{and} \qquad C = 3\bar{A}_r, \tag{2.60a,b}$$

which solved, yield

$$\bar{A}_r = \frac{i(ik)^{\frac{1}{3}}|k|}{i(ik)^{\frac{1}{3}}|k| - 3\varkappa Ai'(0)|K_\infty|^{\frac{1}{2}}}\bar{F}, \tag{2.61a}$$

$$C = \frac{3i(ik)^{\frac{1}{3}}|k|}{i(ik)^{\frac{1}{3}}|k| - 3\varkappa Ai'(0)|K_\infty|^{\frac{1}{2}}}\bar{F}. \tag{2.61b}$$

This allows us to write the steady problem solution for longitudinal and transverse velocities in the Fourier space as

$$\bar{u}_r = \bar{F}(k)\Phi\left(z; k, K_\infty\right) \qquad \text{and} \qquad \bar{v}_r = \bar{F}(k)\Psi\left(z; k, K_\infty\right), \tag{2.62a,b}$$

where

$$\Phi\left(z; k, K_\infty\right) = \frac{3i(ik)^{\frac{1}{3}}|k|}{i(ik)^{\frac{1}{3}}|k| - 3\varkappa Ai'(0)|K_\infty|^{\frac{1}{2}}} \int_0^z Ai(s)\, ds, \tag{2.63a}$$

$$\Psi\left(z; k, K_\infty\right) = -(ik)^{\frac{2}{3}} \int_0^z \Phi\left(s; k, K_\infty\right)\, ds. \tag{2.63b}$$

2.5.2 Unsteady problem

Returning back to the viscous-inviscid problem (2.34-2.37) and expansions (2.38), we deduce that working with $O(\alpha h)$ quantities, leads to the following set of equations in the viscous sublayer

$$\frac{\partial u'}{\partial x} + \frac{\partial v'}{\partial y} = 0, \tag{2.64a}$$

$$\frac{\partial u'}{\partial t} + y\frac{\partial u'}{\partial x} + v' + U_s\frac{\partial u_r}{\partial x} + v_r\frac{\partial U_s}{\partial y} = -\frac{\partial p'}{\partial x} + \frac{\partial^2 u'}{\partial y^2}, \tag{2.64b}$$

which are subject to the following boundary conditions

$$u' = v' = 0 \quad \text{at} \quad y = 0, \tag{2.65a}$$

$$u' = A' \quad \text{as} \quad y \to \infty, \tag{2.65b}$$

$$u' = 0 \quad \text{as} \quad x \to -\infty. \tag{2.65c}$$

In the upper deck we obtain

$$\frac{\partial^2 P'}{\partial x \partial t} + K_\infty \frac{\partial^2 P'}{\partial x^2} - \frac{\partial^2 P'}{\partial Y^2} = 0, \tag{2.66}$$

with boundary conditions being

$$P' = p' \quad \text{and} \quad \frac{\partial P'}{\partial Y} = \frac{\partial^2 A'}{\partial x^2} \quad \text{at} \quad Y = 0, \tag{2.67a,b}$$

$$P' \to 0 \quad \text{as} \quad Y \to \infty. \tag{2.67c}$$

Solution of the unsteady problem

The solution of the unsteady problem is sought in the time-periodic form, namely,

$$(u',\ v',\ p',\ P',\ A',\ U_s') = \left(\tilde{u},\ \tilde{v},\ \tilde{p},\ \tilde{P},\ \tilde{A},\ \tilde{U}_s\right) e^{i\omega t} + c.c., \tag{2.68}$$

where

$$\tilde{U}_s = \frac{i}{\omega}\left[e^{-(i+1)\sqrt{\frac{\omega}{2}}y} - 1\right]. \tag{2.69}$$

Substitution of (2.68), (2.69) into (2.64) and (2.65) lead to

$$\frac{\partial \tilde{u}}{\partial x} + \frac{\partial \tilde{v}}{\partial \bar{Y}} = 0, \tag{2.70a}$$

$$i\omega\tilde{u} + y\frac{\partial \tilde{u}}{\partial x} + \tilde{v} + \tilde{U}_s\frac{\partial u_r}{\partial x} + v_r\frac{\partial \tilde{U}_s}{\partial y} = -\frac{\partial \tilde{p}}{\partial x} + \frac{\partial^2 \tilde{u}}{\partial y^2}, \tag{2.70b}$$

and

$$\tilde{u} = \tilde{v} = 0 \qquad \text{at} \qquad y = 0, \tag{2.71a}$$

$$\tilde{u} = \tilde{A} \qquad \text{as} \qquad y \to \infty, \tag{2.71b}$$

$$\tilde{u} = 0 \qquad \text{as} \qquad x \to -\infty, \tag{2.71c}$$

Similarly, the upper deck equations (2.66), (2.67) reduce to

$$i\omega\frac{\partial \tilde{P}}{\partial x} + K_\infty\frac{\partial^2 \tilde{P}}{\partial x^2} - \frac{\partial^2 \tilde{P}}{\partial Y^2} = 0, \tag{2.72}$$

and

$$\tilde{P} = \tilde{p} \qquad \text{and} \qquad \frac{\partial \tilde{P}}{\partial Y} = \frac{\partial^2 \tilde{A}}{\partial x^2} \qquad \text{at} \qquad Y = 0, \tag{2.73a,b}$$

$$\tilde{P} \to 0 \qquad \text{as} \qquad Y \to \infty. \tag{2.73c}$$

These equations are manipulated in the same way as the corresponding steady flow equations. We start by applying the Fourier transform and differentiating (2.70b) with respect to y. Combining the result with the continuity equation (2.70a) gives

$$i(ky+\omega)\frac{d\check{u}}{dy} + ik\check{U}_s\frac{d\bar{u}_r}{dy} + \bar{v}_r\frac{d^2\check{U}_s}{dy^2} = \frac{d^3\check{u}}{dy^3}. \tag{2.74}$$

This equation has to be solved with the boundary conditions

$$\check{u} = 0 \qquad \text{at} \qquad y = 0, \tag{2.75a}$$

$$\check{u} = \check{A} \qquad \text{as} \qquad y \to \infty. \tag{2.75b}$$

The Fourier transform of the upper deck equations lead to

$$\frac{d^2\check{P}}{dY^2} + \left(\omega k + k^2 K_\infty\right)\check{P} = 0, \tag{2.76}$$

and

$$\check{P} = \check{p} \qquad \text{at} \qquad Y = 0 \tag{2.77a}$$

$$\frac{d\check{P}}{dY} = -k^2 \check{A} \qquad \text{at} \qquad Y = 0, \tag{2.77b}$$

$$\check{P} \to 0 \qquad \text{as} \qquad Y \to \infty. \tag{2.77bc}$$

The general solution of the upper deck equation (2.76) is written as

$$\check{P} = B_1 e^{i\sqrt{\omega k + k^2 K_\infty} Y} + B_2 e^{-i\sqrt{\omega k + k^2 K_\infty} Y}. \tag{2.78}$$

It can be seen that the solution depends on the sign of K_∞. If $K_\infty > 0$, then the solution satisfying the boundary conditions at $Y = \infty$, is written as

$$\check{P} = B_{21} e^{i\sqrt{|\omega k + k^2 K_\infty|} Y} \qquad k \in \left(-\infty, -\frac{\omega}{|K_\infty|}\right), \tag{2.79a}$$

$$\check{P} = B_{12} e^{-\sqrt{|-\omega k - k^2 K_\infty|} Y} \qquad k \in \left[-\frac{\omega}{|K_\infty|}, 0\right], \tag{2.79b}$$

$$\check{P} = B_{13} e^{i\sqrt{|\omega k + k^2 K_\infty|} Y} \qquad k \in (0, \infty). \tag{2.79c}$$

The solution with negative values of K_∞ has a similar form. Combining these solutions, we can write the solution in the more general form

$$\check{P} = B_* \, e^{i\sigma Y}, \tag{2.80}$$

where

$$\sigma = \begin{cases} |\omega k + k^2 K_\infty|^{\frac{1}{2}} & k \in \left(-\infty, -\frac{\omega}{|K_\infty|}\right) \cup (0, \infty) \\ i|\omega k + k^2 K_\infty|^{\frac{1}{2}} & k \in \left[-\frac{\omega}{|K_\infty|}, 0\right] \end{cases} \quad \text{for } K_\infty > 0, \tag{2.81a,b}$$

$$\sigma = \begin{cases} |\omega k + k^2 K_\infty|^{\frac{1}{2}} & k \in \left(0, \frac{\omega}{|K_\infty|}\right) \\ i|\omega k + k^2 K_\infty|^{\frac{1}{2}} & k \in (-\infty, 0] \cup \left[\frac{\omega}{|K_\infty|}, \infty\right) \end{cases} \quad \text{for } K_\infty < 0. \tag{2.81c,d}$$

Combining (2.77b) and (2.80) we find that

$$B_* = ik^2 \check{A} \sigma^{-1}, \tag{2.82}$$

which together with (2.75a), (2.77a) and (2.80) in (2.74) yields an additional boundary condition

$$\frac{d^2\breve{u}}{dy^2} = i(ik)k^2\breve{A}\sigma^{-1} \qquad \text{at} \qquad y=0. \tag{2.83}$$

Equations (2.62) suggest that the solution for the equation (2.74) may be represented as

$$\breve{u} = \bar{F}(k)\bar{\bar{u}} \qquad \text{and} \qquad \breve{A} = \bar{F}(k)\bar{\bar{A}}, \tag{2.84a,b}$$

which, when substituting it into (2.74), yields

$$\frac{d^3\bar{\bar{u}}}{dy^3} - i(ky+\omega)\frac{d\bar{\bar{u}}}{dy} = H(y;k,\omega,K_\infty). \tag{2.85a}$$

Here

$$H(y;k,\omega,K_\infty) = ik\breve{U}_s\frac{d\Phi}{dy} + \Psi\frac{d^2\breve{U}_s}{dy^2} = (ik)^{\frac{4}{3}}\breve{U}_s\frac{d\Phi}{dz} + \Psi\frac{d^2\breve{U}_s}{dy^2}. \tag{2.85b}$$

The boundary conditions (2.75) and (2.83) stay the same with the understanding that $\breve{u}$ and $\breve{A}$ are substituted by $\bar{\bar{u}}$ and $\bar{\bar{A}}$ respectively.

Introducing the new independent variable

$$\zeta = \theta y + \zeta_0, \qquad \text{where} \qquad \theta = (ik)^{\frac{1}{3}}, \qquad \zeta_0 = \frac{i\omega}{(ik)^{\frac{2}{3}}}, \tag{2.86}$$

we obtain the inhomogeneous Airy equation

$$\frac{d^3\bar{\bar{u}}}{d\zeta^3} - \zeta\frac{d\bar{\bar{u}}}{d\zeta} = \bar{\bar{H}}(\zeta;k,\omega,K_\infty), \tag{2.87a}$$

$$\bar{\bar{H}}(\zeta;k,\omega,K_\infty) = (ik)^{\frac{1}{3}}\breve{U}_s\frac{d\Phi}{dz} + (ik)^{-1}\frac{d^2\breve{U}_s}{dy^2}\Psi, \tag{2.87b}$$

which should be solved subject to the following boundary conditions

$$\bar{\bar{u}} = 0 \qquad \text{at} \qquad \zeta = \zeta_0, \tag{2.88a}$$

$$\frac{d^2\bar{\bar{u}}}{d\zeta^2} = i(ik)^{\frac{1}{3}}k^2\bar{\bar{A}}\sigma^{-1} \qquad \text{as} \qquad \zeta = \zeta_0, \tag{2.88b}$$

$$\bar{\bar{u}} = \bar{\bar{A}} \qquad \text{as} \qquad \zeta \to \infty. \tag{2.88c}$$

The general solution of (2.87a) is a composition of two complementary solutions of the Airy equation and a particular integral, and has the form

$$\frac{d\bar{\bar{u}}}{d\zeta} = C_1 Ai(\zeta) + C_2 Bi(\zeta) + \varphi(\zeta), \tag{2.89}$$

where the function $\varphi(\zeta)$ is the solution of the following boundary-value problem,

$$\varphi'' - \zeta\varphi = \bar{\bar{H}}, \tag{2.90a}$$

$$\varphi'(\zeta_0) = 0, \tag{2.90b}$$

$$\varphi(\infty) = 0. \tag{2.90c}$$

In order to find the constants C_1 and C_2 we apply the same arguments as previously in description of the steady problem (sec. 2.5.1). In order to avoid exponential growth of the solution as $\zeta \to \infty$, we set $C_2 = 0$ and therefore (2.89) is written as

$$\frac{d\bar{\bar{u}}}{d\zeta} = C_1 Ai(\zeta) + \varphi(\zeta). \tag{2.91}$$

Applying the boundary conditions (2.88) we obtain two equations relating the constant C_1 and the displacement function $\bar{\bar{A}}$, which are written as

$$C_1 Ai'(\zeta_0) = i(ik)^{\frac{1}{3}} k^2 \bar{\bar{A}} \sigma^{-1}, \qquad C_1 \int\limits_{\zeta_0}^{\infty} Ai(s)\, ds + \int\limits_{\zeta_0}^{\infty} \varphi(s)\, ds = \bar{\bar{A}}, \tag{2.92a,b}$$

Eliminating C_1 from (2.92), we find that

$$\bar{\bar{A}} = \frac{Ai'(\zeta_0) \int\limits_{\zeta_0}^{\infty} \varphi(s)\, ds}{Ai'(\zeta_0) - i(ik)^{\frac{1}{3}} k^2 \sigma^{-1} \int\limits_{\zeta_0}^{\infty} Ai(s)\, ds}. \tag{2.93}$$

Substituting this expression back into the equations relating the pressure and the displacement function, and taking into account that $\check{A} = \bar{F}(k)\bar{\bar{A}}$, we deduce that the pressure in Fourier space is

$$\check{P} = \frac{ik^2 Ai'(\zeta_0) \bar{F}(k) \int\limits_{\zeta_0}^{\infty} \varphi(s)\, ds}{\sigma Ai'(\zeta_0) - i(ik)^{\frac{1}{3}} k^2 \int\limits_{\zeta_0}^{\infty} Ai(s)\, ds}. \tag{2.94}$$

2.6 Receptivity coefficient

In order to return back from Fourier to physical space it is necessary to perform the inverse Fourier transform

$$P(t,x) = \frac{e^{i\omega t}}{2\pi} \int_{-\infty}^{\infty} \frac{ik^2 Ai'(\zeta_0) \int_{\zeta_0}^{\infty} \varphi(s)\, ds}{\sigma Ai'(\zeta_0) - i(ik)^{\frac{1}{3}} k^2 \int_{\zeta_0}^{\infty} Ai(s)\, ds} \bar{F}(k) e^{ikx}\, dk. \tag{2.95}$$

The integration here is performed along the real axis in the k-plane. Nevertheless it is convenient to take the analytic extension of the integrands into the complex k-plane, where according to Cauchy's theorem, the contour of integration can be deformed. As the main interest is in the behaviour of the perturbations downstream of the roughness, for positive x it is convenient to consider an analytical extension of the integrand into the upper half plane. When deforming the contour, it might cross a point where the denominator of the integrand is zero, therefore is necessary to start with a study of the roots of the dispersion equation.

2.6.1 Dispersion relation

The dispersion relation is obtained from equation (2.94) by equating the denominator to zero:

$$\sigma Ai'(\zeta_0) - i(ik)^{\frac{1}{3}} k^2 \int_{\zeta_0}^{\infty} Ai(s)\, ds = 0, \tag{2.96}$$

with σ and ζ_0 defined as in (2.81) and (2.86) respectively.

Solving the equation (2.96) we will assume that the frequency, ω, is real and positive. Our task will be to find the wavenumber, k, which in general case is complex and is a function of ω and K_∞. We expect the Tollmien-Schlichting waves to propagate downstream, which happens when the real part of the wavenumber is negative and real part of $\sqrt{\omega k + k^2 K_\infty}$ is positive.

We start by assuming that $\omega \to 0$ and ζ_0 is finite, which consequently leads to the limit $k \to 0$. In addition from (2.86) it can be deduced that ω is $O\left(k^{2/3}\right)$ quantity and thus σ is of order k. Taking into the account all these limits the dispersion equation (2.96) reduces to

$$\frac{dAi(\zeta)}{d\zeta} = 0 \qquad \text{at} \qquad \zeta = \zeta_0, \tag{2.97}$$

which has infinite number of roots and all lie on the negative real semi-axis in ζ_0-plane,

	$Ai'(\zeta_0)$	$\int_{\zeta_0}^{\infty} Ai(s)\, ds$
1	-1.01879	$-4.10699 + 1.14416i$
2	-3.24819	$-4.10699 - 1.14416i$
3	-4.82009	$-6.79814 + 1.03515i$
4	-6.16330	$-6.79814 - 1.03515i$
5	-7.37217	$-9.03091 + 0.96940i$

Table 2.1: First five roots, ζ_0, of $Ai(\zeta_0) = 0$ and $\int\limits_{\zeta_0}^{\infty} Ai(s)\, ds = 0$

the first five roots are shown in Table 2.1. These roots may be used as an initial guess in the iterative solution of the dispersion equation for a small value of ω. The dispersion relation (2.96) is solved using MatLab®, were the frequency ω is kept fixed until the iteration process converges and the corresponding value of ζ_0 is found. The process is then repeated for a new ω, which is increased by a small value $d\omega$.

From the solution of the dispersion equation we see, Figure 2.5, that when ω increases each root of the equation tend to a certain point in ζ_0-plane, except the first root which tends to infinity.

To find these points we look at roots of the dispersion equation for large values of ω. We assume that $\omega \to \infty$ and ζ_0 is finite, and following similar arguments as deriving the expression (2.97) the dispersion equation (2.96) reduces to

$$\int\limits_{\zeta_0}^{\infty} Ai(s)\, ds = 0 \tag{2.98}$$

This equation has an infinite number of roots which all come in complex conjugate pairs and lie in the left half of the complex ζ_0-plane, see Table 2.1.

As mentioned earlier the behaviour of the first root is different from that of the other roots. In the k-plane it stays in the second quadrant until the frequency reaches its critical value, ω_0, which depends on the Kármán-Guderley parameter. Increasing the frequency further the trajectory of the first root crosses the real axis at the point k_0 and remains in the third quadrant for all $\omega > \omega_0$. In addition it can be seen that as the value of the Kármán-Guderley parameter increases, the neutral point k_0 approaches zero. This root represents the Tollmien-Schlichting wave.

In order to find how the neutral wavenumber, k_r depends on the Kármán-Guderley parameter we start by introducing the phase velocity $c = \omega/k_r$. Denoting by c_0^* and k_0^* the neutral values of the phase velocity and wavenumber in incompressible flow (Smith, 1979a), we perform transformations: $c = ac_0^*$ and $k_r = a^{-3}k_0^*$, see Timoshin (1990),

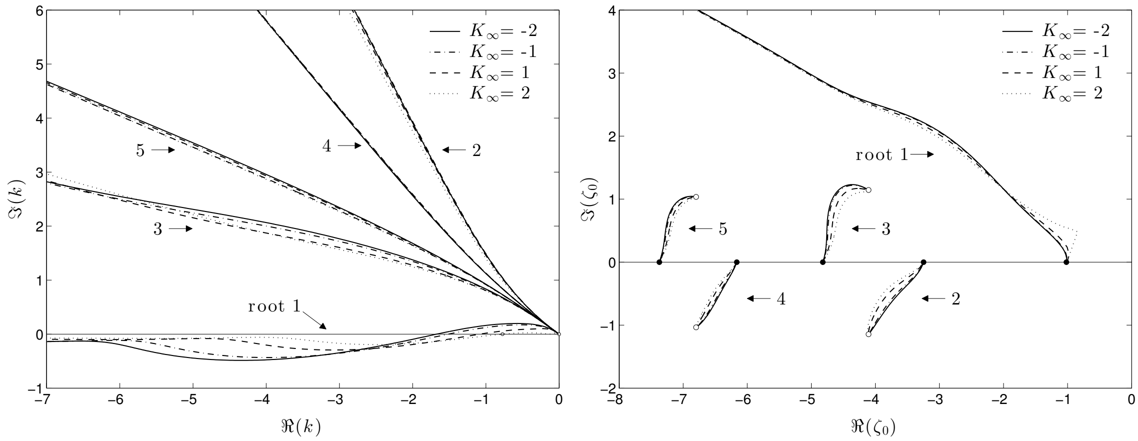

(a) k-plane (b) ζ_0-plane

Figure 2.5: The first five roots of the dispersion equation (2.96).

and then the dispersion equation (2.96) can be rewritten as

$$(ik_0^*)^{1/3}|k_0^*|\,[Ai'(\zeta_0^*)]^{-1}\int_{\zeta_0^*}^{\infty} Ai(s)\,ds = a^4\,(-ac_0^* - K_\infty)^{\frac{1}{2}}\,, \tag{2.99}$$

where a is a constant. In incompressible flow the dispersion equation is

$$(ik)^{1/3}|k|\,[Ai'(\zeta_0)]^{-1}\int_{\zeta_0}^{\infty} Ai(s)\,ds = 1. \tag{2.100}$$

It has only one unstable root and the neutral point is positioned at $\omega_0^* = 2.29797$ and $k_0^* = -1.00049$. Comparison of (2.100) with (2.99) leads to the following equation for constant a:

$$a^8\,(ac_0^* + K_\infty) = -1, \tag{2.101}$$

where $c_0^* = -2.296$. This equation has only one real root, which gives the sought neutral point position $(\omega_0,\, k_0)$ for each value of K_∞, see Figure 2.6.

Returning back to the integral (2.95) we shall distinguish between two cases: $K_\infty < 0$ and $K_\infty > 0$, where our task is to determine the amplitude of the Tollmien-Schlichting waves. To calculate the integral in both cases we consider a value of the frequency that is smaller than the critical frequency. For such ω the roots of (2.96) lie in the second quadrant of the complex k-plane. In addition, one has to remember that when introducing an analytical branch of the function $(ik)^{1/3}$ we had to make a branch cut

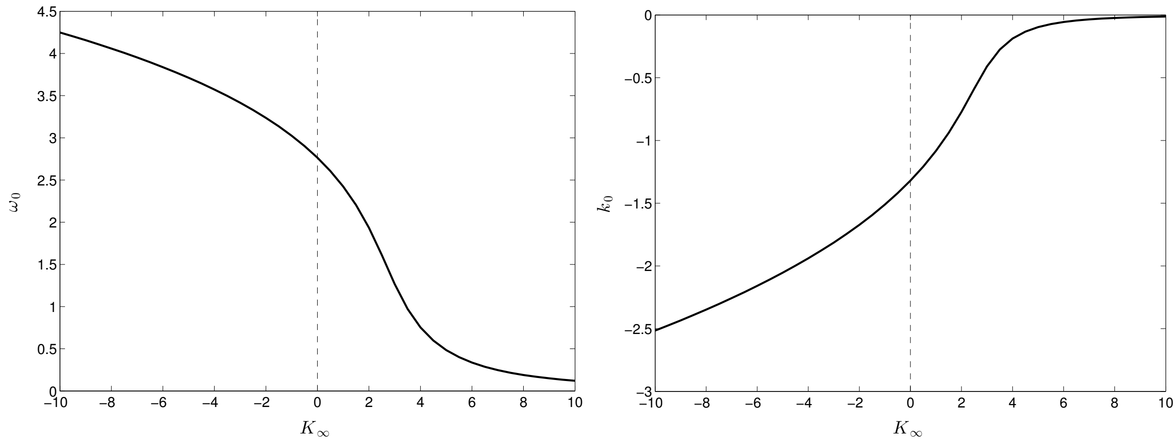

(a) Frequency, ω_0 (b) Wavenumber, k_0

Figure 2.6: Position of neutral points (ω_0, k_0) as a function of the Kármán-Guderley parameter.

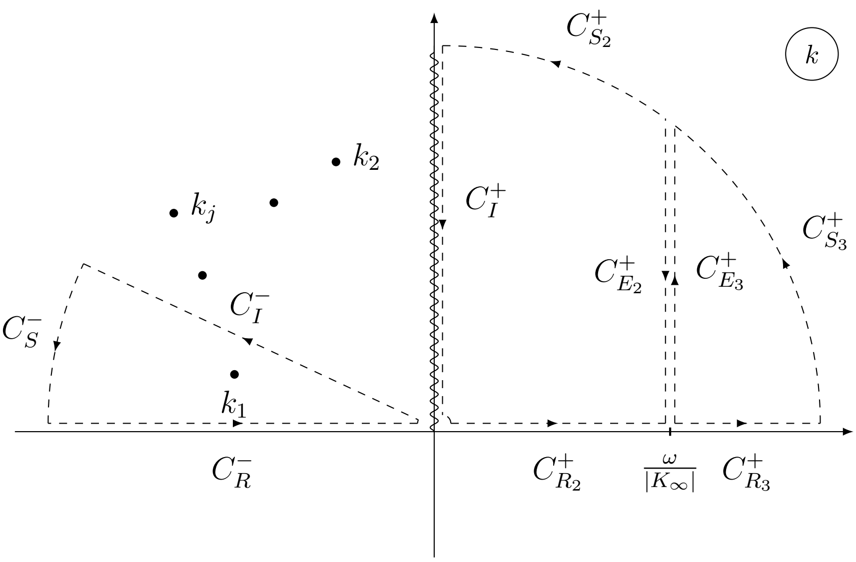

Figure 2.7: The contour of integration in k-plane in the case of the negative transonic parameter, $K_\infty < 0$

along the positive imaginary axis in the k-plane, which suggest that the branch cut here have to be extended to the entire imaginary axis. Therefore, we can split the integration interval into two parts, negative and positive real semi-axes.

In the case of the negative Kármán-Guderley parameter the contour along the real negative semi-axis is closed with the arc C^-_S with large radius, R, and ray C^-_R originating at the coordinate origin, see Figure 2.7. The angle between the negative real semi-axis and C^-_I is chosen so that the closed contour encloses only one root k_j. For the real positive semi-axis, the contour consists of two closed contours $(C^+_{R_2}, C^+_{E_2}, C^+_{S_2}, C^+_I)$ and $(C^+_{R_3}, C^+_{S_3}, C^+_{E_3})$ where position of the $C^+_{E_2}$ and $C^+_{E_3}$ depends on value of $\frac{\omega}{|K_\infty|}$.

The analytic extensions of the integrand (2.94) in the region enclosed inside of each contour is given by expressions

$$\check{P}_1^- = \frac{k^2 Ai'(\zeta_0)\bar{F}(k)\int\limits_{\zeta_0}^{\infty}\varphi(s)\,ds}{(-\omega k - k^2K_\infty)^{\frac{1}{2}}\,Ai'(\zeta_0) - (ik)^{\frac{1}{3}}k^2\int\limits_{\zeta_0}^{\infty}Ai(s)\,ds} \qquad k_r \in (-\infty, 0)\,, \tag{2.102a}$$

$$\check{P}_2^- = \frac{ik^2 Ai'(\zeta_0)\bar{F}(k)\int\limits_{\zeta_0}^{\infty}\varphi(s)\,ds}{(\omega k + k^2K_\infty)^{\frac{1}{2}}\,Ai'(\zeta_0) - i(ik)^{\frac{1}{3}}k^2\int\limits_{\zeta_0}^{\infty}Ai(s)\,ds} \qquad k_r \in \left(0, \frac{\omega}{|K_\infty|}\right), \tag{2.102b}$$

$$\check{P}_3^- = \frac{k^2 Ai'(\zeta_0)\bar{F}(k)\int\limits_{\zeta_0}^{\infty}\varphi(s)\,ds}{(-\omega k - k^2K_\infty)^{\frac{1}{2}}\,Ai'(\zeta_0) - (ik)^{\frac{1}{3}}k^2\int\limits_{\zeta_0}^{\infty}Ai(s)\,ds} \qquad k_r \in \left(\frac{\omega}{|K_\infty|}, \infty\right). \tag{2.102c}$$

In addition the integral (2.95) can be split into the sum of three integrals as

$$P(t,x) = \frac{e^{i\omega t}}{2\pi}\int\limits_{C_R^-}\check{P}_1^- e^{ikx}\,dk + \frac{e^{i\omega t}}{2\pi}\int\limits_{C^+_{R_2}}\check{P}_2^- e^{ikx}\,dk + \frac{e^{i\omega t}}{2\pi}\int\limits_{C^+_{R_3}}\check{P}_3^- e^{ikx}\,dk. \tag{2.103}$$

The first integral in (2.103) is found using the residue theorem

$$\int\limits_{C_R^-}\check{P}_1^- e^{ikx}\,dk + \int\limits_{C_I^-}\check{P}_1^- e^{ikx}\,dk + \int\limits_{C_S^-}\check{P}_1^- e^{ikx}\,dk = 2i\pi \mathrm{Res}\left\{P_1^-; k_1\right\}. \tag{2.104}$$

Note that the expression (2.102a) is in the form

$$\check{P}_1^- = \frac{N(k)}{D(k)}, \tag{2.105}$$

where

$$N(k) = k^2 Ai'(\zeta_0)\bar{F}(k)e^{ikx}\int\limits_{\zeta_0}^{\infty}\varphi(s)\,ds, \tag{2.106a}$$

$$D(k) = \left(-\omega k - k^2K_\infty\right)^{\frac{1}{2}}Ai'(\zeta_0) - (ik)^{\frac{1}{3}}k^2\int\limits_{\zeta_0}^{\infty}Ai(s)\,ds. \tag{2.106b}$$

Residue of the function $\check{P}_1^-$ at the point k_1, which is the simple pole, is found by differentiating the denominator (2.106b) at the pole, which leads to the expression

$$-\frac{6q_1k_1^2Ai'(\zeta_0)\bar{F}(k_1)e^{ik_1x}\int\limits_{\zeta_0}^{\infty}\varphi(s)\,ds}{3Ai'(\zeta_0)\left\{2K_\infty k_1+\omega\right\}+2q_1(ik_1)^{\frac{1}{3}}\left[2Ai(\zeta_0)\zeta_0\left(q_1\frac{\omega}{k_1^2}+k_1\right)+7k_1I_{\zeta_0}\right]}, \tag{2.107}$$

where $I_{\zeta_0}=\int\limits_{\zeta_0}^{\infty}Ai(s)\,ds$, $q_1=(-K_\infty k_1^2-\omega k_1)^{\frac{1}{2}}$ and $\zeta_0=\frac{i\omega}{(ik_1)^{\frac{2}{3}}}$.

The second and third integral in (2.103) is found using Cauchy's theorem. As the dispersion equations do not have roots in the first quadrant (figure. 2.7), then the integral over the closed contour is equal to zero, thus

$$\int\limits_{C^+_{R_2}}\check{P}_2^-e^{ikx}\,dk=-\int\limits_{C^+_I}\check{P}_2^-e^{ikx}\,dk-\int\limits_{C^+_{S_2}}\check{P}_2^-e^{ikx}\,dk-\int\limits_{C^+_{E_2}}\check{P}_2^-e^{ikx}\,dk, \tag{2.108a}$$

$$\int\limits_{C^+_{R_3}}\check{P}_3^-e^{ikx}\,dk=-\int\limits_{C^+_{S_3}}\check{P}_3^-e^{ikx}\,dk-\int\limits_{C^+_{E_3}}\check{P}_3^-e^{ikx}\,dk. \tag{2.108b}$$

Substituting (2.104), (2.107) and (2.108) into (2.103) we obtain

$$\begin{aligned}P(t,x)=&-\frac{6iq_1k_1^2Ai'(\zeta_0)\int\limits_{\zeta_0}^{\infty}\varphi(s)\,ds\;\bar{F}(k_1)e^{i(\omega t+k_1x)}}{3Ai'(\zeta_0)\left[2K_\infty k_1+\omega\right]+2q_1(ik_1)^{\frac{1}{3}}\left[2Ai(\zeta_0)\zeta_0\left(q_1\frac{\omega}{k_1^2}+k_1\right)+7k_1I_{\zeta_0}\right]}\\&-\frac{e^{i\omega t}}{2\pi}\left[\int\limits_{C^-_I}\check{P}_1^-(k)e^{ikx}\,dk+\int\limits_{C^-_S}\check{P}_1^-(k)e^{ikx}\,dk\right.\\&\left.+\int\limits_{C^+_I}\check{P}_2^-(k)e^{ikx}\,dk+\int\limits_{C^+_{S_2}}\check{P}_2^-(k)e^{ikx}\,dk+\int\limits_{C^+_{S_3}}\check{P}_3^-(k)e^{ikx}\,dk\right],\end{aligned} \tag{2.109}$$

where the integrals along $C^+_{E_2}$ and $C^+_{E_3}$ cancel each other as the integration is performed along the same line but in the opposite directions.

In order calculate the remaining five integrals in (2.109), at first we consider the integrals along the arcs $C^-_S, C^+_{S_2}$ and $C^+_{S_3}$, where we will show that the integrals tend to zero as the arc radius tends to infinity.

We start with the study of the solution of the boundary-value problem (2.90) at the limit

$$k \to \infty, \qquad \omega = O(1). \tag{2.110}$$

Returning to (2.63) and setting $k \to \infty$ we deduce

$$\Phi^- \approx 3 \int_0^z Ai(s)\,ds, \qquad \Psi^- \approx -3(ik)^{\frac{2}{3}} \int_0^z \left[\int_0^s Ai(s')\,ds' \right] ds. \tag{2.111a,b}$$

With z being an order one quantity, $y = (ik)^{-\frac{1}{3}} z$ is small, and therefore the function (2.69) may be approximated as

$$\tilde{U}_s \approx -\frac{1-i}{\sqrt{2\omega}} y + O(y^2). \tag{2.112}$$

Substituting (2.111) and (2.112) into (2.87b) we find that at large values of k the right-hand side of the equation (2.90) becomes

$$\bar{\bar{H}} \approx -3\frac{1-i}{\sqrt{2\omega}} z Ai(z) + O(k^{-\frac{1}{3}}). \tag{2.113}$$

If $k \to \infty$, then ζ_0 tends to zero and therefore the boundary-value problem (2.90) reduces to

$$\varphi'' - \zeta\varphi \approx -3\frac{1-i}{\sqrt{2\omega}} z Ai(z), \tag{2.114a}$$

$$\varphi'(0) = 0, \qquad \varphi(\infty) = 0. \tag{2.114b,c}$$

The solution to this problem, φ, is an order one quantity. Hence the integral

$$\int_{\zeta_0}^{\infty} \varphi(s)\,ds = \int_0^{\infty} \varphi(s)\,ds = O(1). \tag{2.115}$$

Returning back to (2.102a) and representing this expression in the form

$$\check{P}_1^- = \Pi_1^-(k,\omega)\bar{F}(k), \tag{2.116}$$

where

$$\Pi_1^-(k,\omega) = \frac{k^2 Ai'(\zeta_0) \int\limits_{\zeta_0}^{\infty} \varphi(s)\, ds}{(-k^2 K_\infty - \omega k)^{\frac{1}{2}}\, Ai'(\zeta_0) - (ik)^{\frac{1}{3}} k^2 \int\limits_{\zeta_0}^{\infty} Ai(s)\, ds}, \tag{2.117}$$

it can be seen that Π_1^- is of order $k^{-\frac{1}{3}}$ when $k \to \infty$. Therfore if we assume that the function $F(x)$ representing the wall roughness shape is integrable on the interval $x \in (-\infty, \infty)$ together with its modulus, then there exist a positive constant B such that

$$\left|\bar{F}(k)\right| = \left| \int\limits_{-\infty}^{\infty} F(x) e^{-ikx}\, dx \right| \leq \int\limits_{-\infty}^{\infty} |F(x)|\, dx \leq B \tag{2.118}$$

It follows from (2.117) and (2.118) that the expression (2.102a) satisfies the conditions of Jordan's lemma, which allows to conclude that for all $x > 0$ the integral along C_S^- tend to zero as the radius becomes large. Similarly we may show that the integrals along $C_{S_2}^+$ and $C_{S_3}^+$ satisfy Jordan's lemma and therefore, when the radius tends to infinity the integrals along theses arcs also tend to zero.

The remaining integrals in (2.109), along the rays C_I^- and C_I^+, represent the continuous spectrum of the perturbation field, which decay further downstream of the wall roughness. Both integrals are of Laplace type and they may be evaluated with the help of Watson's lemma. In order to use the lemma it is necessary to know the behaviour of the integrands (2.102) at small values of k. Keeping this in mind, we return to the boundary-value problem (2.90), and take a limit

$$k \to 0, \qquad \omega = O(1). \tag{2.119}$$

Applying the limit to (2.90) it is convenient to recast the independent variable using $z = \zeta - \zeta_0$, therefore we obtain

$$\varphi_z'' - (\zeta_0 + z)\varphi_z = \bar{\bar{H}}, \tag{2.120a}$$

$$\varphi_z'(0) = 0, \quad \varphi_z(\infty) = 0. \tag{2.120b,c}$$

Since the integrands (2.102) involve the integral of φ it is sufficient to determine the behaviour of the function φ when $y \to \infty$ but $z = O(1)$. Substituting (2.63) and (2.69) into (2.87b) we see that the right head side of (2.90) is

$$\bar{\bar{H}} \approx -\frac{i(ik)^{\frac{2}{3}}|k|}{\omega Ai'(0)|K_\infty|^{\frac{1}{2}}} Ai(z). \tag{2.121}$$

In the region of interest ζ_0 tend to infinity, therefore the second term on the left hand side of (2.120a) is large compared to the first term, which leads to the equation

$$-\zeta_0\varphi_z = \bar{\bar{H}}. \tag{2.122}$$

Sunstituting (2.121) into (2.122), we find that

$$\varphi \approx \frac{i(ik)^{\frac{4}{3}}|k|}{\omega^2 Ai'(0)|K_\infty|^{\frac{1}{2}}}Ai(z), \tag{2.123}$$

and consequently

$$\int\limits_{\zeta_0}^{\infty}\varphi(s)\,ds \approx \int\limits_{0}^{\infty}\varphi(s)\,ds \approx \frac{i(ik)^{\frac{4}{3}}|k|}{3\omega^2 Ai'(0)|K_\infty|^{\frac{1}{2}}}. \tag{2.124}$$

This allows us to continue with the analysis of (2.102) in the limit (2.119). Since in this limit ζ_0 is large, the derivative and integral of the Airy function can be substituted by their asymptotic formulae (Abramowitz & Stegun, 1965)

$$Ai'(\zeta_0) = -\frac{1}{2}\pi^{-\frac{1}{2}}\zeta_0{}^{\frac{1}{4}}e^{-\frac{2}{3}\zeta_0{}^{3/2}} + \dots, \tag{2.125a}$$

$$\int\limits_{\zeta_0}^{\infty} Ai(s)\,ds = \frac{1}{2}\pi^{-\frac{1}{2}}\zeta_0{}^{-\frac{3}{4}}e^{-\frac{2}{3}\zeta_0{}^{\frac{3}{2}}} + \dots. \tag{2.125b}$$

Using these in (2.102), we have

$$\check{P} \approx -\frac{k^2(ik)^{\frac{4}{3}}|k|}{3\omega^2\sigma Ai'(0)|K_\infty|^{\frac{1}{2}}}\bar{F}(0). \tag{2.126}$$

Returning back to (2.109), we see that the integrals along C_I^- and C_I^+ can be rewritten as

$$\int\limits_{C_I^\pm}\check{P}e^{ikx}\,dk \approx -\frac{\bar{F}(0)}{3\omega^2 Ai'(0)|K_\infty|^{\frac{1}{2}}}\int\limits_{C_I^\pm}k^2(ik)^{\frac{4}{3}}|k|\sigma^{-1}e^{ikx}\,dk. \tag{2.127}$$

The integrand in (2.127) is analytic in the entire k-plane with the branch cut along the imaginary positive semi-axis. Therefore, instead of integrating along the rays C_I^- and C_I^+, we can choose any other ray as long as it stays in the upper half plane. For the ray C_I^- it is convenient to perform the calculations along the left hand side of the branch cut, in which case

$$k = se^{-\frac{3i\pi}{2}} = is, \qquad s \in [0, \infty). \tag{2.128}$$

Consequently it allows to express the integral (2.127) as

$$\int_{C_I^-} \check{P}_1^-(k) e^{ikx}\, dk \approx \frac{\bar{F}(0)}{3\omega^{\frac{5}{2}} Ai'(0)|K_\infty|^{\frac{1}{2}}} \frac{(1+i)}{\sqrt{2}} \int_0^\infty s^{\frac{23}{6}} e^{-sx}\, ds. \tag{2.129}$$

Performing the change of the integration variable, $t = sx$, we obtain

$$\begin{aligned} \int_{C_I^-} \check{P}_1^-(k) e^{ikx}\, dk &\approx \frac{\bar{F}(0)}{3\omega^{\frac{5}{2}} Ai'(0)|K_\infty|^{\frac{1}{2}}} \frac{(1-i)}{x^{\frac{29}{6}}\sqrt{2}} \int_0^\infty t^{\frac{23}{6}} e^{-t}\, dt \\ &= \frac{\bar{F}(0)}{3\omega^{\frac{5}{2}} Ai'(0)|K_\infty|^{\frac{1}{2}}} \frac{(1-i)}{x^{\frac{29}{6}}\sqrt{2}} \Gamma\left(\frac{29}{6}\right). \end{aligned} \tag{2.130}$$

The integral along C_I^+ is found in a similar way to the above except that now

$$k = se^{\frac{i\pi}{2}} = is, \qquad s \in [\infty, 0). \tag{2.131}$$

Thus we can write

$$\int_{C_I^+} \check{P}_1^-(k) e^{ikx}\, dk \approx \frac{\bar{F}(0)}{3\omega^{\frac{5}{2}} Ai'(0)|K_\infty|^{\frac{1}{2}}} \frac{(1+i)}{x^{\frac{29}{6}}\sqrt{2}} \Gamma\left(\frac{29}{6}\right) \qquad \text{as} \qquad x \to \infty. \tag{2.132}$$

Substituting (2.130) and (2.132) back into (2.109) we obtain the solution for the pressure at large values of x and negative values of the Kármán-Guderley parameter

$$P(t,x) = \frac{1}{2}\mathcal{K}(\omega, K_\infty)\bar{F}(k_1)e^{i(\omega t + k_1 x)} - \frac{\sqrt{2}\Gamma\left(29/6\right)}{3\omega^{\frac{5}{2}} Ai'(0)|K_\infty|^{\frac{1}{2}}} \bar{F}(0) \frac{e^{i\omega t}}{x^{\frac{29}{6}}} + \ldots, \tag{2.133}$$

where

$$\mathcal{K} = -\frac{12iq_1k_1^2 Ai'(\zeta_0) \int\limits_{\zeta_0}^{\infty} \varphi(s)\, ds}{3Ai'(\zeta_0)\left[2K_\infty k_1 + \omega\right] + 2q_1(ik_1)^{\frac{1}{3}}\left[2Ai(\zeta_0)\zeta_0\left(q_1\frac{\omega}{k_1^2} + k_1\right) + 7k_1 I_{\zeta_0}\right]}. \tag{2.134}$$

This function, $\mathcal{K}(\omega, K_\infty)$ is called the receptivity coefficient. It is a function of the frequency, ω and the Kármán-Guderley parameter, K_∞, only.

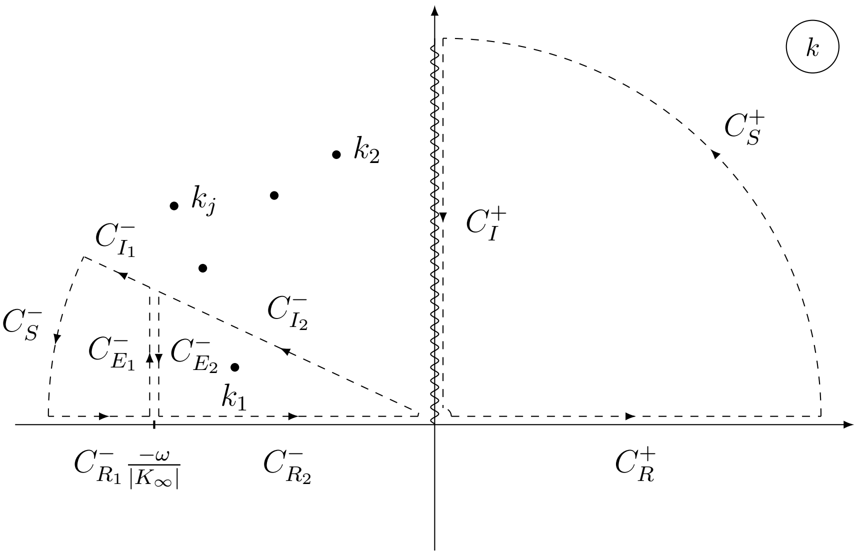

Figure 2.8: The contour of integration in k-plane in the case of the positive transonic parameter, $K_\infty > 0$

Calculation of the inverse integral for the pressure for positive values of the Kármán-Guderley parameter can be achieved using a similar procedure, with the exception that in this case the contour of integration in the k-plane is chosen such as shown in Figure 2.8. Performing this analysis, it is found that the receptivity coefficient in the case of $K_\infty > 0$ is expressed again by (2.134).

Hence the receptivity coefficient of the boundary-layer to an acoustic perturbation with a phase velocity of $O(1)$ can be calculated using the expression (2.134) as long as $\sqrt{\omega k + k^2 K_\infty}$ is positive.

Numerical calculations of the receptivity coefficient are performed in the following way. First, we choose real values of the frequency and Kármán-Guderley parameter, then from the dispersion equation (2.96) we find values of k and ζ_0 of the first root, see Figure 2.5. Values of the Airy function and its derivative and the integral at the point ζ_0 were found by solving the initial-value problem for the Airy equation along the straight line connecting ζ_0 with the origin in the complex z-plane. These calculations employed the Runge-Kutta algorithm with calculations starting at the origin, $\zeta = 0$, where the values of the Airy function and its derivatives are well known (see for an example, Abramowitz & Stegun (1965)). Finally, the function φ is found by solving the boundary-value problem (2.90), which using standard second order central finite differences scheme was decomposed into the tridiagonal matrix system. This system later was solved using the Thomas algorithm, which is based on LU decomposition of the original matrix system. During the calculations of the receptivity coefficient we

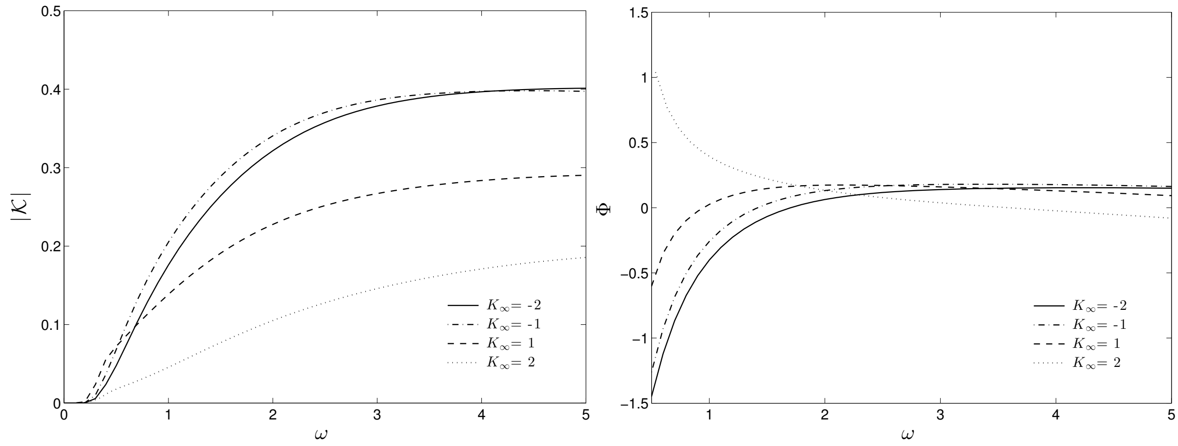

(a) Modulus of the receptivity coefficient (b) Argument of the receptivity coefficient

Figure 2.9: Receptivity coefficient dependence on the frequency and the Kármán-Guderley parameter.

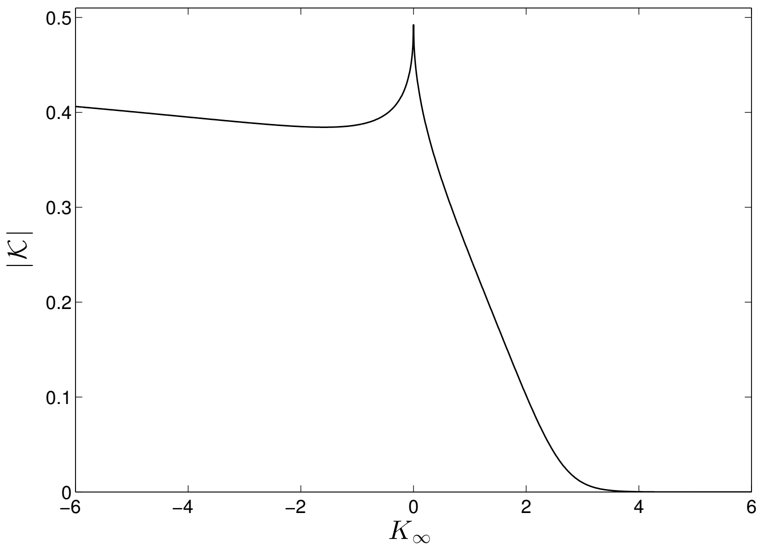

Figure 2.10: Modulus of the receptivity coefficient and its dependence on the Kármán-Guderley parameter for neutral points (ω_0, k_0).

varied the size of the domain, y, and the mesh size, N in order to find optimal values. The results presented here were obtained by setting the domain size to 10 and the mesh size to 100.

2.7 Discussion of the results

This study have shown that in the transonic regime the receptivity coefficient depends not only on the initial frequency of the perturbations, as it was in the case of the subsonic flow (see Ruban, 1984), it also depends on the free-stream Mach number. The receptivity coefficient is complex quantity and thus may be represented in the exponential form, $\mathcal{K} = |\mathcal{K}|e^{i\Phi}$. Results of the calculation of the receptivity coefficient are presented in Figure 2.9, where Figure 2.9(a) shows the modulus of the receptivity coefficient and its argument is shown in Figure 2.9(b). Figure 2.10 shows the modulus of the receptivity coefficient dependence on the Kármán-Guderley parameter for neutral state of the Tollmien-Schlichting wave with parameters (ω_0, k_0).

It is observed that the maximum value for the receptivity coefficient (see Figure 2.10) is achieved when the Kármán-Guderley parameter, K_∞, tends to zero, or equivalently the Mach number is one. This point of the maximum value in undefined in the scope of the theory presented here as it is not valid when the Kármán-Guderley parameter is equal to zero. Thus in order to find the correct value for the maximum it is necessary to consider higher order approximations around this point. Increasing the Kármán-Guderley parameter we observe that the modulus of the receptivity coefficient decreases rapidly and calculations show that when K_∞ reaches 5 the receptivity coefficient practically becomes zero. On the another hand when the Kármán-Guderley parameter becomes negative the modulus of the receptivity coefficient at the first instance decreases and then starts to grow. Further decrease in K_∞ is not practical as from the assumptions made at the beginning it should be an order of one quantity.

From Figure 2.9(a) it can be seen that, when the frequency increases, the receptivity coefficient tends to a certain value, which increasing the Kármán-Guderley parameter decreases. Similar behaviour may be observed for the argument of the receptivity coefficient (see Figure 2.9(b)), where increasing the frequency of the acoustic perturbations, the phase levels at a certain value close to zero.

3 Receptivity of the Boundary Layer to an Oblique Acoustic Wave Traveling Upstream in Transonic flow

3.1 Introduction

In Subsection 2.3.1 it was established that in the transonic flow regime, $M^2 - 1 = O(Re^{-\frac{1}{9}})$, the governing equation in the unsteady potential flow describes two distinct waves. Previous chapter considered only the “fast” wave and its interaction with the isolated wall roughness. In this chapter we study the generation of Tollmien-Schlichting waves in the boundary-layer on a flat plate due to the “slow”, upstream-travelling external acoustic wave, which is considered to be an oblique wave. As before, in order to satisfy the resonance conditions it is necessary to introduce a wall roughness on the plate surface, which produces steady perturbations of the boundary layer. These perturbations induce viscous-inviscid interaction between the boundary-layer and the outer regions. The inviscid flow and the interaction region can be modelled by a triple-deck structure, where the characteristic features of unsteady transonic flow can be taken into account.

The layout of this chapter follows the layout of the previous chapter, where the mathematical formulation of the problem is given in Section 3.2. The flow in vicinity of the wall roughness is described by the triple-deck theory and presented in Section 3.3. It is followed by formulation of the viscous-inviscid interaction problem, which is split into steady and unsteady problems, Section 3.4. Section 3.6 concludes the analysis of the problem by showing that in the vicinity of the roughness the flow perturbation field is composed of discrete and continuous spectrums. It is shown that the continuous spectrum perturbations decay downstream of the roughness uniformly with respect to the frequency of oscillations, and so do all the perturbations of the discrete spectrum except the one which represents the Tollmien-Schlichting wave. The amplitude of the latter is found in an analytic form.

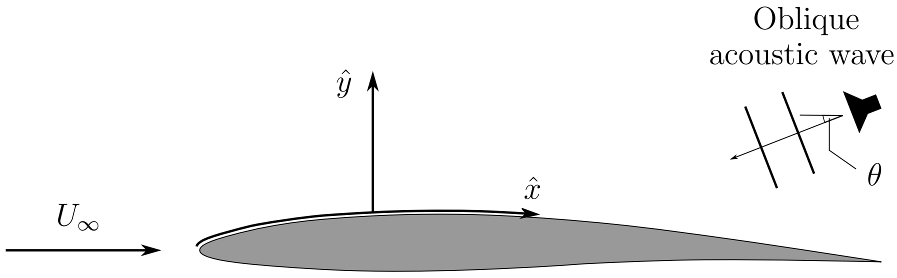

Figure 3.1: Layout of the problem

3.2 Problem Formulation

Consider an aerofoil placed in a uniform two-dimensional flow of a perfect gas with an oblique plane acoustic wave as shown in Figure 3.1. In order to generalise the analysis in what follows we shall use the body-fitted curvilinear orthogonal coordinate system $(\hat{x}, \hat{y})$ with $\hat{x}$ measured along the aerofoil surface from its leading edge, and $\hat{y}$ in the normal direction. The aerofoil contour curvature is assumed to be small. The dimensional velocity components are denoted $(\hat{u}, \hat{v})$ and time by $\hat{t}$. In addition, the gas density is denoted by $\hat{\rho}$, the pressure $\hat{p}$, the enthalpy $\hat{h}$ and the dynamic viscosity coefficient $\hat{\mu}$.

The flow analysis will be conducted using the non-dimensional compressible Navier-Stokes equations; see Appendix A.1. As in Chapter 2, we will conduct the asymptotic analysis of theNavier-Stokes equations (A.6) using the limits

$$Re \to \infty, \qquad Q_\infty = O(1), \tag{3.1a,b}$$

where Q_∞ is the Kármán-Guderley parameter. Here, in contrast to the previous problem 2, we will be consider only negative values of the Q_∞.

Analysis of the steady flow in the compressible boundary layer is presented in Appendix A.2

3.3 Formulation of the triple-deck problem

This chapter covers the interaction process of the roughness in the boundary layer with an upstream propagating acoustic wave. The analysis is performed under the assumption that the frequency of the acoustic wave, $\omega_* = O\left(Re^{2/9}\right)$, and the Kármán-Guderley parameter, Q_∞, is an order one quantity. Further, bases on the result obtained in Subsection 2.3.1, this leads to the conclusion that in the presence of the acoustic per-

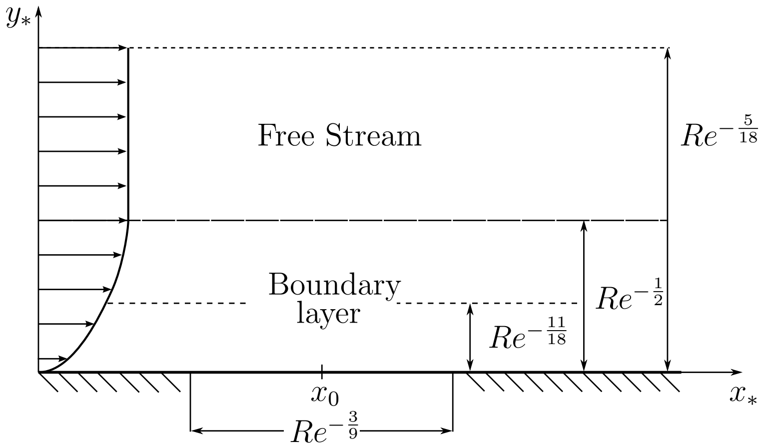

Figure 3.2: Triple-deck structure in transonic flow.

turbations the governing equation in the potential flow describes two waves. In this problem we consider only the "slow" wave, which propagates with the phase velocity of order $Re^{-1/9}$ and may change propagation direction depending on the Mach number of the flow. The wavenumber of the "slow" wave now is of $O\left(Re^{3/9}\right)$ quantity, which is a significant difference compared to the problem analysed in the Chapter 2. In this situation the wavelength already has required scale and does not require shortening as it was for the previous problem.

In addition it is assumed that the shape of the roughness is given by the equation

$$y_* = hRe^{-\frac{11}{18}}\bar{G}\left(\frac{x_* - x_0}{Re^{-3/9}}\right). \tag{3.2}$$

Consequently the streamwise extent of the roughness is assumed to be $O\left(Re^{-3/9}\right)$ quantity, which will allow us to satisfy the resonance conditions between the external perturbations and the Tollmien-Schlichting wave.

Under these conditions it is known that the process is described by the transonic version of the triple-deck theory: see Figure 3.2, see Timoshin (1990) or Bowles & Smith (1993).

3.3.1 Viscous sublayer

The characteristic thickness of the viscous sublayer is an $O\left(Re^{-11/18}\right)$ quantity, so that it occupies an $O\left(Re^{-1/9}\right)$ portion of the boundary layer. Correspondingly, the flow velocity in this region is estimated to be an $O\left(Re^{-1/9}\right)$ quantity, relative to the free-stream velocity. We shall assume that the roughness height parameter, h, and acoustic wave amplitude, σ, are small. Under these assumptions the solution of the Navier-Stokes equations (A.6) in the viscous sublayer is sought in the form

$$u_* = Re^{-\frac{1}{9}} \left\{ \tau_0 \tilde{y} + h\breve{u}_r\left(\tilde{x}, \tilde{y}\right) + \sigma \breve{u}_a\left(\tilde{t}, \tilde{x}, \tilde{y}\right) + h\sigma \breve{u}_i\left(\tilde{t}, \tilde{x}, \tilde{y}\right) \right\} + \cdots, \tag{3.3a}$$

$$v_* = Re^{-\frac{7}{18}} \left\{ h\breve{v}_r\left(\tilde{x}, \tilde{y}\right) + \sigma \breve{v}_a\left(\tilde{t}, \tilde{x}, \tilde{y}\right) + h\sigma \breve{v}_i\left(\tilde{t}, \tilde{x}, \tilde{y}\right) \right\} + \cdots, \tag{3.3b}$$

$$p_* = Re^{-\frac{2}{9}} \left\{ h\breve{p}_r\left(\tilde{x}, \tilde{y}\right) + \sigma \breve{p}_a\left(\tilde{t}, \tilde{x}, \tilde{y}\right) + h\sigma \breve{p}_i\left(\tilde{t}, \tilde{x}, \tilde{y}\right) \right\} + \cdots, \tag{3.3c}$$

$$h_* = h_w + \cdots, \tag{3.3d}$$

$$\rho_* = \rho_w + \cdots, \tag{3.3e}$$

$$\mu_* = \mu_w + \cdots. \tag{3.3f}$$

Here $\tau_0 = \lambda \rho_w$ denotes the value of function (A.34) at $x_* = x_0$.

The independent variables in the region are scaled as

$$t_* = Re^{-\frac{2}{9}}\tilde{t}, \qquad x_* = x_0 + Re^{-\frac{3}{9}}\tilde{x}, \qquad y_* = Re^{-\frac{11}{18}}\tilde{y}. \tag{3.4a-c}$$

The structure of the solution (3.3) may be explained as follows. We start with the asymptotic expansion for the longitudinal velocity component, u_*. The leading order term, $\tau_0 \tilde{y}$, in this expansion represents the unperturbed steady boundary layer, and would be the only term if neither the roughness nor the acoustic wave were present. The next two terms, $h\breve{u}_r\left(\tilde{x}, \tilde{y}\right)$ and $\sigma \breve{u}_a\left(\tilde{t}, \tilde{x}, \tilde{y}\right)$, represent the perturbations produced by the roughness and the acoustic wave, respectively. Finally, the fourth term, $h\sigma \breve{u}_i\left(\tilde{t}, \tilde{x}, \tilde{y}\right)$, represents the perturbations produced in the boundary layer due to the interaction of the acoustic wave with the steady flow field around the roughness.

Substitution of (3.3) and (3.4) into (A.6) results, for $O\left(hRe^{1/9}\right)$ terms, in similar equations to (2.39) describing the steady flow past the roughness.

$$\rho_w \tau_0 \left(\tilde{y} \frac{\partial \breve{u}_r}{\partial \tilde{x}} + \breve{v}_r \right) = -\frac{\partial \breve{p}_r}{\partial \tilde{x}} + \mu_w \frac{\partial^2 \breve{u}_r}{\partial \tilde{y}^2}, \tag{3.5a}$$

$$\frac{\partial \breve{u}_r}{\partial \tilde{x}} + \frac{\partial \breve{v}_r}{\partial \tilde{y}} = 0. \tag{3.5b}$$

The difference from (2.39) arise because we have not performed the affine transformation yet. This set of equations is subject to the no-slip condition on the surface of the roughness and the condition at the outer edge of the region,

$$\breve{u}_r = \breve{v}_r = 0 \qquad \text{at} \qquad \tilde{y} = 0, \tag{3.6a}$$
$$\breve{u}_r = \breve{A}_r\left(\tilde{x}\right) \qquad \text{as} \qquad \tilde{y} \to \infty, \tag{3.6b}$$
$$\breve{u}_r = 0 \qquad \text{as} \qquad \tilde{x} \to -\infty, \tag{3.6c}$$

where $\breve{A}_r(\tilde{x})$ is unknown displacement function.

In the next order approximation, $\sigma Re^{1/9}$, the governing equations describe the Stokes layer produced by the acoustic wave,

$$\rho_w\left(\frac{\partial \breve{u}_a}{\partial \tilde{t}} + \tau_0\tilde{y}\frac{\partial \breve{u}_a}{\partial \tilde{x}} + \tau_0\breve{v}_a\right) = -\frac{\partial \breve{p}_a}{\partial \tilde{x}} + \mu_w\frac{\partial^2 \breve{u}_a}{\partial \tilde{y}^2}, \tag{3.7a}$$
$$\frac{\partial \breve{u}_a}{\partial \tilde{x}} + \frac{\partial \breve{v}_a}{\partial \tilde{y}} = 0. \tag{3.7b}$$

These have to be solved subject the boundary conditions

$$\breve{u}_a = \breve{v}_a = 0 \qquad \text{at} \qquad \tilde{y} = 0, \tag{3.8a}$$
$$\breve{u}_a = \breve{A}_a\left(\tilde{t}, \tilde{x}\right) \qquad \text{as} \qquad \tilde{y} \to \infty. \tag{3.8b}$$
$$\breve{u}_a = 0 \qquad \text{as} \qquad \tilde{x} \to -\infty, \tag{3.8c}$$

Here we impose the no-slip condition at the surface and condition at the outer edge of the region. As before, the displacement function $\breve{A}_a(\tilde{t}, \tilde{x})$ is unknown at the moment.

The third set of equations, which describe the interaction between the wall roughness and the acoustic wave, is obtained retaining $O\left(h\sigma Re^{1/9}\right)$ terms, after substituting (3.3) and (3.4) into (A.6),

$$\begin{aligned}\rho_w\left(\frac{\partial \breve{u}_i}{\partial \tilde{t}} + \tau_0\tilde{y}\frac{\partial \breve{u}_i}{\partial \tilde{x}} + \tau_0\breve{v}_i\right) &= -\frac{\partial \breve{p}_i}{\partial \tilde{x}} + \mu_w\frac{\partial^2 \breve{u}_i}{\partial \tilde{y}^2} \\ &\quad - \rho_w\left(\frac{\partial\left[\breve{u}_a\breve{u}_r\right]}{\partial \tilde{x}} + \breve{v}_a\frac{\partial \breve{u}_r}{\partial \tilde{y}} + \breve{v}_r\frac{\partial \breve{u}_a}{\partial \tilde{y}}\right),\end{aligned} \tag{3.9a}$$
$$\frac{\partial \breve{u}_i}{\partial \tilde{x}} + \frac{\partial \breve{v}_i}{\partial \tilde{y}} = 0. \tag{3.9b}$$

The boundary conditions are

$$\breve{u}_i = \breve{v}_i = 0 \qquad \text{at} \qquad \tilde{y} = 0, \tag{3.10a}$$
$$\breve{u}_i = \breve{A}_i\left(\tilde{t}, \tilde{x}\right) \qquad \text{as} \qquad \tilde{y} \to \infty, \tag{3.10b}$$
$$\breve{u}_i = 0 \qquad \text{as} \qquad \tilde{x} \to -\infty, \tag{3.10c}$$

where $\breve{A}_i\left(\tilde{t},\tilde{x}\right)$ is unknown displacement function.

Note that comparing (3.9) to (2.64), we can see that the in this problem governing equations contain extra two terms. The first involves perturbation in wall normal direction, $\breve{v}_a$ and the other a product of the steady perturbation, caused by the wall roughness, and a gradient of the perturbation in the Stokes layer caused by the acoustic perturbations in the streamwise direction.

In all approximations the pressure does not change across the boundary layer,

$$\frac{\partial \breve{p}_a}{\partial \breve{y}} = \frac{\partial \breve{p}_r}{\partial \breve{y}} = \frac{\partial \breve{p}_i}{\partial \breve{y}} = 0, \tag{3.11}$$

which may be obtained from the lateral momentum equation (A.6b).

3.3.2 Main part of the boundary layer

The solution in the main part of the boundary layer is sought in the form

$$u_* = U_0(\tilde{x}_0, Y) + Re^{-\frac{1}{9}}\left\{h\breve{u}_r(\tilde{x},Y) + \sigma\breve{u}_a(\tilde{t},\tilde{x},Y) + h\sigma\breve{u}_i(\tilde{t},\tilde{x},Y)\right\} + \cdots, \tag{3.12a}$$

$$v_* = Re^{-\frac{5}{18}}\left\{h\breve{v}_r(\tilde{x},Y) + \sigma\breve{v}_a(\tilde{t},\tilde{x},Y) + h\sigma\breve{v}_i(\tilde{t},\tilde{x},Y)\right\} + \cdots, \tag{3.12b}$$

$$p_* = Re^{-\frac{2}{9}}\left\{h\breve{p}_r(\tilde{x},Y) + \sigma\breve{p}_a(\tilde{t},\tilde{x},Y) + h\sigma\breve{p}_i(\tilde{t},\tilde{x},Y)\right\} + \cdots, \tag{3.12c}$$

$$\rho_* = R_0(\tilde{x}_0, Y) + Re^{-\frac{1}{9}}\left\{h\breve{\rho}_r(\tilde{x},Y) + \sigma\breve{\rho}_a(\tilde{t},\tilde{x},Y) + h\sigma\breve{\rho}_i(\tilde{t},\tilde{x},Y)\right\} + \cdots, \tag{3.12d}$$

$$h_* = H_0(\tilde{x}_0, Y) + Re^{-\frac{1}{9}}\left\{h\breve{h}_r(\tilde{x},Y) + \sigma\breve{h}_a(\tilde{t},\tilde{x},Y) + h\sigma\breve{h}_i(\tilde{t},\tilde{x},Y)\right\} + \cdots, \tag{3.12e}$$

$$\mu_* = \mu_0(\tilde{x}_0, Y) + Re^{-\frac{1}{9}}\left\{h\breve{\mu}_r(\tilde{x},Y) + \sigma\breve{\mu}_a(\tilde{t},\tilde{x},Y) + h\sigma\breve{\mu}_i(\tilde{t},\tilde{x},Y)\right\} + \cdots, \tag{3.12f}$$

Substituting expressions (3.12) into the Navier-Stokes equations and retaining terms of order $hRe^{2/9}$, we obtain

$$U_0\frac{\partial \breve{u}_r}{\partial \tilde{x}} + \breve{v}_r\frac{dU_0}{dY} = 0, \tag{3.13a}$$

$$U_0\frac{\partial \breve{\rho}_r}{\partial \tilde{x}} + \breve{v}_r\frac{dR_0}{dY} = 0, \tag{3.13b}$$

$$R_0\frac{\partial \breve{u}_r}{\partial \tilde{x}} + U_0\frac{\partial \breve{\rho}_r}{\partial \tilde{x}} + \frac{\partial (R_0\breve{v}_r)}{\partial Y} = 0. \tag{3.13c}$$

The solution of this set of equations may be found by matching the slope angles, ϑ, of the streamlines in the viscous sublayer and the main part of the boundary layer. It follows that solution is

$$\breve{u}_r = \breve{A}_r\frac{dU_0}{dY}, \qquad \breve{v}_r = -U_0\frac{d\breve{A}_r}{d\tilde{x}}, \qquad \breve{\rho}_r = \breve{A}_r\frac{dR_0}{dY}, \tag{3.14a-c}$$

Retaining order $\sigma Re^{2/9}$ and $h\sigma Re^{2/9}$ terms we obtain similar equations to (3.13), but for variables describing the acoustic wave propagation in the main part of the boundary layer and interaction between the roughness and the acoustic wave, respectively. The solution of these equations may be written as

$$\breve{u}_j = \breve{A}_j \frac{dU_0}{dY}, \qquad \breve{v}_j = -U_0 \frac{\partial \breve{A}_j}{\partial \tilde{x}}, \qquad \breve{\rho}_j = \breve{A}_j \frac{dR_0}{dY}, \tag{3.15a-c}$$

where j is a in the case of the acoustic wave problem and i for the interaction problem.

These equations are written in the body-fitted coordinates with x_* lying on the roughness surface. In the upper deck the flow analysis will be conducted in coordinates with the x_*-axis following the body contour without the roughness. Therefore, performing the matching of the streamlines slopes in the main deck and upper deck, we need to incorporate the slope of the body roughness. Differentiating (3.2) yields

$$\frac{dy_*}{dx_*} = hRe^{-\frac{5}{18}} \frac{d\bar{G}}{d\tilde{x}}. \tag{3.16}$$

From (3.12) and (3.14)-(3.16) follows that the slope of the steamlines in the main part of the boundary layer is written as

$$\vartheta = \frac{v_*}{u_*} = Re^{-\frac{5}{18}} \left[h \left(\frac{d\bar{G}}{d\tilde{x}} - \frac{d\breve{A}_r}{d\tilde{x}} \right) - \sigma \frac{\partial \breve{A}_a}{\partial \tilde{x}} - h\sigma \frac{\partial \breve{A}_i}{\partial \tilde{x}} \right] + \dots. \tag{3.17}$$

This will allow us to deduce the boundary conditions for the upper deck lower edge.

3.3.3 Upper Deck

In the upper deck, the solution is represented in the form

$$\begin{aligned} u_* = 1 &+ Re^{-\frac{2}{9}} \left\{ h\tilde{u}_r(\tilde{x},\bar{y}) + \sigma\tilde{u}_a(\tilde{t},\tilde{x},\bar{y}) + h\sigma\tilde{u}_i(\tilde{t},\tilde{x},\bar{y}) \right\} \\ &+ Re^{-\frac{3}{9}} \left\{ h\tilde{u}'_r(\tilde{x},\bar{y}) + \sigma\tilde{u}'_a(\tilde{t},\tilde{x},\bar{y}) + h\sigma\tilde{u}'_i(\tilde{t},\tilde{x},\bar{y}) \right\} + \cdots, \end{aligned} \tag{3.18a}$$

$$\begin{aligned} v_* = Re^{-\frac{5}{18}} &\left\{ h\tilde{v}_r(\tilde{x},\bar{y}) + \sigma\tilde{v}_a(\tilde{t},\tilde{x},\bar{y}) + h\sigma\tilde{v}_i(\tilde{t},\tilde{x},\bar{y}) \right\} \\ &+ Re^{-\frac{7}{18}} \left\{ h\tilde{v}'_r(\tilde{x},\bar{y}) + \sigma\tilde{v}'_a(\tilde{t},\tilde{x},\bar{y}) + h\sigma\tilde{v}'_i(\tilde{t},\tilde{x},\bar{y}) \right\} + \cdots, \end{aligned} \tag{3.18b}$$

$$\begin{aligned} p_* = Re^{-\frac{2}{9}} &\left\{ h\tilde{p}_r(\tilde{x},\bar{y}) + \sigma\tilde{p}_a(\tilde{t},\tilde{x},\bar{y}) + h\sigma\tilde{p}_i(\tilde{t},\tilde{x},\bar{y}) \right\} \\ &+ Re^{-\frac{3}{9}} \left\{ h\tilde{p}'_r(\tilde{x},\bar{y}) + \sigma\tilde{p}'_a(\tilde{t},\tilde{x},\bar{y}) + h\sigma\tilde{p}'_i(\tilde{t},\tilde{x},\bar{y}) \right\} + \cdots, \end{aligned} \tag{3.18c}$$

$$\begin{aligned} \rho_* = 1 &+ Re^{-\frac{2}{9}} \left\{ h\tilde{\rho}_r(\tilde{x},\bar{y}) + \sigma\tilde{\rho}_a(\tilde{t},\tilde{x},\bar{y}) + h\sigma\tilde{\rho}_i(\tilde{t},\tilde{x},\bar{y}) \right\} \\ &+ Re^{-\frac{3}{9}} \left\{ h\tilde{\rho}'_r(\tilde{x},\bar{y}) + \sigma\tilde{\rho}'_a(\tilde{t},\tilde{x},\bar{y}) + h\sigma\tilde{\rho}'_i(\tilde{t},\tilde{x},\bar{y}) \right\} + \cdots, \end{aligned} \tag{3.18d}$$

where the independent variables are defined as

$$t_* = Re^{-\frac{2}{9}}\tilde{t}, \qquad x_* = x_0 + Re^{-\frac{3}{9}}\tilde{x}, \qquad y_* = Re^{-\frac{5}{18}}\bar{y}. \tag{3.19a-c}$$

Substitution of (3.18) into the Navier-Stokes equations and working with the leading order terms results in the following equations for the steady perturbations

$$\tilde{p}_r = \tilde{\rho}_r = -\tilde{u}_r, \qquad \frac{\partial \tilde{v}_r}{\partial \tilde{x}} = -\frac{\partial \tilde{p}_r}{\partial \bar{y}}, \tag{3.20a,b}$$

These expressions could be used to determine $\tilde{u}_r$, $\tilde{v}_r$, $\tilde{\rho}_r$, if $\tilde{p}_r$ was known. In order to deduce an equation for the pressure we need to analyse the equations for the next order terms

$$\frac{\partial \tilde{u}_r'}{\partial \tilde{x}} = -\frac{\partial \tilde{p}_r'}{\partial \tilde{x}}, \tag{3.21a}$$

$$\frac{\partial \tilde{v}_r}{\partial \bar{y}} + \frac{\partial \tilde{u}_r'}{\partial \tilde{x}} + \frac{\partial \tilde{\rho}_r'}{\partial \tilde{x}} = 0, \tag{3.21b}$$

$$\frac{\partial \tilde{\rho}_r'}{\partial \tilde{x}} + Q_\infty \frac{\partial \tilde{\rho}_r}{\partial \tilde{x}} = \frac{\partial \tilde{p}_r'}{\partial \tilde{x}}. \tag{3.21c}$$

Using (3.20) the set of equations (3.21) may be reduced to a single equation for the pressure

$$Q_\infty \frac{\partial^2 \tilde{p}_r}{\partial \tilde{x}^2} - \frac{\partial^2 \tilde{p}_r}{\partial \bar{y}^2} = 0. \tag{3.22}$$

The slope angle of the streamlines in the main part of the boundary layer is given by (3.17). The corresponding equation in the upper deck is deduced using the asymptotic expansions for v_* and u_* in (3.18), which lead to

$$\frac{v_*}{u_*} = Re^{-\frac{5}{18}}\left\{h\tilde{v}_r + \sigma\tilde{v}_a + h\sigma\tilde{v}_i\right\} + \dots. \tag{3.23}$$

This allows us to deduce the boundary condition on the lower edge of the region. Matching the slope angles of the streamlines (3.17) and (3.23), and setting $\bar{y} = 0$, from (3.20) we obtain

$$\frac{\partial \tilde{p}_r}{\partial \bar{y}} = \frac{d^2 \breve{A}_r}{d\tilde{x}^2} - \frac{d^2 \bar{G}}{d\tilde{x}^2} \qquad \text{at} \qquad \bar{y} = 0. \tag{3.24a}$$

The second boundary condition is the attenuation condition

$$\tilde{p}_r(\tilde{x}, \bar{y}) \to 0 \qquad \text{as} \qquad \tilde{x}^2 + \bar{y}^2 \to \infty. \tag{3.24b}$$

Similarly, we can deduce that for the unsteady acoustic perturbations we have the two-dimensional small perturbation equation

$$2\frac{\partial^2 \tilde{p}_a}{\partial \tilde{x}\partial \tilde{t}} + Q_\infty \frac{\partial^2 \tilde{p}_a}{\partial \tilde{x}^2} - \frac{\partial^2 \tilde{p}_a}{\partial \bar{y}^2} = 0. \tag{3.25}$$

The boundary condition at the bottom of the region is

$$\frac{\partial \tilde{p}_a}{\partial \bar{y}} = \frac{d^2 \breve{A}_a}{d\tilde{x}^2} \qquad \text{at} \qquad \bar{y} = 0. \tag{3.26}$$

The second boundary condition specifies the acoustic field impinging upon the boundary layer. In what follows we shall assume that the boundary layer is exposed to a simple acoustic wave, which may be represented in the form

$$\tilde{p}_a(\tilde{t}, \tilde{x}, \bar{y}) = f\left(\tilde{\omega}\tilde{t} + \tilde{k}\tilde{x} + \tilde{\beta}\bar{y}\right), \tag{3.27}$$

where $\tilde{k}$ and $\tilde{\beta}$ are characteristic wavenumbers in streamwise and normal directions, respectively.

Substitution of (3.27) into (3.25) leads to

$$Q_\infty \tilde{k}^2 + 2\tilde{\omega}\tilde{k} - \tilde{\beta}^2 = 0. \tag{3.28}$$

If we assume that the frequency, $\tilde{\omega}$, and the wavenumber in the normal direction, $\tilde{\beta}$, are given, then the equation above can be used to determine the streamwise wavenumber

$$\tilde{k} = -\frac{\tilde{\omega}}{Q_\infty} \pm \frac{\sqrt{\tilde{\omega}^2 + Q_\infty \tilde{\beta}^2}}{Q_\infty}. \tag{3.29}$$

There are two pairs of solutions representing the acoustic waves with the phase speeds in the streamwise direction given as

$$c_x = -\frac{\tilde{\omega}}{\tilde{k}} = \frac{\tilde{\omega}\, Q_\infty}{\tilde{\omega} \mp \sqrt{\omega^2 + Q_\infty \tilde{\beta}^2}}. \tag{3.30}$$

In the following analysis we assume that the frequency is positive and the acoustic wave propagates against the flow, that is $Q_\infty < 0$ (subsonic flow regime). This means that in (3.29) we have to choose a minus sign in front of the square-root.

$$\tilde{k} = -\frac{\tilde{\omega}}{Q_\infty} - \frac{\sqrt{\tilde{\omega}^2 + Q_\infty \tilde{\beta}^2}}{Q_\infty}. \tag{3.31}$$

Consequently, it can be seen that, for relation (3.31) to be valid in the particular condition the expression under the square-root should remain positive, and therefore setting a limit for the wavenumber in the normal direction

$$-\frac{\tilde{\omega}}{\sqrt{|Q_\infty|}} \leq \tilde{\beta} \leq \frac{\tilde{\omega}}{\sqrt{|Q_\infty|}}. \tag{3.32}$$

In addition, note that positive values of $\tilde{\beta}$ correspond to an incident wave, and negative values correspond to a reflected wave.

Keeping this in mind and simplifying (3.27) further, we assume that the solution to (3.25) can be written as

$$\tilde{p}_a = \tilde{P}_0 \left(e^{i\left(\tilde{\omega}\tilde{t} + \tilde{k}\tilde{x} + |\tilde{\beta}|\bar{y}\right)} + \varkappa e^{i\left(\tilde{\omega}\tilde{t} + \tilde{k}\tilde{x} - |\tilde{\beta}|\bar{y}\right)} \right) + c.c.. \tag{3.33}$$

Here both $\tilde{\omega}$ and $\tilde{\beta}$ are assumed given and positive. The first term in (3.33) represents an incident acoustic wave with amplitude $\tilde{P}_0$ which is assumed to be known. The second term represents a reflected wave with an amplitude $\varkappa\tilde{P}_0$, where the proportionality coefficient $\varkappa$ remains unknown and is found by solving the viscous-inviscid interaction problem.

Similarly as for the previous order of approximation, the unsteady interaction terms may be described by a single equation

$$2\frac{\partial^2 \tilde{p}_i}{\partial \tilde{x} \partial \tilde{t}} + Q_\infty \frac{\partial^2 \tilde{p}_i}{\partial \tilde{x}^2} - \frac{\partial^2 \tilde{p}_i}{\partial \bar{y}^2} = 0, \tag{3.34}$$

which should be solved with

$$\frac{\partial \tilde{p}_i}{\partial \bar{y}} = \frac{d^2 \breve{A}_i}{d\tilde{x}^2} \qquad \text{at} \qquad \bar{y} = 0, \tag{3.35a}$$

and

$$\tilde{p}_i(\tilde{t}, \tilde{x}, \bar{y}) \to 0 \qquad \text{as} \qquad \tilde{x}^2 + \bar{y}^2 \to \infty. \tag{3.35b}$$

This concludes the formulation of the problem. Further analysis is devoted to solving the interaction problem, which involves the analysis of three seemingly unrelated problems. The first problem is due to the flow interaction with the wall roughness. The second is the acoustic wave interaction with the flow and the third is the desired problem, which uses results obtained from the two earlier problems.

3.4 Viscous-inviscid interaction problem

We have found that in order to describe the steady flow past the surface roughness one has to solve the equations (3.5, 3.6) governing the flow in the viscous sublayer coupled with the equations (3.22, 3.24) governing the flow in the upper deck. Similarly for the unsteady acoustic problem (3.7, 3.8, 3.26, 3.33) and the interaction problem (3.9, 3.10, 3.34, 3.35). To reduce the number of variables, we shall write all sets of equations in canonical form, using the following affine transformation

$$\tilde{t} = \frac{t}{(2^2\rho_w^{-1}\mu_w^5\tau_0^{14})^{\frac{1}{9}}}, \qquad \tilde{x} = \frac{x}{(2^3\rho_w^3\mu_w^3\tau_0^{12})^{\frac{1}{9}}}, \qquad \tilde{y} = \frac{y}{(2\rho_w^4\mu_w^{-2}\tau_0^7)^{\frac{1}{9}}}, \tag{3.36a-c}$$

$$\breve{v}_j = \frac{v_i}{\left(2^{-1}\rho_w^5\mu_w^{-7}\tau_0^{-7}\right)^{\frac{1}{9}}}, \qquad \breve{u}_j = \frac{u_i}{\left(2\rho_w^4\mu_w^{-2}\tau_0^{-2}\right)^{\frac{1}{9}}}, \qquad \breve{p}_j = \frac{p_i}{\left(2^2\rho_w^{-1}\mu_w^{-4}\tau_0^{-4}\right)^{\frac{1}{9}}}, \tag{3.36d-f}$$

$$\bar{y} = \frac{Y}{(2^7\rho_w\mu_w^4\tau_0^{13})^{\frac{1}{9}}}, \qquad Q_\infty = \frac{K_\infty}{\left(2^{-8}\rho_w^4\mu_w^{-2}\tau_0^{-2}\right)^{\frac{1}{9}}}, \qquad \tilde{p}_j = \frac{P_i}{\left(2^2\rho_w^{-1}\mu_w^{-4}\tau_0^{-4}\right)^{\frac{1}{9}}}, \tag{3.36g-i}$$

and

$$\bar{G} = \frac{F}{(2\rho_w^4\mu_w^{-2}\tau_0^7)^{\frac{1}{9}}}, \qquad \breve{A}_j = \frac{A_j}{(2\rho_w^4\mu_w^{-2}\tau_0^7)^{\frac{1}{9}}}. \tag{3.36j,k}$$

Here j can be r, a and i for steady, acoustic and interaction problem terms, respectively.

3.4.1 Steady problem

Substituting (3.36) into the steady flow problem (3.5, 3.6, 3.22, 3.24) reduces the viscous sublayer equations to

$$y\frac{\partial u_r}{\partial x} + v_r = -\frac{\partial p_r}{\partial x} + \frac{\partial^2 u_r}{\partial y^2}, \tag{3.37a}$$

$$\frac{\partial u_r}{\partial x} + \frac{\partial v_r}{\partial y} = 0, \tag{3.37b}$$

subject to

$$u_r = v_r = 0 \qquad \text{at} \qquad y = 0, \tag{3.38a}$$
$$u_r = A_r(x) \qquad \text{as} \qquad y \to \infty. \tag{3.38b}$$

The upper deck equation (3.22) becomes

$$K_\infty \frac{\partial^2 P_r}{\partial x^2} - \frac{\partial^2 P_r}{\partial Y^2} = 0, \tag{3.39}$$

with the boundary conditions

$$\frac{\partial P_r}{\partial Y} = \frac{d^2 A_r}{dx^2} - \frac{d^2 F}{dx^2} \qquad \text{at} \qquad Y = 0, \tag{3.40a}$$
$$P_r \to 0 \qquad \text{as} \qquad Y \to \infty. \tag{3.40b}$$

This problem, as expected, is exactly the same as described in Subsection 2.5.1.

3.4.2 Unsteady acoustic problem

Applying the affine transformation (3.36) to the unsteady acoustic problem, turns the viscous sublayer equations (3.7) into

$$\frac{\partial u_a}{\partial t} + y\frac{\partial u_a}{\partial x} + v_a = -\frac{\partial p_a}{\partial x} + \frac{\partial^2 u_a}{\partial y^2}, \tag{3.41a}$$
$$\frac{\partial u_a}{\partial x} + \frac{\partial v_a}{\partial y} = 0, \tag{3.41b}$$

Consequently, the boundary conditions (3.8) for these equations assume the form

$$u_a = v_a = 0 \qquad \text{at} \qquad y = 0, \tag{3.42a}$$
$$u_a = A_a(t, x) \qquad \text{as} \qquad y \to \infty. \tag{3.42b}$$

The solution of the corresponding upper deck problem (3.33) takes the form

$$P_a = P_0 \left(e^{i(\omega t + kx + |\beta| Y)} + \varkappa e^{i(\omega t + kx - |\beta| Y)} \right) + c.c., \tag{3.43}$$

where

$$\tilde{\omega} = \left(2^2 \rho_w^{-1} \mu_w^5 \tau_0^{14}\right)^{\frac{1}{9}} \omega, \qquad \tilde{k} = \left(2^3 \rho_w^3 \mu_w^3 \tau_0^{12}\right)^{\frac{1}{9}} k, \qquad \tilde{\beta} = \left(2^7 \rho_w \mu_w^4 \tau_0^{13}\right)^{\frac{1}{9}} \beta. \tag{3.44a-c}$$

and the amplitude is scaled as

$$\tilde{P}_0 = \frac{P_0}{\left(2^2 \rho_w^{-1} \mu_w^{-4} \tau_0^{-4}\right)^{\frac{1}{9}}}. \tag{3.44d}$$

The boundary condition at the bottom of the region (3.26) reduces to

$$\frac{\partial P_a}{\partial Y} = \frac{\partial^2 A_a}{\partial x^2} \qquad \text{at} \qquad Y = 0. \tag{3.45}$$

3.4.3 Interaction problem

The viscous sublayer equations (3.9) in this problem reduces to

$$\frac{\partial u_i}{\partial t} + y\frac{\partial u_i}{\partial x} + v_i = -\frac{\partial p_i}{\partial x} + \frac{\partial^2 u_i}{\partial y^2} - H(t,x,y), \tag{3.46a}$$

$$\frac{\partial u_i}{\partial \tilde{x}} + \frac{\partial v_i}{\partial \tilde{y}} = 0, \tag{3.46b}$$

where

$$H(t,x,y) = u_a\frac{\partial u_r}{\partial x} + u_r\frac{\partial u_a}{\partial x} + v_a\frac{\partial u_r}{\partial y} + v_r\frac{\partial u_a}{\partial y}. \tag{3.46c}$$

The boundary conditions (3.10) become

$$u_i = v_i = 0 \qquad \text{at} \qquad y = 0, \tag{3.47a}$$

$$u_i = A_i\,(t,x) \qquad \text{as} \qquad y \to \infty. \tag{3.47b}$$

The corresponding upper deck problem (3.34, 3.35) is written as

$$\frac{\partial^2 P_i}{\partial x \partial t} + K_\infty \frac{\partial^2 P_i}{\partial x^2} - \frac{\partial^2 P_i}{\partial Y^2} = 0, \tag{3.48}$$

and

$$\frac{\partial P_i}{\partial Y} = \frac{\partial^2 A_i}{\partial x^2} \qquad \text{at} \qquad Y = 0, \tag{3.49a}$$

$$P_i \to 0 \qquad \text{as} \qquad x^2 + Y^2 \to \infty. \tag{3.49b}$$

3.5 Solution of the viscous-inviscid interaction problem

The steady, unsteady acoustic and interaction problems can be solved by means of the Fourier transform technique.

The solution of the steady problem (3.37-3.40) has been described in detail in Chapter 2, therefore only the final solution is presented here:

$$\bar{u}_r = \bar{F}(k)\Phi\left(z;k,K_\infty\right) \qquad \text{and} \qquad \bar{v}_r = \bar{F}(k)\Psi\left(z;k,K_\infty\right), \tag{3.50a,b}$$

where

$$\Phi\left(z;k,K_\infty\right) = \frac{3(ik)^{\frac{1}{3}}|k|}{(ik)^{\frac{1}{3}}|k| - 3Ai'(0)|K_\infty|^{\frac{1}{2}}} \int\limits_0^z Ai(s')\,ds', \tag{3.51a}$$

$$\Psi\left(z;k,K_\infty\right) = -(ik)^{\frac{2}{3}} \int\limits_0^z \Phi\left(s;k,K_\infty\right)\,ds. \tag{3.51b}$$

Here "bar" denotes the Fourier transformed quantities and Ai is the Airy function.

3.5.1 Unsteady acoustic problem

The next problem looks at the unsteady acoustic perturbations. The analysis of this problem (3.41-3.45), similarly as for the steady problem, will allow us to deduce velocity perturbations in streamwise $\breve{u}_a$ and longitudinal $\breve{v}_a$ directions.

Solutions of the problem is sought in the form

$$\left(u_a, v_a, p_a, P_a, A_a\right) = \left(\bar{u}'_a, \bar{v}'_a, \bar{p}'_a, \bar{P}'_a, \bar{A}'_a\right) e^{i(\omega t + kx)} + c.c., \tag{3.52}$$

Substituting (3.52) into (3.43) yields the following expression for the pressure in the upper deck

$$\bar{P}'_a(k,Y) = P_0\left(e^{i|\beta|Y} + \varkappa e^{-i|\beta|Y}\right) + c.c.. \tag{3.53}$$

The boundary condition (3.45) at the bottom of the upper deck reduces to

$$\frac{d\bar{P}'_a}{dY} = -k^2\bar{A}'_a(k) \qquad \text{at} \qquad Y = 0. \tag{3.54}$$

Substituting (3.53) into (3.54) we find that the proportionality coefficient, $\varkappa$, is

$$\varkappa = 1 - i\frac{k^2}{|\beta|}\frac{\bar{A}_a'}{P_0}. \tag{3.55}$$

Returning back to the equations in the viscous sublayer and setting $Y = 0$ in (3.53) we deduce that the pressure in this region may be written as

$$\bar{p}_a'(k) = 2P_0 - i\frac{k^2}{|\beta|}\bar{A}_a'. \tag{3.56}$$

Using (3.52) in (3.41) turns the viscous sublayer problem into

$$i\left(\omega + ky\right)\bar{u}_a' + \bar{v}_a' = -ik\bar{p}_a' + \frac{d^2\bar{u}_a'}{dy^2}, \tag{3.57a}$$

$$ik\bar{u}_a' + \frac{d\bar{v}_a'}{dy} = 0, \tag{3.57b}$$

and

$$\bar{u}_a' = \bar{v}_a' = 0 \qquad \text{at} \quad y = 0, \tag{3.58a}$$

$$\frac{d^2\bar{u}_a'}{dy^2} = ik\left(2P_0 - i\frac{k^2}{|\beta|}\bar{A}_a'\right) \qquad \text{at} \quad y = 0, \tag{3.58b}$$

$$\bar{u}_a' = \bar{A}_a' \qquad \text{as} \quad y \to \infty. \tag{3.58c}$$

Differentiating (3.57a) with respect to y and using (3.57b) we obtain

$$\frac{d^3\bar{u}_a'}{dy^3} - i\left(\omega + ky\right)\frac{d\bar{u}_a'}{dy} = 0. \tag{3.59}$$

Now performing the change of variables

$$\zeta = \theta y + \zeta_0 \qquad \text{where} \qquad \theta = (ik)^{1/3}, \quad \zeta_0 = i\omega/(ik)^{2/3}, \tag{3.60}$$

reduces (3.59) to the Airy equation

$$\frac{d^3\bar{u}_a'}{d\zeta^3} - \zeta\frac{d\bar{u}_a'}{d\zeta} = 0. \tag{3.61}$$

The boundary conditions (3.58) are reduced to

$$\bar{u}'_a = \bar{v}'_a = 0 \qquad \text{at} \quad \zeta = \zeta_0, \tag{3.62a}$$
$$\frac{d^2\bar{u}'_a}{d\zeta^2} = (ik)^{\frac{1}{3}} \left(2P_0 - i\frac{k^2}{|\beta|}\bar{A}'_a\right) \qquad \text{at} \quad \zeta = \zeta_0, \tag{3.62b}$$
$$\bar{u}'_a = \bar{A}'_a \qquad \text{as} \quad \zeta \to \infty. \tag{3.62c}$$

The solution of the Airy equation, that does not grow exponentially as $\zeta \to \infty$, is written as

$$\frac{d\bar{u}'_a}{d\zeta} = C Ai(\zeta). \tag{3.63}$$

Subtituting (3.63) into (3.62b) we find that

$$(ik)^{\frac{2}{3}} C|\beta| Ai'(\zeta_0) = 2ik|\beta|P_0 + k^3\bar{A}'_a. \tag{3.64a}$$

Using (3.62c) we find that the second relation for C and $\bar{A}'_a$ is

$$C\int_{\zeta_0}^{\infty} Ai(s')\, ds' = \bar{A}'_a. \tag{3.64b}$$

Solving (3.64a) and (3.64b) for $\bar{A}'_a$ and C, we have

$$\bar{A}'_a = \frac{2ik|\beta|\int_{\zeta_0}^{\infty} Ai(s')\, ds'}{(ik)^{2/3}|\beta|Ai'(\zeta_0) - k^3\int_{\zeta_0}^{\infty} Ai(s')\, ds'}\, P_0, \tag{3.65a}$$
$$C = \frac{2ik|\beta|}{(ik)^{2/3}|\beta|Ai'(\zeta_0) - k^3\int_{\zeta_0}^{\infty} Ai(s')\, ds'}\, P_0, \tag{3.65b}$$

and thus from (3.57b), (3.63) and (3.65) it follows that

$$\bar{u}'_a = \phi\left(\zeta;\omega,\beta,K_\infty\right) P_0 \qquad \text{and} \qquad \bar{v}'_a = \psi\left(\zeta;\omega,\beta,K_\infty\right) P_0, \tag{3.66a,b}$$

where

$$\phi\left(\zeta;\omega,\beta,K_\infty\right) = \frac{2ik|\beta|}{(ik)^{2/3}|\beta|Ai'(\zeta_0) - k^3\int_{\zeta_0}^{\infty} Ai(s')\, ds'} \int_{\zeta_0}^{\zeta} Ai(s')\, ds', \tag{3.67a}$$

$$\psi\left(\zeta;\omega,\beta,K_\infty\right) = -(ik)^{\frac{2}{3}} \int_{\zeta_0}^{\zeta} \phi\left(s;\omega,\beta,K_\infty\right)\, ds. \tag{3.67b}$$

This concludes the analysis of the individual components, which influence the flow and the next problem will consider the interaction between these components.

3.5.2 Interaction problem

The solution of the problem of interaction between the acoustic wave and the surface roughness is sought in the time periodic form

$$(u_i, v_i, p_i, P_i, A_i, H) = (u_i', v_i', p_i', P_i', A_i', H')\, e^{i\omega t} + c.c., \tag{3.68}$$

Substituting (3.68) into the interaction problem (3.46-3.49) and performing the Fourier transform, leads to the equations in the upper deck to be written as

$$\frac{d^2 \bar{P}_i'}{dY^2} + \left(\omega k + k^2 K_\infty\right) \bar{P}_i' = 0, \tag{3.69}$$

subject to

$$\frac{\partial \bar{P}_i'}{\partial Y} = -k^2 \bar{A}_i'(k) \qquad \text{at} \qquad Y = 0, \tag{3.70a}$$

$$\bar{P}_i' \to 0 \qquad \text{as} \qquad Y \to \infty. \tag{3.70b}$$

The general solution of the equation (3.69) is

$$\bar{P}_i' = B_1 e^{i\sqrt{\omega k + k^2 K_\infty}\, Y} + B_2 e^{-i\sqrt{\omega k + k^2 K_\infty}\, Y}. \tag{3.71}$$

It can be seen that when the Kármán-Guderley parameter is negative, the expression under the square-root changes the sign at points $k_1 = 0$ and $k_2 = \omega/|K_\infty|$, which splits the solution into three regions. Keeping this in mind and satisfying the attenuation condition, we can write the solution in the form

$$\bar{P}_i' = B_*\, e^{i\Lambda Y}, \tag{3.72}$$

where

$$\Lambda = \begin{cases} |\omega k + k^2 K_\infty|^{\frac{1}{2}} & k \in \left(0, \dfrac{\omega}{|K_\infty|}\right) \\ i|\omega k + k^2 K_\infty|^{\frac{1}{2}} & k \in \left(-\infty, 0\right] \cup \left[\dfrac{\omega}{|K_\infty|}, \infty\right) \end{cases} \tag{3.73a,b}$$

Setting $Y = 0$ in (3.72) and make use of (3.70a) allows to obtain the Fourier transform of the pressure in the viscous sublayer

$$\bar{p}_i' = ik^2\Lambda^{-1}\bar{A}_i'(k). \tag{3.74}$$

Now we turn to the viscous problem (3.46), which is written in terms of the Fourier transform as

$$i(\omega + ky)\,\bar{u}_i' + \bar{v}_i' = -ik\bar{p}_i' + \frac{d^2\bar{u}_i'}{dy^2} - \bar{H}', \tag{3.75a}$$

$$ik\bar{u}_i' + \frac{d\bar{v}_i'}{dy} = 0. \tag{3.75b}$$

The boundary conditions (3.47) are

$$\bar{u}_i' = \bar{v}_i' = 0 \qquad \text{at} \qquad y = 0, \tag{3.76a}$$

$$\bar{u}_i' = \bar{A}_i'(k) \qquad \text{as} \qquad y \to \infty. \tag{3.76b}$$

Equations (3.75, 3.76) may be manipulated in the same way as the corresponding steady flow equations. We start by eliminating $\bar{v}_i'$, which is achieved through differentiation of (3.75a) with respect to y. This leads to the equation

$$i(\omega + ky)\frac{d\bar{u}_i'}{dy} = \frac{d^3\bar{u}_i'}{dy^3} - \frac{d\bar{H}'}{dy}. \tag{3.77}$$

Since we are dealing with a third order differential equation, an additional boundary condition for $\bar{u}_i'$ is required. It is obtained by setting $y = 0$ in (3.75a), and as $\bar{u}_i'$, $\bar{v}_i'$, $\bar{u}_a'$, $\bar{v}_a'$, $\bar{u}_r$ and $\bar{v}_r$ are all zero at $y = 0$, we obtain

$$\frac{d^2\bar{u}_i'}{dy^2} = ik\bar{p}_i' = -k^3\Lambda^{-1}\bar{A}_i'(k). \tag{3.78}$$

Performing the change of variables (3.60), the equation (3.77) assumes the form

$$\frac{d^3\bar{u}_i'}{d\zeta^3} - \zeta\frac{d\bar{u}_i'}{d\zeta} = (ik)^{-\frac{2}{3}}\frac{d\bar{H}'}{d\zeta}. \tag{3.79}$$

For the boundary conditions (3.76) and (3.78) we deduce

$$\bar{u}_i' = 0 \qquad \text{at} \qquad \zeta_0 = 0, \tag{3.80a}$$

$$\frac{d^2\bar{u}_i'}{d\zeta^2} = i(ik)^{1/3}k^2\Lambda^{-1}\bar{A}_i'(k) \qquad \text{at} \qquad \zeta_0 = 0, \tag{3.80b}$$

$$\bar{u}_i' = \bar{A}_i'(k) \qquad \text{as} \qquad \zeta \to \infty. \tag{3.80c}$$

The general solution of (3.79) is composition of the solution of the Airy equation and a particular solution, and can be written as

$$\frac{d\bar{u}_i'}{d\zeta} = CAi(\zeta) + \varphi(\zeta), \tag{3.81}$$

where function $\varphi(\zeta)$ is the solution of the following boundary-value problem,

$$\varphi'' - \zeta\varphi = (ik)^{-\frac{2}{3}}\frac{d\bar{H}'}{d\zeta}, \tag{3.82a}$$

$$\varphi'(\zeta_0) = 0, \tag{3.82b}$$

$$\varphi(\infty) = 0. \tag{3.82c}$$

Applying the boundary conditions (3.80) we obtain two equations relating the constant, C, and the Fourier transform of the displacement function. These are:

$$CAi'(\zeta_0) = i(ik)^{\frac{1}{3}}k^2\Lambda^{-1}\bar{A}_i', \qquad C\int_{\zeta_0}^{\infty} Ai(s')\,ds' + \int_{\zeta_0}^{\infty}\varphi(s')\,ds' = \bar{A}_i'. \tag{3.83a,b}$$

Eliminating C from (3.83), we deduce that the displacement function my be written as

$$\bar{A}_i' = \frac{Ai'(\zeta_0)\int_{\zeta_0}^{\infty}\varphi(s')\,ds'}{Ai'(\zeta_0) - i(ik)^{\frac{1}{3}}k^2\Lambda^{-1}\int_{\zeta_0}^{\infty}Ai(s')\,ds'}. \tag{3.84}$$

It remains to substitute the above equation into (3.74), which yields that the Fourier transform of the pressure in the viscous sublayer is

$$\bar{p}_i' = \frac{ik^2Ai'(\zeta_0)\int_{\zeta_0}^{\infty}\varphi(s')\,ds'}{\Lambda Ai'(\zeta_0) - i(ik)^{\frac{1}{3}}k^2\int_{\zeta_0}^{\infty}Ai(s')\,ds'}. \tag{3.85}$$

Comparing expression for the Fourier transform of the pressure (3.85) with the equivalent expression in the previous chapter (2.94), we see that the only difference arise in the numerator. In this problem the numerator does not contain the shape of the wall roughens explicitly as it is in (2.94), but now it is part of the function φ. As it is expected the denominator remains the same, therefore the dispersion relation and its solutions are the same described in Subsection 2.6.1.

3.6 Receptivity coefficient

In order to find the pressure in the physical space it is necessary to perform the inverse Fourier transform of (3.85)

$$P_i(t,x) = \frac{e^{i\omega t}}{2\pi} \int_{-\infty}^{\infty} \frac{ik^2 Ai'(\zeta_0) \int_{\zeta_0}^{\infty} \varphi(s')\,ds'}{\Lambda Ai'(\zeta_0) - i(ik)^{\frac{1}{3}} k^2 \int_{\zeta_0}^{\infty} Ai(s')\,ds'} e^{ikx}\,dk. \tag{3.86}$$

The integration procedure is omitted here as it has been studied in detail in Chapter 2, and only the solution for the pressure at large values of x and negative values of the Kármán-Guderley parameter, disregarding the continuous spectrum contribution, is presented here

$$P_i(t,x) = \frac{1}{2}\mathcal{K}(\omega, K_\infty, \beta, \bar{F}) e^{i(\omega t + k_1 x)} + \dots, \tag{3.87}$$

where

$$\mathcal{K} = -\frac{12iq_1 k_1^2 Ai'(\zeta_0) \int_{\zeta_0}^{\infty} \varphi(s')\,ds'}{3Ai'(\zeta_0)\left[2K_\infty k_1 + \omega\right] + 2q_1(ik_1)^{\frac{1}{3}}\left[2Ai(\zeta_0)\zeta_0\left(q_1\frac{\omega}{k_1^2} + k_1\right) + 7k_1 I_{\zeta_0}\right]}. \tag{3.88}$$

This function, $\mathcal{K}(\omega, K_\infty, \beta, \bar{F})$ is the receptivity coefficient and now it is a function of the acoustic perturbation frequency, ω, the Kármán-Guderley parameter, K_∞, the Fourier transform of the shape of the roughness, $\bar{F}$, and the angle at which acoustic wave impinges the boundary layer, β. Similarly as in the case of the expression for the Fourier transform of the pressure (3.85), the expression of the receptivity coefficient (3.88) is similar to the expression (2.134). The only difference is in the function φ.

Numerical calculations of the receptivity coefficient (3.88) are performed following the same steps as described at the end of Section 2.6. The exception is in the calculation of the function φ, which is found by solving the boundary-value problem (3.82). This

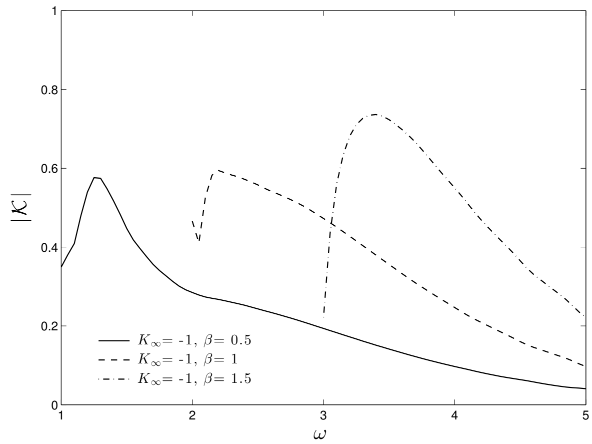

(a) Modulus of the receptivity coefficient

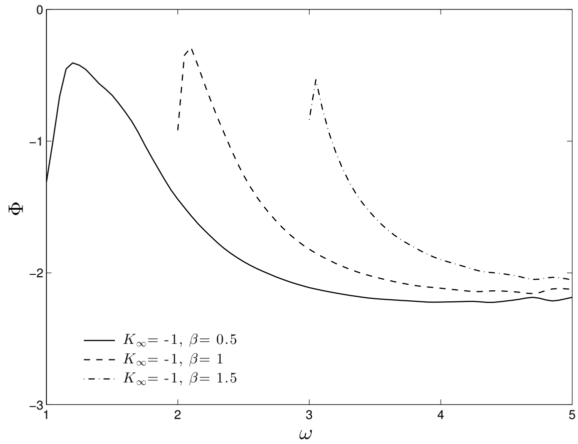

(b) Argument of the receptivity coefficient

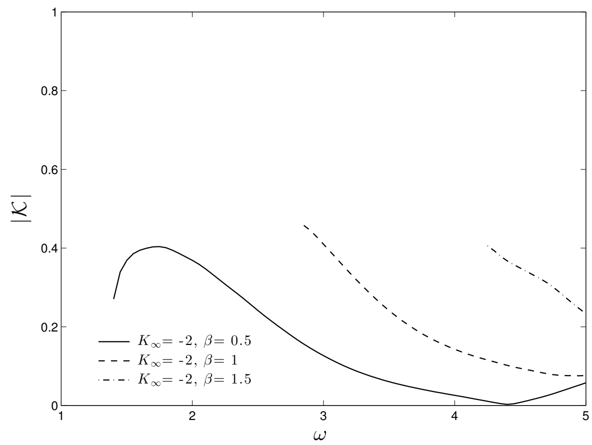

(c) Modulus of the receptivity coefficient

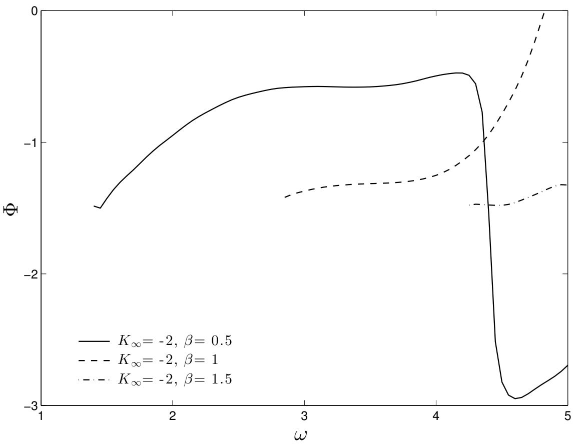

(d) Argument of the receptivity coefficient

Figure 3.3: Receptivity coefficient dependence on frequency, the Kármán-Guderley parameter and transverse wavenumber

calculation involves direct use of functions (3.50) and (3.66) and its inverse Fourier transforms in order to determine function H in (3.46c).

Results of the numerical calculations are presented in Figure 3.3, where shape of the roughness is described by the Gaussian function and the amplitude of the impinging acoustic waves, P_0 is set to be one. Here the receptivity coefficient is represented in the exponential form, $\mathcal{K} = |\mathcal{K}|e^{i\Phi}$.

3.7 Discussion of the results

This study has shown that the receptivity coefficient now depends on the shape of the roughness itself as well as acoustic wave parameters and the free-stream Mach number. Results are presented in Figure 3.3, where the shape of the roughness is described by the Gaussian function. It may be observed that the receptivity coefficient is not available for small acoustic wave frequencies. This limit comes from the restriction set by the condition (3.32). In addition, the receptivity coefficient increases when the transverse wavenumber increases and the Kármán-Guderley parameter decreases. It may also be observed that increasing the frequency of the perturbations the modulus of the receptivity coefficient decreases and tends to zero.

4 Receptivity of the boundary layer to vibrations of the wing surface

4.1 Introduction

In this chapter we study the generation of Tollmien-Schlichting waves in the boundary layer on the wing surface due to elastic vibrations of the wing. This form of the receptivity was not highlighted by experimentalists, probably, because laminar-turbulent transition experiments are normally conducted on rigid surfaces. Meanwhile, a real aircraft wing has a flexible surface which is susceptible to elastic vibrations. Also modern jet engine nacelles are known to exhibit oscillations. We shall show that the boundary layer displays high sensitivity to this form of excitation.

This work differs from two works presented previously (see Chapters 2 and 3) in two ways: in current analysis we consider only the subsonic flow regime whereas previously it was the transonic regime, and external perturbations are due to wing vibrations and not from the acoustic disturbances in the free-steam as before.

The layout of the chapter is as follows. The mathematical formulation of the problem is given in section 4.2, followed by the flow analysis outside the boundary layer. It is shown that unless the Mach number is very small the pressure perturbation field may be calculated using piston theory (see, for example, Liepmann & Roshko, 1957). As the pressure perturbations penetrate into the boundary layer, the Stokes layer forms near the body surface; this process is studied in section 4.3. In order to simplify the flow analysis we assume that the amplitude of the wall vibrations is small. We find that if the wave length, ℓ, of the vibrations of the wing surface is an order $Re^{-1/8}$ quantity, then the oscillations of the longitudinal velocity in the Stokes layer are caused by both the longitudinal pressure gradient and by the pressure oscillations in time. In section 4.4 we analyse the flow in the triple-deck region which forms as a result of the interaction of the Stokes layer with a roughness on the wing surface. With $\ell = O(Re^{-1/8})$ the flow appears to be compressible even in the near-wall region 1. The solution of the triple-deck problem is presented in section 4.5. We show that in the vicinity of the roughness the flow perturbation field is composed of discrete and continuous spectra. We show that the continuous spectrum perturbations decay downstream of the roughness, and so do all the perturbations of the discrete spectrum except the one which

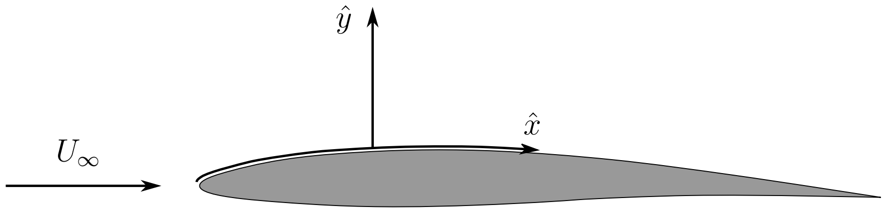

Figure 4.1: Layout of the problem

represents the Tollmien-Schlichting wave. The amplitude of the latter is found in an analytic form.

The analysis presented here is conducted in collaboration with Prof. Anatoly I. Ruban and David Pryce, and it is published in Journal of Fluid Mechanics, (Ruban *et al.*, 2013).

4.2 Problem formulation

Let us consider a uniform two-dimensional subsonic flow of a perfect gas and an aerofoil placed in it as shown in Figure 4.1.

In what follows we shall use the body-fitted curvilinear orthogonal coordinate system $(\hat{x}, \hat{y})$ with $\hat{x}$ measured along the aerofoil surface from its leading edge, and $\hat{y}$ in the normal direction. The velocity components in these coordinates are denoted as $(\hat{u}, \hat{v})$. We shall further denote the gas density by $\hat{\rho}$, the pressure $\hat{p}$, the enthalpy $\hat{h}$ and the dynamic viscosity coefficient $\hat{\mu}$. The "hat" is used to signify that the corresponding variables are dimensional.

Similarly as in the previous chapter, the flow analysis will be conducted using the Navier-Stokes equations written in the body-fitted coordinates (A.5). When solving these equations we shall assume that the Reynolds number is large. Here U_∞ is the free-stream velocity, L is the aerofoil cord length, and ρ_∞ and μ_∞ are the values of the gas density, $\hat{\rho}$, and viscosity coefficient, $\hat{\mu}$, in the free stream.

We shall assume that the surface of the aerofoil performs small amplitude vibrations the form of which will be now defined. An efficient generation of Tollmien-Schlichting waves in the boundary layer is expected to take place when a part of the spectrum of the wing vibrations comes in resonance with the Tollmien-Schlichting waves. For this to happen the period of the vibrations, T, has to be

$$T \sim \frac{L}{U_\infty} Re^{-1/4}. \tag{4.1}$$

Keeping this in mind we shall write the equation for the aerofoil contour as

$$\hat{y}_w = \varepsilon L f\left(\frac{\hat{t}}{\frac{L}{U_\infty}Re^{-1/4}}, \frac{\hat{x}}{L\delta_x}\right). \tag{4.2}$$

Here we use the coordinates, $(\hat{x}, \hat{y})$, fitted in the undisturbed aerofoil shape.

In the following subsection we will fist establish restrictions on the amplitude of the aerofoil surface vibrations, ε, and on the characteristic wave length, δ_x in therms of Re. As the result this will allows us to determine appropriate scalings for the particular problem.

4.2.1 Piston theory

We shall start our study by analysing the pressure perturbations in the inviscid part of the flow outside the boundary layer. The following arguments may be used in order to determine the form of the solution in this region. If the perturbations induced in the flow by the vibrating wing surface are small, then they will propagate with the speed of sound, a_∞, and over the time (4.1) cover the distance

$$\hat{y} \sim a_\infty T \sim \frac{L}{M_\infty} Re^{-1/4}. \tag{4.3}$$

The gas velocity component normal to the aerofoil surface may be estimated by differentiating (4.2) with respect to time,

$$\hat{v} \sim \frac{\partial \hat{y}_w}{\partial \hat{t}} \sim U_\infty \varepsilon Re^{1/4}. \tag{4.4}$$

In order to evaluate the pressure perturbations produced by the vibrating wall we use the $\hat{y}$-momentum equation (A.5b). We assume (subject to subsequent confirmation) that the local acceleration term, $\hat{\rho}\,\partial\hat{v}/\partial\hat{t}$, is dominant on the left hand side of this equation, and therefore, has to be in balance with the pressure gradient on the right hand side of (A.5b),

$$\hat{\rho}\frac{\partial \hat{v}}{\partial \hat{t}} \sim \frac{\partial \hat{p}}{\partial \hat{y}}. \tag{4.5}$$

Assuming that the perturbations are small we can approximate the gas density as $\hat{\rho} \sim \rho_\infty$. The other quantities in the above equation can be estimated with the help of equations (4.4), (4.1) and (4.3) which leads to

$$\rho_\infty \frac{U_\infty \varepsilon Re^{1/4}}{\frac{L}{U_\infty}Re^{-1/4}} \sim \frac{\Delta \hat{p}}{\frac{L}{M_\infty}Re^{-1/4}}. \tag{4.6}$$

Solving this equation for $\Delta\hat{p}$, we find

$$\Delta\hat{p} \sim \rho_\infty U_\infty^2 \frac{\varepsilon Re^{1/4}}{M_\infty}. \tag{4.7}$$

The principle balance in the energy equation (A.5c) is

$$\hat{\rho}\frac{\partial\hat{h}}{\partial\hat{t}} \sim \frac{\partial\hat{p}}{\partial\hat{t}}, \tag{4.8}$$

which shows that the perturbations of enthalpy

$$\Delta\hat{h} \sim \frac{\Delta\hat{p}}{\rho_\infty}. \tag{4.9}$$

Substituting (4.7) into (4.9) we find

$$\Delta\hat{h} \sim \frac{\Delta\hat{p}}{\rho_\infty} \sim U_\infty^2 \frac{\varepsilon Re^{1/4}}{M_\infty}. \tag{4.10}$$

The density perturbations can now be estimated using the state equation (A.5e). We write it as

$$\hat{\rho} = \frac{\gamma}{\gamma-1}\frac{\hat{p}}{\hat{h}}, \tag{4.11}$$

and introducing the perturbations of the thermodynamic function with respect to their values in the free stream,

$$\rho_\infty + \Delta\hat{\rho} = \frac{\gamma}{\gamma-1}\frac{p_\infty + \Delta\hat{p}}{h_\infty + \Delta\hat{h}} = \frac{\gamma}{\gamma-1}\frac{p_\infty}{h_\infty}\frac{\left(1 + \Delta\hat{p}/p_\infty\right)}{\left(1 + \Delta\hat{h}/h_\infty\right)}. \tag{4.12}$$

Taking into account that $\rho_\infty = \frac{\gamma}{\gamma-1}\frac{p_\infty}{h_\infty}$ and assuming $\Delta\hat{p}/p_\infty$ and $\Delta\hat{h}/h_\infty$ small, we arrive at a conclusion that

$$1 + \frac{\Delta\hat{\rho}}{\rho_\infty} = \left(1 + \frac{\Delta\hat{p}}{p_\infty}\right)\left(1 - \frac{\Delta\hat{h}}{h_\infty}\right) = 1 + O\big(M_\infty \varepsilon Re^{1/4}\big). \tag{4.13}$$

Hence,

$$\Delta\hat{\rho} \sim \rho_\infty M_\infty \varepsilon Re^{1/4}. \tag{4.14}$$

Finally, it remains to find an estimate for the perturbations of the longitudinal velocity component, $\hat{u}$. For this purpose the $\hat{x}$-momentum equation (A.5a) has to be used. We write

$$\hat{\rho}\frac{\partial\hat{u}}{\partial\hat{t}} \sim \frac{\partial\hat{p}}{\partial\hat{x}}. \tag{4.15}$$

Approximating the derivatives in this equation by finite differences,

$$\rho_\infty \frac{\Delta \hat{u}}{T} \sim \frac{\Delta \hat{p}}{L\delta_x}, \tag{4.16}$$

and using (4.1) and (4.7) for the characteristic time and pressure perturbations, respectively, we find that

$$\Delta \hat{u} \sim U_\infty \frac{\varepsilon}{M_\infty \delta_x}. \tag{4.17}$$

We are now in a position to formulate the restrictions that should be imposed on the flow parameters (the free-stream Mach number, M_∞, the Reynolds number, Re, and the amplitude of the wall vibrations, ε,) for the piston theory to be valid. Firstly, from (4.7), (4.10) and (4.14) it is easily seen that relative variations of the thermodynamic quantities, $\Delta\hat{p}/p_\infty$, $\Delta\hat{h}/h_\infty$ and $\Delta\hat{\rho}/\rho_\infty$, are small provided that

$$M_\infty \varepsilon Re^{1/4} \ll 1. \tag{4.18}$$

Secondly, we shall assume that the distance (4.3) the perturbations travel during one period of oscillations is small as compared to the characteristic wave length of the aerofoil surface vibrations, $L\delta_x$. This condition is satisfied if

$$\delta_x \gg \frac{Re^{-1/4}}{M_\infty}. \tag{4.19}$$

We shall see that under the conditions (4.18) and (4.19) the flow outside the boundary layer is described by the linear, quasi-one-dimensional unsteady equations of the classical piston theory. In what follows we shall assume that the free-stream Mach number, M_∞, is an order one quantity, in which case the conditions (4.18), (4.19) may be written as

$$\varepsilon Re^{1/4} \ll 1, \qquad \delta_x \gg Re^{-1/4}. \tag{4.20}$$

Being guided by (4.1), (4.3), (4.4)–(4.17) we represent the solution of the Navier-Stokes equations (A.5) in the region considered in the form

$$\begin{gathered} \hat{u} = U_\infty + U_\infty \frac{\varepsilon}{\delta_x} u'(t, \breve{x}', y), \qquad \hat{v} = U_\infty \varepsilon Re^{1/4} v'(t, \breve{x}', y), \\ \hat{\rho} = \rho_\infty + \rho_\infty \varepsilon Re^{1/4} \rho'(t, \breve{x}', y), \qquad \hat{p} = p_\infty + \rho_\infty U_\infty^2 \varepsilon Re^{1/4} p'(t, \breve{x}', y), \\ \hat{h} = h_\infty + U_\infty^2 \varepsilon Re^{1/4} h'(t, \breve{x}', y), \end{gathered} \tag{4.21a-e}$$

with the independent variables, t, $\breve{x}'$ and y, being the non-dimensional time, longitudinal and normal coordinates introduced through the scalings

$$\hat{t} = \frac{L}{U_\infty} Re^{-1/4} t, \qquad \hat{x} = L\delta_x \breve{x}', \qquad \hat{y} = L Re^{-1/4} y. \tag{4.22}$$

Substituting (4.21), (4.22) into the Navier-Stokes equations (A.5), and setting $Re \to \infty$ and $\varepsilon \to 0$ such that the conditions (4.20) are observed, we arrive at the following set of equations,

$$\frac{\partial u'}{\partial t} = -\frac{\partial p'}{\partial \breve{x}'}, \tag{4.23a}$$
$$\frac{\partial v'}{\partial t} = -\frac{\partial p'}{\partial y}, \tag{4.23b}$$
$$\frac{\partial h'}{\partial t} = \frac{\partial p'}{\partial t}, \tag{4.23c}$$
$$\frac{\partial \rho'}{\partial t} + \frac{\partial v'}{\partial y} = 0, \tag{4.23d}$$
$$h' + \frac{\rho'}{(\gamma-1)M_\infty^2} = \frac{\gamma}{\gamma-1} p'. \tag{4.23e}$$

It is easy to see that the $\hat{x}$-momentum equation (4.23a) separates from the rest of the equations in (4.23). It may be used to determine the longitudinal velocity perturbation function, u', once the pressure perturbation field, p', is found. The equation for p'

$$M_\infty^2 \frac{\partial^2 p'}{\partial t^2} - \frac{\partial^2 p'}{\partial y^2} = 0 \tag{4.24}$$

is deduced by eliminating h', ρ' and v' from the (4.23b)–(4.23e). In order to deduce a boundary condition for this equation we notice that the flow considered is inviscid, and therefore, has to satisfy the impermeability condition on the aerofoil surface,

$$\hat{v} = \frac{\partial \hat{y}_w}{\partial \hat{t}} + \frac{\hat{u}}{1+\kappa\hat{y}} \frac{\partial \hat{y}_w}{\partial \hat{x}} \quad \text{at} \quad \hat{y} = \hat{y}_w(\hat{t}, \hat{x}). \tag{4.25}$$

Using (4.2) and (4.21) in (4.25) we have in the leading order

$$v'\Big|_{y=0} = \frac{\partial f}{\partial t}. \tag{4.26}$$

This condition can be converted into a condition for p' through making use of the

$\hat{y}$-momentum equation. We find that

$$\left.\frac{\partial p'}{\partial y}\right|_{y=0} = -\frac{\partial^2 f}{\partial t^2}. \tag{4.27}$$

The general solution of equation (4.24) is written as

$$p' = \varphi(\xi; \breve{x}') + \psi(\eta; \breve{x}'), \tag{4.28}$$

where

$$\xi = t - M_\infty y, \qquad \eta = t + M_\infty y, \tag{4.29a,b}$$

and $\breve{x}'$ plays the role of a parameter. Since we are interested in the perturbations emanating from the aerofoil surface we have to disregard the second term, $\psi(\eta; \breve{x}')$, on the right hand side of (4.28). The function $\varphi(\xi; \breve{x}')$ is then found from the boundary condition (4.27),

$$\varphi(\xi; \breve{x}') = \frac{1}{M_\infty}\frac{\partial f}{\partial t}(\xi, \breve{x}'). \tag{4.30}$$

Consequently, at any point in the flow field

$$p'(t, y; \breve{x}') = \frac{1}{M_\infty}\frac{\partial f}{\partial t}(t - M_\infty y, \breve{x}'). \tag{4.31}$$

Now, using (4.31) in (4.23) we find that

$$\begin{aligned} u' &= -\frac{1}{M_\infty}\frac{\partial f}{\partial \breve{x}'}(t - M_\infty y, \breve{x}'), \qquad & v' &= \frac{\partial f}{\partial t}(t - M_\infty y, \breve{x}'), \\ h' &= \frac{1}{M_\infty}\frac{\partial f}{\partial t}(t - M_\infty y, \breve{x}'), \qquad & \rho' &= M_\infty \frac{\partial f}{\partial t}(t - M_\infty y, \breve{x}'). \end{aligned} \tag{4.32a-d}$$

Of particular interest is the pressure on the aerofoil surface. It is found by setting $y = 0$ in (4.31). We have

$$\left. p' \right|_{y=0} = \frac{1}{M_\infty}\frac{\partial f}{\partial t}(t, \breve{x}'). \tag{4.33}$$

In what follows we shall assume that the vibrations of the aerofoil surface are time periodic, namely,

$$f(t, \breve{x}') = e^{i\breve{\omega}t}\breve{F}(\breve{x}') + c.c.. \tag{4.34}$$

Here the frequency, $\breve{\omega}$, and phase, Φ, are real while $\breve{F}(\breve{x}')$ is a complex function of real variable $\breve{x}'$; *c.c.* denotes the complex conjugate of $e^{i\breve{\omega}t}\breve{F}(\breve{x}')$. Substituting (4.34) into

(4.33) and then into the asymptotic expansion for $\hat{p}$ in (4.21) yields

$$\hat{p} = p_\infty + \rho_\infty U_\infty^2 \varepsilon Re^{1/4}\left\{\frac{i\breve{\omega}}{M_\infty}\breve{F}(\breve{x}')e^{i\breve{\omega}t} + c.c.\right\}. \tag{4.35}$$

4.3 Boundary-layer analysis

We shall now turn our attention to the boundary layer on the aerofoil surface. If the flow was steady then the solution in the boundary layer could be represented by the asymptotic expansions,

$$\begin{aligned} &\hat{u} = U_\infty U_0(x,Y) + \cdots, && \hat{v} = U_\infty Re^{-1/2} V_0(x,Y) + \cdots, \\ &\hat{p} = p_\infty + \rho_\infty U_\infty^2 P_0(x,Y) + \cdots, && \hat{\rho} = \rho_\infty R_0(x,Y) + \cdots, \\ &\hat{h} = U_\infty^2 h_0(x,Y) + \cdots, && \hat{\mu} = \mu_\infty \mu_0(x,Y) + \cdots. \end{aligned} \tag{4.36a-f}$$

Here the dimensionless coordinates, (x, Y), are introduced by means of the transformations,

$$\hat{x} = Lx, \qquad \hat{y} = LRe^{-1/2}Y. \tag{4.37a,b}$$

Substitution of (4.36), (4.37) into the Navier-Stokes equations (A.5) leads to the classical boundary-layer equations,

$$R_0\left(U_0\frac{\partial U_0}{\partial x} + V_0\frac{\partial U_0}{\partial Y}\right) = -\frac{\partial P_0}{\partial x} + \frac{\partial}{\partial Y}\left(\mu_0\frac{\partial U_0}{\partial Y}\right), \tag{4.38a}$$

$$\frac{\partial P_0}{\partial Y} = 0, \tag{4.38b}$$

$$R_0\left(U_0\frac{\partial h_0}{\partial x} + V_0\frac{\partial h_0}{\partial Y}\right) = U_0\frac{\partial P_0}{\partial x} + \frac{1}{Pr}\frac{\partial}{\partial Y}\left(\mu_0\frac{\partial h_0}{\partial Y}\right) + \mu_0\left(\frac{\partial U_0}{\partial Y}\right)^2, \tag{4.38c}$$

$$\frac{\partial(R_0U_0)}{\partial x} + \frac{\partial(R_0V_0)}{\partial Y} = 0, \tag{4.38d}$$

$$h_0 = \frac{1}{(\gamma-1)R_0} + \frac{\gamma}{\gamma-1}\frac{P_0}{R_0}. \tag{4.38e}$$

When solving these equations one needs to pose the following boundary conditions. Firstly, at the front stagnation point,

$$U_0 = 0, \quad h_0 = H_0 \quad \text{at} \quad x = 0, \tag{4.39a,b}$$

with $H_0 = \frac{1}{2} + \frac{1}{(\gamma-1)M_\infty^2}$ being the total enthalpy. Secondly, the solution has to satisfy the no-slip condition on the aerofoil surface,

$$U_0 = V_0 = 0 \quad \text{at} \quad Y = 0. \tag{4.40a}$$

It has to be supplemented with an appropriate thermal condition. If, for example, the temperature distribution on the aerofoil surface, $\hat{T}_w(x)$, is known, then

$$h_0 = \frac{1}{(\gamma-1)M_\infty^2}\frac{\hat{T}_w(x)}{T_\infty} \quad \text{at} \quad Y = 0. \tag{4.40b}$$

If, on the other hand, it is known that the aerofoil is thermally isolated, then (4.40b) has to be substituted by

$$\frac{\partial h_0}{\partial Y} = 0 \quad \text{at} \quad Y = 0. \tag{4.40c}$$

Finally, at the outer edge of the boundary layer,

$$U_0 = U_e(x), \quad h_0 = h_e(x) \quad \text{at} \quad Y = \infty. \tag{4.41a,b}$$

Here $U_e(x)$ and $h_e(x)$ are the tangential velocity and enthalpy on the aerofoil surface as given by the solution of the inviscid equations of motion.

Through these functions the solution to the boundary-value problem (4.38)–(4.41) depends on the aerofoil shape. In the general case the solution has to be constructed numerically. However, for the receptivity analysis we only need know the behaviour of the fluid dynamic functions at the "bottom" of the boundary layer near the aerofoil surface. It is easily seen that

$$\left.\begin{aligned} U_0(x,Y) &= \tau_w(x)Y + O(Y^2), \qquad & h_0(x,Y) &= \rho_w(x) + O(Y),\\ \rho_0(x,Y) &= \rho_w(x) + O(Y), \qquad & \mu_0(x,Y) &= \mu_w(x) + O(Y) \end{aligned}\right\} \quad \text{as} \quad Y \to 0, \tag{4.42a-d}$$

where $\tau_w(x)$ denotes the skin friction, and $\rho_w(x)$, $\mu_w(x)$ are the gas density and dynamic viscosity coefficient on the aerofoil surface.

We shall now study the perturbations produced in the boundary layer due to the wall vibrations. When performing this task we shall still use the body fitted coordinates (see Figure 4.1) which now move up and down with the aerofoil surface. As the coordinate system is no longer inertial, we need to see if the inertial force changes the pressure distribution in the boundary layer. With the aerofoil surface given by equation (4.2) the inertial force is calculated as

$$\mathbf{F}_{\text{inertial}} = \hat{\rho}\frac{\partial^2 \hat{y}_w}{\partial \hat{t}^2}\mathbf{e}_y, \tag{4.43}$$

where $\mathbf{e}_y$ is a unit vector along the $\hat{y}$-axis. The pressure at the outer edge of the boundary layer is given by (4.35). We need to estimate the effect of the inertial force on the pressure variation across the boundary layer. We write

$$\mathbf{F}_{\text{inertial}} \sim \frac{\partial \hat{p}}{\partial \hat{y}}\mathbf{e}_y. \tag{4.44}$$

Using (4.2) in (4.43) we find,

$$\left|\mathbf{F}_{\text{inertial}}\right| \sim \frac{\rho_\infty U_\infty^2}{L}\,\varepsilon Re^{1/2}. \tag{4.45}$$

With $\Delta\hat{p}$ denoting the pressure variation due to the action of the inertial force, we can estimate the right hand side of (4.44) as

$$\frac{\partial \hat{p}}{\partial \hat{y}} \sim \frac{\Delta\hat{p}}{LRe^{-1/2}}. \tag{4.46}$$

Substituting (4.45) and (4.46) into (4.44) yields

$$\Delta\hat{p} \sim \rho_\infty U_\infty^2 \varepsilon, \tag{4.47}$$

which is $Re^{1/4}$ times smaller than the pressure (4.35) at the outer edge of the boundary layer. Hence, in the flow considered the inertial force can be disregarded.

4.3.1 Stokes layer

As the pressure perturbations (4.35) penetrate into the boundary layer, they cause a Stokes layer to form near the aerofoil surface. The thickness of this layer is easily found by comparing the instantaneous acceleration term with the viscous forces in the longitudinal momentum equation (A.5a),

$$\hat{\rho}\,\frac{\partial \hat{u}}{\partial \hat{t}} \sim \frac{\partial}{\partial \hat{y}}\left(\hat{\mu}\frac{\partial \hat{u}}{\partial \hat{y}}\right). \tag{4.48}$$

Taking into account that $\hat{\rho} \sim \rho_\infty$, $\hat{\mu} \sim \mu_\infty$ and using equation (4.1) for the characteristic time, we find that

$$\hat{y} \sim L Re^{-5/8}. \tag{4.49}$$

Let us now estimate the perturbations, $\Delta\hat{u}$, of the longitudinal velocity component. There are two physical mechanisms which lead to oscillations of the longitudinal velocity in the Stokes layer. In the first one the acceleration and deceleration of fluid particles are caused by the pressure variations along the body surface. This process is expressed by the following balance in the $\hat{x}$-momentum equation (A.5a),

$$\hat{\rho}\frac{\partial \hat{u}}{\partial \hat{t}} \sim \frac{\partial \hat{p}}{\partial \hat{x}}. \tag{4.50}$$

Using the results of the piston theory (4.35),

$$\Delta\hat{p} \sim \rho_\infty U_\infty^2 \varepsilon Re^{1/4}, \tag{4.51}$$

and the fact that the characteristic time and the length scale are

$$\hat{t} \sim \frac{L}{U_\infty} Re^{-1/4}, \qquad \hat{x} \sim L\delta_x, \tag{4.52}$$

we find from (4.50) that

$$\Delta\hat{u} \sim U_\infty \frac{\varepsilon}{\delta_x}. \tag{4.53}$$

The second mechanism is attributed to the compressibility of the flow. When the pressure at the outer edge of the boundary layer varies periodically in time, the gas in the Stokes layer undergoes periodic compression and expansion, which leads to an oscillatory motion of fluid particles in the direction normal to the wall. The characteristic velocity, $\hat{v}$, of this motion may be estimated using the following balance in the continuity equation (A.5d),

$$\frac{\partial \hat{\rho}}{\partial \hat{t}} \sim \hat{\rho}\frac{\partial \hat{v}}{\partial \hat{y}}. \tag{4.54}$$

With the pressure perturbations given by (4.51), the density perturbations are estimated as

$$\Delta\hat{\rho} \sim \rho_\infty \varepsilon Re^{1/4}. \tag{4.55}$$

Using (4.55) and (4.1) the derivative $\partial\hat{\rho}/\partial\hat{t}$ on the left hand side of (4.54) may be estimated as

$$\frac{\partial \hat{\rho}}{\partial \hat{t}} \sim \frac{\rho_\infty U_\infty}{L} \varepsilon Re^{1/2}. \tag{4.56}$$

On the right hand side of (4.54) we substitute $\hat{\rho}$ by ρ_∞ and evaluate the derivative $\partial \hat{v}/\partial \hat{y}$ keeping in mind that the thickness of the Stokes layer is given by (4.49). We have

$$\hat{\rho}\frac{\partial \hat{v}}{\partial \hat{y}} \sim \rho_\infty \frac{\hat{v}}{LRe^{-5/8}}. \tag{4.57}$$

It remains to substitute (4.56) and (4.57) into (4.54) and solve the resulting equation for $\hat{v}$. We find

$$\hat{v} \sim U_\infty \varepsilon Re^{-1/8}. \tag{4.58}$$

As the fluid particles migrate from a region with lower basic flow velocity $\hat{u}$ into a region with larger $\hat{u}$ and then return back, an exchange between the instantaneous acceleration of the fluid particles and the convective acceleration takes place, which is represented by the following balance in the longitudinal momentum equation (A.5a),

$$\frac{\partial \hat{u}}{\partial \hat{t}} \sim \hat{v}\frac{\partial \hat{u}}{\partial \hat{y}}. \tag{4.59}$$

The derivative $\partial \hat{u}/\partial \hat{y}$ on the right hand side of (4.59) is approximated using the steady solution in the boundary layer,

$$\frac{\partial \hat{u}}{\partial \hat{y}} \sim \frac{U_\infty}{LRe^{-1/2}}, \tag{4.60}$$

which being substituted together with (4.58) into (4.59) yields

$$\frac{\Delta \hat{u}}{\frac{L}{U_\infty} Re^{-1/4}} \sim U_\infty \varepsilon Re^{-1/8} \frac{U_\infty}{LRe^{-1/2}}. \tag{4.61}$$

We arrive at a conclusion that

$$\Delta \hat{u} \sim U_\infty \varepsilon Re^{1/8}. \tag{4.62}$$

Comparing (4.62) with (4.53) one can see that the two physical mechanisms appear to be equally important if

$$\delta_x = Re^{-1/8}, \tag{4.63}$$

which is consistent with the restriction (4.20). Equation (4.63) defines a distinguished flow regime which will now be studied using standard asymptotic analysis.

Notice that the perturbations (4.62), (4.53) should be superimposed on the steady flow solution which, according to (4.36) and (4.42), is written in the Stokes layer as

$$\hat{u} = U_\infty Re^{-1/8}\tau_w(x)\breve{Y}_* + \cdots, \qquad \breve{Y}_* = Re^{1/8}Y. \tag{4.64}$$

This suggests that in the Stokes layer the solution of the Navier-Stokes equations (A.5) has to be represented in the form

$$\hat{u} = U_\infty\Big\{Re^{-1/8}\tau_w(x)\breve{Y}_* + \varepsilon Re^{1/8}\breve{u}(t,\breve{x}',\breve{Y}_*) + \cdots\Big\}, \tag{4.65a}$$

$$\hat{v} = U_\infty\Big\{\varepsilon Re^{-1/8}\breve{v}(t,\breve{x}',\breve{Y}_*) + \cdots\Big\}, \tag{4.65b}$$

$$\hat{p} = p_\infty + \rho_\infty U_\infty^2\Big\{P_0(x) + \varepsilon Re^{1/4}\breve{p}(t,\breve{x}') + \cdots\Big\}, \tag{4.65c}$$

$$\hat{h} = U_\infty^2\Big\{h_w(x) + \varepsilon Re^{1/4}\breve{h}(t,\breve{x}',\breve{Y}_*) + \cdots\Big\}, \tag{4.65d}$$

$$\hat{\rho} = \rho_\infty\Big\{\rho_w(x) + \varepsilon Re^{1/4}\breve{\rho}(t,\breve{x}',\breve{Y}_*) + \cdots\Big\}, \tag{4.65e}$$

$$\hat{\mu} = \mu_\infty\Big\{\mu_w(x) + \varepsilon Re^{1/4}\breve{\mu}(t,\breve{x}',\breve{Y}_*) + \cdots\Big\}, \tag{4.65f}$$

with the independent variables t, $\breve{x}'$ and $\breve{Y}_*$ introduced by

$$\hat{t} = \frac{L}{U_\infty}Re^{-1/4}t, \qquad \hat{x} = LRe^{-1/8}\breve{x}', \qquad \hat{y} = LRe^{-5/8}\breve{Y}_*. \tag{4.66a-c}$$

Notice that the scale time t, and longitudinal coordinate $\breve{x}'$ are the same as in (4.22).

Substitution of (4.65) into (A.5) results in

$$\rho_w\frac{\partial\breve{u}}{\partial t} + \rho_w\tau_w\breve{v} = -\frac{\partial\breve{p}}{\partial\breve{x}'} + \mu_w\frac{\partial^2\breve{u}}{\partial\breve{Y}_*^2}, \tag{4.67a}$$

$$\frac{\partial\breve{p}}{\partial\breve{Y}_*} = 0, \tag{4.67b}$$

$$\rho_w\frac{\partial\breve{h}}{\partial t} = \frac{\partial\breve{p}}{\partial t} + \mu_w\frac{\partial^2\breve{h}}{\partial\breve{Y}_*^2}, \tag{4.67c}$$

$$\frac{\partial\breve{\rho}}{\partial t} + \rho_w\frac{\partial\breve{v}}{\partial\breve{Y}_*} = 0, \tag{4.67d}$$

$$h_w(x) = \frac{1}{(\gamma-1)M_\infty^2}\frac{1}{\rho_w(x)}, \qquad \breve{h} = \frac{\gamma}{\gamma-1}\frac{1}{\rho_w}\bigg(\breve{p} - \frac{\breve{\rho}}{\gamma M_\infty^2\rho_w}\bigg). \tag{4.67e}$$

We start with the energy equation (4.67c). We shall seek the solution to this equation in the class of functions which are time periodic and do not show exponential growth as $\breve{Y}_* \to \infty$. If the aerofoil surface is thermally isolated, i.e.

$$\left.\frac{\partial \breve{h}}{\partial \breve{Y}_*}\right|_{\breve{Y}_*=0} = 0, \tag{4.68}$$

then the suitable solution is given by

$$\breve{h} = \frac{\breve{p}}{\rho_w}, \tag{4.69}$$

which is independent of the $\breve{Y}_*$.

Substitution of (4.69) into the state equation (4.67e) yields

$$\breve{\rho} = M_\infty^2 \rho_w \breve{p}, \tag{4.70}$$

and then the continuity equation (4.67d) may be expressed in the form

$$\frac{\partial \breve{v}}{\partial \breve{Y}_*} = -M_\infty^2 \frac{\partial \breve{p}}{\partial t}. \tag{4.71}$$

The solution of (4.71) satisfying the impermeability condition on the aerofoil surface

$$\left.\breve{v}\right|_{\breve{Y}_*=0} = 0, \tag{4.72}$$

is written as

$$\breve{v} = -M_\infty^2 \frac{\partial \breve{p}}{\partial t} \breve{Y}_*. \tag{4.73}$$

With (4.73) the $\hat{x}$-momentum equation (4.67a) assumes the form

$$\rho_w \frac{\partial \breve{u}}{\partial t} - \rho_w \tau_w M_\infty^2 \frac{\partial \breve{p}}{\partial t} \breve{Y}_* = -\frac{\partial \breve{p}}{\partial \breve{x}'} + \mu_w \frac{\partial^2 \breve{u}}{\partial \breve{Y}_*^2}. \tag{4.74}$$

Notice that, according to (4.67b), the pressure does not change with $\breve{Y}_*$ making the inviscid solution (4.35) applicable inside the Stokes layer. It is written in non-dimensional variables (4.65) as

$$\breve{p} = \frac{i\breve{\omega}}{M_\infty} \breve{F}(\breve{x}') e^{i\breve{\omega} t} + c.c.. \tag{4.75}$$

This suggests that the solution of equation (4.74) should be sought in the form

$$\breve{u}(t, \breve{x}', \breve{Y}_*) = e^{i\breve{\omega} t} U(\breve{x}', \breve{Y}_*) + c.c.. \tag{4.76}$$

Substitution of (4.75) and (4.76) into (4.74) results in the following equation for U,

$$\mu_w \frac{\partial^2 U}{\partial \breve{Y}_*^2} - i\breve{\omega}\rho_w U = \frac{i\breve{\omega}}{M_\infty}\frac{d\breve{F}}{d\breve{x}'} + \rho_w \tau_w M_\infty \breve{\omega}^2 \breve{F}(\breve{x}')\breve{Y}_*. \tag{4.77}$$

The solution of this equation which satisfies the no-slip condition on the aerofoil surface

$$U\Big|_{\breve{Y}_*=0} = 0, \tag{4.78}$$

and does not grow exponentially at the outer edge of the Stokes layer has the form,

$$U = \frac{d\breve{F}/d\breve{x}'}{M_\infty \rho_w}\left[e^{-(1+i)\sqrt{\frac{\breve{\omega}\rho_w}{2\mu_w}}\breve{Y}_*} - 1\right] + i\breve{\omega}\tau_w M_\infty \breve{F}(\breve{x}')\breve{Y}_*. \tag{4.79}$$

4.3.2 The main part of the boundary layer

The form of the asymptotic expansions of the fluid dynamic function in the main part of the boundary layer, where $\hat{y} \sim LRe^{-1/2}$, may be predicted with the help of the following procedure which is based on the principle of matching of asymptotic expansions. We shall describe the procedure using as an example the longitudinal velocity component $\hat{u}$. Substituting (4.79) into (4.76) and setting $\breve{Y}_* \to \infty$, we find that at the outer edge of the Stokes layer

$$\breve{u} = i\breve{\omega}\tau_w M_\infty \breve{F}(\breve{x}')\breve{Y}_* e^{i\breve{\omega}t} + c.c.. \tag{4.80}$$

Comparing (4.80) with (4.75) one can see that

$$\breve{u} = \tau_w M_\infty^2 \breve{p}(t, \breve{x}')\breve{Y}_* + \cdots \quad \text{as} \quad \breve{Y}_* \to \infty. \tag{4.81}$$

It remains to substitute (4.81) into the asymptotic expansion for $\hat{u}$ in (4.65), and we will find that "the outer expansion of the inner solution" has the form

$$\hat{u} = U_\infty\Big\{Re^{-1/8}\tau_w(x)\breve{Y}_* + \varepsilon Re^{1/8}\tau_w M_\infty^2 \breve{p}(t, \breve{x}')\breve{Y}_* + \cdots\Big\}. \tag{4.82}$$

If we now recast the above equation in terms of the outer variable, $Y = Re^{-1/8}\breve{Y}_*$, then we will find that "the inner expansion of the outer solution" has to have the form

$$\hat{u} = U_\infty\Big\{\tau_w Y + \varepsilon Re^{1/4}\tau_w(x)M_\infty^2 \breve{p}(t, \breve{x}')Y + \cdots\Big\}. \tag{4.83}$$

This suggests that the solution in the main part of the boundary layer has to be written in the form

$$\hat{u} = U_\infty \Big\{ U_0(x, Y) + \varepsilon Re^{1/4} U_1(t, \breve{x}', Y) + \cdots \Big\}, \tag{4.84}$$

where the functions $U_0(x, Y)$ and $U_1(t, \breve{x}', Y)$ are such that

$$\left.\begin{aligned} U_0 &= \tau_w(x) Y + \cdots, \\ U_1 &= \tau_w(x) M_\infty^2 \breve{p}(t, \breve{x}') Y + \cdots \end{aligned}\right\} \quad \text{as} \quad Y \to 0. \tag{4.85a,b}$$

Repeating this procedure with the other fluid dynamic functions we find that in the main part of the boundary layer the solution has to be sought in the form

$$\hat{u} = U_\infty \Big\{ U_0(x, Y) + \varepsilon Re^{1/4} U_1(t, \breve{x}', Y) + \cdots \Big\}, \tag{4.86a}$$

$$\hat{v} = U_\infty \Big\{ \varepsilon V_1(t, \breve{x}', Y) + \cdots \Big\}, \tag{4.86b}$$

$$\hat{p} = p_\infty + \rho_\infty U_\infty^2 \Big\{ P_0(x) + \varepsilon Re^{1/4} p_1(t, \breve{x}', Y) + \cdots \Big\}, \tag{4.86c}$$

$$\hat{h} = U_\infty^2 \Big\{ h_0(x, Y) + \varepsilon Re^{1/4} h_1(t, \breve{x}', Y) + \cdots \Big\}, \tag{4.86d}$$

$$\hat{\rho} = \rho_\infty \Big\{ R_0(x, Y) + \varepsilon Re^{1/4} \rho_1(t, \breve{x}', Y) + \cdots \Big\}, \tag{4.86e}$$

with

$$\hat{t} = \frac{L}{U_\infty} Re^{-1/4} t, \qquad \hat{x} = L Re^{-1/8} \breve{x}', \qquad \hat{y} = L Re^{-1/2} Y. \tag{4.87a-c}$$

The matching conditions with the solution in the Stokes layer are

$$\left.\begin{aligned} U_0 &= \tau_w(x) Y + \cdots, \\ U_1 &= \tau_w(x) M_\infty^2 \breve{p}(t, \breve{x}') Y + \cdots, \\ p_1 &= \breve{p}(t, \breve{x}') + \cdots, \\ V_1 &= -M_\infty^2 \frac{\partial \breve{p}}{\partial t} Y + \cdots, \\ h_1 &= \frac{1}{\rho_w(x)} \breve{p}(t, \breve{x}') + \cdots, \\ \rho_1 &= M_\infty^2 \rho_w(x) \breve{p}(t, \breve{x}') + \cdots \end{aligned}\right\} \quad \text{as} \quad Y \to 0. \tag{4.88a-f}$$

Substitution of (4.86) into the Navier-Stokes equations (A.5) results in

$$\frac{\partial U_1}{\partial t} + V_1 \frac{\partial U_0}{\partial Y} = 0, \tag{4.89a}$$

$$\frac{\partial p_1}{\partial Y} = 0, \tag{4.89b}$$

$$\frac{\partial h_1}{\partial t} + V_1 \frac{\partial h_0}{\partial Y} = \frac{1}{R_0}\frac{\partial p_1}{\partial t}, \tag{4.89c}$$

$$\frac{\partial \rho_1}{\partial t} + V_1 \frac{\partial R_0}{\partial Y} + R_0 \frac{\partial V_1}{\partial Y} = 0, \tag{4.89d}$$

$$h_0 = \frac{1}{(\gamma-1)M_\infty^2 R_0}, \qquad h_1 = \frac{\gamma}{\gamma-1}\frac{1}{R_0}\left(p_1 - \frac{1}{\gamma M_\infty^2}\frac{\rho_1}{R_0}\right). \tag{4.89e}$$

The solution to the set of equation (4.89) is written as

$$\begin{gathered} p_1 = \frac{1}{M_\infty}\frac{\partial f}{\partial t}, \qquad U_1 = M_\infty Y \frac{\partial U_0}{\partial Y}\frac{\partial f}{\partial t}, \qquad V_1 = -M_\infty Y \frac{\partial^2 f}{\partial t^2}, \\ \rho_1 = M_\infty \frac{\partial (R_0 Y)}{\partial Y}\frac{\partial f}{\partial t}, \qquad h_1 = \frac{\gamma}{\gamma-1}\frac{1}{M_\infty R_0}\left[1 - \frac{1}{\gamma R_0}\frac{\partial (R_0 Y)}{\partial Y}\right]\frac{\partial f}{\partial t}. \end{gathered} \tag{4.90a-e}$$

4.4 Formulation of the triple-deck problem

The Stokes layer on its own cannot produce the Tollmien-Schlichting wave because the characteristic length, $\delta_x \sim Re^{-1/8}$, of the flow oscillations in the Stokes layer is too large as compared to the wave length of the Tollmien-Schlichting wave. Keeping this in mind, we shall assume that there is a roughness on the aerofoil surface centred at the point $\hat{x} = \hat{x}_0$ whose shape is given by the equation,

$$\hat{y} = LRe^{-5/8}\delta \breve{G}\left(\frac{\hat{x} - \hat{x}_0}{LRe^{-3/8}}\right). \tag{4.91}$$

Here we choose the longitudinal extent of the roughness, $\hat{x} - \hat{x}_0$, to be an order $O(LRe^{-3/8})$ quantity. This is to satisfy the conditions of the resonance between the external perturbations and the Tollmien-Schlichting wave, and, indeed, we shall see that with the roughness shape defined by (4.91) the flow is capable of extracting from the entire spectrum of steady perturbations (produced by the roughness) the mode with required wave number.

This is the main difference from the two previously described problems, where the characteristic length of the flow oscillations in the Stokes layer was an $O\left(Re^{-1/9}\right)$. As before the flow past a roughness is described by triple-deck theory, see Figure 4.2).

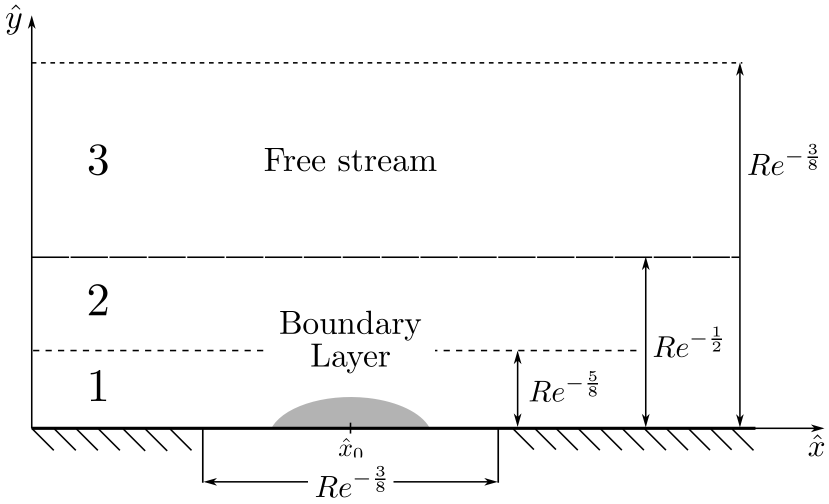

Figure 4.2: The flow in the vicinity of the wall roughness.

4.4.1 Region 1

Assuming that the amplitude of the pulsations in the Stokes layer, $\sigma = \varepsilon Re^{1/4}$, and the roughness height parameter, δ, are small, we can represent the solution in region 1 in the form

$$\hat{u} = U_\infty Re^{-1/8}\Big\{\tau_w \breve{Y}_* + \sigma \breve{u}_S(t, \breve{Y}_*) + \delta \breve{U}_r(\breve{x}_*, \breve{Y}_*) + \sigma\delta \breve{U}_*(t, \breve{x}_*, \breve{Y}_*) + \cdots\Big\}, \tag{4.92a}$$

$$\hat{v} = U_\infty Re^{-3/8}\Big\{\sigma \breve{v}_S(t, \breve{Y}_*) + \delta \breve{V}_r(\breve{x}_*, \breve{Y}_*) + \sigma\delta \breve{V}_*(t, \breve{x}_*, \breve{Y}_*) + \cdots\Big\}, \tag{4.92b}$$

$$\hat{p} = p_\infty + \rho_\infty U_\infty^2\Big\{\sigma P_0(t) + Re^{-1/4}\sigma p_0(t)\breve{x}_* + Re^{-1/4}\delta \breve{P}_r(\breve{x}_*) + \\ + Re^{-1/4}\sigma\delta \breve{P}_*(t, \breve{x}_*) + \cdots\Big\}, \tag{4.92c}$$

$$\hat{h} = U_\infty^2\Big\{h_w + \sigma h_0(t) + \cdots\Big\}, \tag{4.92d}$$

$$\hat{\rho} = \rho_\infty\Big\{\rho_w + \sigma \rho_0(t) + \cdots\Big\}, \tag{4.92e}$$

$$\hat{\mu} = \mu_\infty\Big\{\mu_w + \sigma \mu_0(t) + \cdots\Big\}, \tag{4.92f}$$

with the independent variables, t, $\breve{x}_*$ and $\breve{Y}_*$, defined by the equations,

$$\hat{t} = \frac{L}{U_\infty} Re^{-1/4} t, \qquad \hat{x} = \hat{x}_0 + L Re^{-3/8}\breve{x}_*, \qquad \hat{y} = L Re^{-5/8}\breve{Y}_*. \tag{4.93a-c}$$

The structure of the solution (4.92) may be explained as follows. We start with the asymptotic expansion for the longitudinal velocity component, $\hat{u}$. The leading order term, $\tau_w \breve{Y}_*$, in this expansion represents the unperturbed steady boundary layer, and would be the only term if neither the Stokes layer nor roughness were present. It is obtained by re-expanding the steady solution (4.36), (4.42) in terms of the variables, $\breve{x}_*$, $\breve{Y}_*$, of region 1. In (4.92) the skin friction, τ_w, is a constant being equal to the value of the function $\tau_w(x)$ at the position of the roughness. The next two terms, $\sigma\breve{u}_S(t,\breve{Y}_*)$ and $\delta\breve{U}_r(\breve{x}_*,\breve{Y}_*)$, represent the perturbations produced by the Stokes layer and the roughness, respectively; the function $\breve{u}_S$ is obtained by setting $\breve{x}'$ in (4.76), (4.79) to its value, $\breve{x}'_0$ at the position of the roughness. We have

$$\breve{u}_S = e^{i\breve{\omega}t}\left\{\frac{\frac{d\breve{F}}{d\breve{x}'}(\breve{x}'_0)}{M_\infty\rho_w}\left[e^{-(1+i)\sqrt{\frac{\breve{\omega}\rho_w}{2\mu_w}}\breve{Y}_*}-1\right]+i\breve{\omega}\tau_w M_\infty\breve{F}(\breve{x}'_0)\breve{Y}_*\right\}+c.c.. \tag{4.94}$$

Finally, the fourth term, $\sigma\delta\breve{U}_*(t,\breve{x}_*,\breve{Y}_*)$, represents the perturbations produced in the boundary layer due to the interaction of the Stokes layer with the steady flow field around the roughness.

Similarly, the function $\breve{v}_S$ in the asymptotic expansion of $\hat{v}$ is obtained by substituting (4.75) into (4.73) and choosing $\breve{x}'=\breve{x}'_0$,

$$\breve{v}_S = M_\infty\breve{\omega}^2\breve{F}(\breve{x}'_0)\breve{Y}_* e^{i\breve{\omega}t}+c.c.. \tag{4.95}$$

The first two terms in the asymptotic expansion of the pressure $\hat{p}$ in (4.92) are obtained by setting $\breve{x}'=\breve{x}'_0+Re^{-1/4}\breve{x}_*$ in (4.35) and using the Taylor expansion of the function $\breve{F}(\breve{x}')$. This yields

$$P_0(t)=\frac{i\breve{\omega}}{M_\infty}\breve{F}(\breve{x}'_0)e^{i\breve{\omega}t}+c.c., \tag{4.96a}$$

$$p_0(t)=\frac{i\breve{\omega}}{M_\infty}\frac{d\breve{F}}{d\breve{x}'}(\breve{x}'_0)e^{i\breve{\omega}t}+c.c.. \tag{4.96b}$$

The third term, $Re^{-1/4}\delta\breve{P}_r(\breve{x}_*)$, describes the steady perturbations produced by the roughness, and the fourth term, $Re^{-1/4}\sigma\delta\breve{P}_*(t,\breve{x}_*)$, is due to the interaction of the Stokes layer with the roughness.

For our purposes it is sufficient to keep only two terms in the asymptotic expansions (4.92) of the enthalpy, $\hat{h}$, density, $\hat{\rho}$, and viscosity coefficient, $\hat{\mu}$. In the leading order approximation these quantities are constant in region 1, with h_w, ρ_w and μ_w denoting the values of functions $h_w(x)$, $\rho_w(x)$ and $\mu_w(x)$ in the solution (4.42) of the boundary-layer equations (4.38) at the position, $x=x_0$, of the roughness. The next order terms, $\sigma h_0(t)$, $\sigma\rho_0(t)$, $\sigma\mu_0(t)$, are caused by the pressure pulsations in time. With $P_0(t)$ given by (4.96a) we can find the functions $h_0(t)$ and $\rho_0(t)$ by substituting (4.92) into the energy equation (A.5c). This results in

$$\rho_w \frac{dh_0}{dt} = \frac{dP_0}{dt}. \tag{4.97}$$

It further follows from the state equation (A.5e) that

$$h_w = \frac{1}{(\gamma - 1)M_\infty^2} \frac{1}{\rho_w}, \qquad \rho_w h_0 + h_w \rho_0 = \frac{\gamma}{\gamma - 1} P_0. \tag{4.98a,b}$$

The time periodic solution of (4.97) is

$$h_0 = \frac{P_0}{\rho_w}, \tag{4.99}$$

which being substituted into (4.98) yields

$$\rho_0 = \rho_w M_\infty^2 P_0. \tag{4.100}$$

In order to progress further we need to introduce a viscosity-temperature law. We shall assume that relationship between viscosity and temperature is described by so called the power law and is written as

$$\hat{\mu} = C\hat{h}^n, \tag{4.101}$$

with C and n being constants. This equation is often used in analytical investigations as the more precise Sutherland's law is complex (Rogers, 1992). Substituting asymptotic expansion for $\hat{\mu}$ and $\hat{h}$ from (4.92) into (4.101), and working with $O(1)$ and $O(\sigma)$ terms, one can easily show that

$$\frac{\mu_0}{\mu_w} = n\frac{h_0}{h_w}. \tag{4.102}$$

Substituting (4.99) and the first of equations (4.98) into (4.102) we finally find that

$$\mu_0 = n(\gamma - 1)M_\infty^2 \mu_w P_0. \tag{4.103}$$

Substitution of (4.92) into the longitudinal momentum (A.5a) and continuity (A.5d) equations results in the following set of equations describing the steady flow past the roughness,

$$\begin{aligned} \rho_w \tau_w \breve{Y}_* \frac{\partial \breve{U}_r}{\partial \breve{x}_*} + \rho_w \tau_w \breve{V}_r = -\frac{d\breve{P}_r}{d\breve{x}_*} + \mu_w \frac{\partial^2 \breve{U}_r}{\partial \breve{Y}_*^2}, \\ \frac{\partial \breve{U}_r}{\partial \breve{x}_*} + \frac{\partial \breve{V}_r}{\partial \breve{Y}_*} = 0. \end{aligned} \tag{4.104a,b}$$

These have to be solved subject to the boundary conditions

$$\begin{aligned} &\breve{U}_r = \breve{V}_r = 0 && \text{at} && \breve{Y}_* = 0, \\ &\breve{U}_r = \breve{A}_r(\breve{x}_*) && \text{at} && \breve{Y}_* = \infty, \\ &\breve{U}_r = 0 && \text{at} && \breve{x}_* = -\infty. \end{aligned} \tag{4.105a-c}$$

Here we impose the no-slip condition on the surface of the roughness, and the matching conditions with the solution in region 2 (see Figure 4.2), and the solution in the Stokes layer upstream of the roughness.

In the next order approximations, the governing equations are

$$\begin{aligned} \rho_w \frac{\partial \breve{U}_*}{\partial t} + \rho_w \tau_w \breve{Y}_* \frac{\partial \breve{U}_*}{\partial \breve{x}_*} + \rho_w \tau_w \breve{V}_* = -\frac{\partial \breve{P}_*}{\partial \breve{x}_*} + \mu_w \frac{\partial^2 \breve{U}_*}{\partial \breve{Y}_*^2} + \\ + \frac{1}{M_\infty} \frac{d\breve{F}}{d\breve{x}'}(\breve{x}'_0) \breve{Q}_1 e^{i\breve{\omega} t} + M_\infty \breve{F}(\breve{x}'_0) \breve{Q}_2 e^{i\breve{\omega} t} + c.c., \end{aligned} \tag{4.106a}$$

$$\frac{\partial \breve{U}_*}{\partial \breve{x}_*} + \frac{\partial \breve{V}_*}{\partial \breve{Y}_*} = 0, \tag{4.106b}$$

with

$$\begin{aligned} \breve{Q}_1(\breve{x}_*, \breve{Y}_*) &= (1+i)\sqrt{\frac{\breve{\omega}\rho_w}{2\mu_w}} \breve{V}_r e^{-(1+i)\sqrt{\frac{\breve{\omega}\rho_w}{2\mu_w}}\breve{Y}_*} - \left[e^{-(1+i)\sqrt{\frac{\breve{\omega}\rho_w}{2\mu_w}}\breve{Y}_*} - 1 \right] \frac{\partial \breve{U}_r}{\partial \breve{x}_*}, \\ \breve{Q}_2(\breve{x}_*, \breve{Y}_*) &= i\breve{\omega} \left[2\frac{d\breve{P}_r}{d\breve{x}_*} + i\breve{\omega}\rho_w \breve{Y}_* \frac{\partial \breve{U}_r}{\partial \breve{Y}_*} + \big[n(\gamma-1) - 2\big] \mu_w \frac{\partial^2 \breve{U}_r}{\partial \breve{Y}_*^2} \right]. \end{aligned}$$

Equations (4.106) have to be solved with the boundary conditions

$$\begin{aligned} &\breve{U}_* = \breve{V}_* = 0 && \text{at} && \breve{Y}_* = 0, \\ &\breve{U}_* = \breve{A}_*(t, \breve{x}_*) && \text{at} && \breve{Y}_* = \infty, \\ &\breve{U}_* = 0 && \text{at} && \breve{x}_* = -\infty. \end{aligned} \tag{4.107a-c}$$

In both approximations the pressure does not change across the boundary layer,

$$\frac{\partial \breve{P}_r}{\partial \breve{Y}_*} = \frac{\partial \breve{P}_*}{\partial \breve{Y}_*} = 0, \tag{4.108}$$

which may be confirmed by substituting (4.92) into the lateral momentum equation (A.5*b*).

4.4.2 Region 2

The solution in the middle tier (region 2) is sought in the form

$$\hat{u} = U_\infty \Big\{ U_{00}(Y) + \sigma U_1(t,Y) + Re^{-1/8}\sigma U_2(t,Y) + \\ + Re^{-1/8}\delta \widetilde{U}_r(\breve{x}_*, Y) + Re^{-1/8}\sigma\delta \widetilde{U}_*(t, \breve{x}_*, Y) + \cdots \Big\}, \tag{4.109a}$$

$$\hat{v} = U_\infty \Big\{ Re^{-1/4}\sigma V_1(t,Y) + \\ + Re^{-1/4}\delta \widetilde{V}_r(\breve{x}_*, Y) + Re^{-1/4}\delta\sigma \widetilde{V}_*(t, \breve{x}_*, Y) + \cdots \Big\}, \tag{4.109b}$$

$$\hat{p} = p_\infty + \rho_\infty U_\infty^2 \Big\{ \sigma P_0(t) + Re^{-1/4}\sigma p_0(t)\breve{x}_* + \\ + Re^{-1/4}\delta \widetilde{P}_r(\breve{x}_*, Y) + Re^{-1/4}\sigma\delta \widetilde{P}_*(t, \breve{x}_*, Y) + \cdots \Big\}, \tag{4.109c}$$

$$\hat{h} = U_\infty^2 \Big\{ H_{00}(Y) + \sigma H_1(t,Y) + \\ + Re^{-1/8}\delta \widetilde{H}_r(\breve{x}_*, Y) + Re^{-1/8}\sigma\delta \widetilde{H}_*(t, \breve{x}_*, Y) + \cdots \Big\}, \tag{4.109d}$$

$$\hat{\rho} = \rho_\infty \Big\{ R_{00}(Y) + \sigma R_1(t,Y) + \\ + Re^{-1/8}\delta \widetilde{R}_r(\breve{x}_*, Y) + Re^{-1/8}\sigma\delta \widetilde{R}_*(t, \breve{x}_*, Y) + \cdots \Big\}. \tag{4.109e}$$

The terms in the first lines are obtained by re-expanding (4.86) in terms of the variables of region 2,

$$\hat{t} = \frac{L}{U_\infty} Re^{-1/4} t, \qquad \hat{x} = \hat{x}_0 + L Re^{-3/8}\breve{x}_*, \qquad \hat{y} = L Re^{-1/2} Y. \tag{4.110a-c}$$

It follows from (4.90) that

$$P_0 = \frac{1}{M_\infty}\frac{\partial f}{\partial t}, \qquad U_1 = M_\infty Y \frac{dU_{00}}{dY}\frac{\partial f}{\partial t}, \qquad V_1 = -M_\infty Y \frac{\partial^2 f}{\partial t^2}, \\ R_1 = M_\infty \frac{d(R_{00}Y)}{dY}\frac{\partial f}{\partial t}, \qquad H_1 = \frac{1}{M_\infty R_{00}}\left[1 - \frac{Y}{(\gamma-1)R_{00}}\frac{dR_{00}}{dY}\right]\frac{\partial f}{\partial t}. \tag{4.111a-e}$$

The terms in the second lines in (4.109) represent the displacement effect of the viscous sublayer (region 1); see Sychev *et al.* (1998).

Substitution of (4.109) into the Navier-Stokes equations (A.5) shows that the steady perturbations produced by the wall roughness are described by

$$U_{00}\frac{\partial \widetilde{U}_r}{\partial \breve{x}_*}+\widetilde{V}_r\frac{dU_{00}}{dY}=0, \tag{4.112a}$$

$$\frac{\partial \widetilde{P}_r}{\partial Y}=0, \tag{4.112b}$$

$$U_{00}\frac{\partial \widetilde{H}_r}{\partial \breve{x}_*}+\widetilde{V}_r\frac{dH_{00}}{dY}=0, \tag{4.112c}$$

$$R_{00}\frac{\partial \widetilde{U}_r}{\partial \breve{x}_*}+U_{00}\frac{\partial \widetilde{R}_r}{\partial \breve{x}_*}+R_{00}\frac{\partial \widetilde{V}_r}{\partial Y}+\widetilde{V}_r\frac{dR_{00}}{dY}=0, \tag{4.112d}$$

$$H_{00}=\frac{1}{(\gamma-1)M_\infty^2 R_{00}}, \qquad \widetilde{H}_r=-\frac{H_{00}}{R_{00}}\widetilde{R}_r. \tag{4.112e}$$

These equations are easily solved using the following elimination procedure. Substitution of (4.112e) into the energy equation (4.112c) results in

$$U_{00}\frac{\partial \widetilde{R}_r}{\partial \breve{x}_*}+\widetilde{V}_r\frac{dR_{00}}{dY}=0. \tag{4.113}$$

This reduces the continuity equation (4.112d) to

$$\frac{\partial \widetilde{U}_r}{\partial \breve{x}_*}+\frac{\partial \widetilde{V}_r}{\partial Y}=0. \tag{4.114}$$

It remains to eliminate $\partial\widetilde{U}_r/\partial\breve{x}_*$ from (4.112a) and (4.114), and we arrive at a conclusion that

$$\frac{\partial}{\partial Y}\left(\frac{\widetilde{V}_r}{U_{00}}\right)=0. \tag{4.115}$$

The solution of this equation satisfying the condition of matching with the solution in region 1

$$\left.\begin{aligned} \widetilde{V}_r &= -\frac{d\breve{A}_r}{d\breve{x}_*}Y+\cdots, \\ U_{00} &= \tau_w Y+\cdots \end{aligned}\right\} \quad \text{as} \quad Y\to 0 \tag{4.116a,b}$$

is written as

$$\widetilde{V}_r=-\frac{1}{\tau_w}\frac{d\breve{A}_r}{d\breve{x}_*}U_{00}. \tag{4.117}$$

In the next order approximation we have to solve the following set of equations

$$U_{00}\frac{\partial \widetilde{U}_*}{\partial \breve{x}_*}+\widetilde{V}_*\frac{dU_{00}}{dY}+U_1\frac{\partial \widetilde{U}_r}{\partial \breve{x}_*}+\widetilde{V}_r\frac{\partial U_1}{\partial Y}=0, \tag{4.118a}$$

$$\frac{\partial \widetilde{P}_*}{\partial Y}=0, \tag{4.118b}$$

$$U_{00}\frac{\partial \widetilde{H}_*}{\partial \breve{x}_*}+\widetilde{V}_*\frac{dH_{00}}{dY}+U_1\frac{\partial \widetilde{H}_r}{\partial \breve{x}_*}+\widetilde{V}_r\frac{\partial H_1}{\partial Y}=0, \tag{4.118c}$$

$$R_{00}\frac{\partial \widetilde{U}_*}{\partial \breve{x}_*}+U_{00}\frac{\partial \widetilde{R}_*}{\partial \breve{x}_*}+U_1\frac{\partial \widetilde{R}_r}{\partial \breve{x}_*}+R_{00}\frac{\partial \widetilde{V}_*}{\partial Y}+\widetilde{V}_*\frac{dR_{00}}{dY}+\widetilde{V}_r\frac{\partial R_1}{\partial Y}=0, \tag{4.118d}$$

$$H_{00}\widetilde{R}_*+R_{00}\widetilde{H}_*+H_1\widetilde{R}_r+R_1\widetilde{H}_r=0. \tag{4.118e}$$

These may be manipulated in the same way as the equations (4.112). Alternatively one can notice that the flow in region 2 is inviscid which allows to use the entropy conservation law

$$\frac{\partial S}{\partial \hat{t}}+\hat{u}\frac{\partial S}{\partial \hat{x}}+\hat{v}\frac{\partial S}{\partial \hat{y}}=0. \tag{4.119}$$

For our purposes it is convenient to choose the entropy function, S, to be

$$S=\frac{\hat{\rho}/\rho_\infty}{(\hat{p}/p_\infty)^{1/\gamma}}. \tag{4.120}$$

Using the asymptotic expansions for $\hat{p}$ and $\hat{\rho}$ from (4.109) in (4.120) we find that the asymptotic expansion of the entropy function is written as

$$\begin{aligned}\hat{S}=R_{00}(Y)+\sigma\Big[R_1(t,Y)-M_\infty^2R_{00}(Y)P_0(t)\Big]+Re^{-1/8}\delta\widetilde{R}_r(\breve{x}_*,Y)+\\+Re^{-1/8}\sigma\delta\Big[\widetilde{R}_*(t,\breve{x}_*,Y)-M_\infty^2\widetilde{R}_r(\breve{x}_*,Y)P_0(t)\Big]+\cdots.\end{aligned} \tag{4.121}$$

Substituting (4.121) into (4.119) and collecting $O(Re^{1/4}\delta\sigma)$ terms we arrive at the following equation,

$$U_{00}\frac{\partial \widetilde{R}_*}{\partial \breve{x}_*}+\widetilde{V}_*\frac{dR_{00}}{dY}+U_1\frac{\partial \widetilde{R}_r}{\partial \breve{x}_*}+\widetilde{V}_r\frac{\partial R_1}{\partial Y}=0. \tag{4.122}$$

It can be used to eliminate $\partial\widetilde{R}_*/\partial\breve{x}_*$ from the continuity equation (4.118d), which results in

$$\frac{\partial \widetilde{U}_*}{\partial \breve{x}_*}+\frac{\partial \widetilde{V}_*}{\partial Y}=0. \tag{4.123}$$

We can now use (4.123) to eliminate $\partial\widetilde{U}_*/\partial\breve{x}_*$ from the longitudinal momentum equation (4.118a). We find that

$$\frac{\partial}{\partial Y}\left(\frac{\widetilde{V}_*}{U_{00}}\right) = \frac{U_1}{U_{00}^2}\frac{\partial \widetilde{U}_r}{\partial \breve{x}_*} + \frac{\widetilde{V}_r}{U_{00}^2}\frac{\partial U_1}{\partial Y}. \tag{4.124}$$

In order to elucidate the physical meaning of the above equation we shall consider the slope of the streamlines in region 2. Using the asymptotic expansions for $\hat{u}$ and $\hat{v}$ in (4.109) it is easily deduced that

$$\frac{\hat{v}}{\hat{u}} = Re^{-1/4}\sigma\frac{V_1}{U_{00}} + Re^{-1/4}\delta\widetilde{\vartheta}_r + Re^{-1/4}\sigma\delta\widetilde{\vartheta}_* + \cdots\,, \tag{4.125}$$

where

$$\widetilde{\vartheta}_r = \frac{\widetilde{V}_r}{U_{00}}, \qquad \widetilde{\vartheta}_* = \frac{\widetilde{V}_*}{U_{00}} - \frac{U_1\widetilde{V}_r}{U_{00}^2}. \tag{4.126a,b}$$

We know from (4.115) that $\widetilde{\vartheta}_r$ does not change across region 2. Differentiating $\widetilde{\vartheta}_*$ with respect to Y and using equations (4.112a) and (4.112b) we find that

$$\frac{\partial\widetilde{\vartheta}_*}{\partial Y} = \frac{\partial}{\partial Y}\left(\frac{\widetilde{V}_*}{U_{00}}\right) - \frac{U_1}{U_{00}^2}\frac{\partial \widetilde{U}_r}{\partial \breve{x}_*} - \frac{\widetilde{V}_r}{U_{00}^2}\frac{\partial U_1}{\partial Y}, \tag{4.127}$$

which being compared with (4.124) shows that $\widetilde{\vartheta}_*$ also does not change across region 2. It, therefore, may be found through matching with the solution in region 1. It follows from the boundary condition for $\breve{U}_*$ in (4.107) and the continuity equation (4.106b) that at the outer edge of the viscous sublayer the normal velocity component exhibits the following behaviour

$$\breve{V}_* = -\frac{\partial \breve{A}_*}{\partial \breve{x}_*}\breve{Y}_* + \cdots \quad \text{as} \quad \breve{Y}_* \to \infty. \tag{4.128}$$

Consequently, at the bottom of regions 2,

$$\widetilde{V}_* = -\frac{\partial \breve{A}_*}{\partial \breve{x}_*}Y + \cdots \quad \text{as} \quad Y \to 0. \tag{4.129}$$

It further follows from (4.42), (4.111) and (4.117) that

$$\left.\begin{aligned} \widetilde{V}_r &= -\frac{d\breve{A}_r}{d\breve{x}_*}Y + \cdots\,, \\ U_{00} &= \tau_w Y + \cdots\,, \\ U_1 &= M_\infty \tau_w Y\frac{\partial f}{\partial t} + \cdots \end{aligned}\right\} \quad \text{as} \quad Y \to 0. \tag{4.130a,b}$$

Using these on the right hand side of the equation for $\widetilde{\vartheta}_*$ in (4.126) we can conclude that

$$\widetilde{\vartheta}_* = -\frac{1}{\tau_w}\frac{\partial \breve{A}_*}{\partial \breve{x}_*} + \frac{1}{\tau_w}\frac{d\breve{A}_r}{d\breve{x}_*} M_\infty \frac{\partial f}{\partial t} \tag{4.131}$$

everywhere in region 2.

4.4.3 Region 3

The perturbations in region 3 are produced by the vibrations of the wing surface and by the displacement effect of the boundary layer. The former were studied in §2. When doing this we used a stationary coordinates which did not move with the wing surface. We shall now call these the "old" coordinates. The triple-deck flow analysis is conducted in the coordinates which move with the wing surface. These will be called the "new" coordinates. The transformation between the two coordinate systems is given by

$$\begin{gathered}\hat{t}_{\text{old}} = \hat{t}_{\text{new}}, \quad \hat{x}_{\text{old}} = \hat{x}_{\text{new}}, \quad \hat{y}_{\text{old}} = \hat{y}_w + \hat{y}_{\text{new}}, \\ \hat{u}_{\text{old}} = \hat{u}_{\text{new}}, \quad \hat{v}_{\text{old}} = \frac{\partial \hat{y}_w}{\partial \hat{t}} + \hat{v}_{\text{new}},\end{gathered} \tag{4.132a-e}$$

where the function $\hat{y}_w(\hat{t}, \hat{x})$ is given by (4.2).

In region 3 the dimensionless time and coordinates are introduced as

$$\hat{t}_{\text{new}} = \frac{L}{U_\infty} Re^{-1/4} t, \quad \hat{x}_{\text{new}} = \hat{x}_0 + L Re^{-3/8} \breve{x}_*, \quad \hat{y}_{\text{new}} = L Re^{-3/8} \tilde{y}_*. \tag{4.133a-c}$$

Let us now reexpand the solution of the piston theory in terms of the variables (4.133) of region 3. We start with the vertical velocity component. According to (4.21) and (4.32),

$$\hat{v}_{\text{old}} = U_\infty \varepsilon Re^{1/4} \frac{\partial f}{\partial t}\big(t - M_\infty y, \breve{x}'\big). \tag{4.134}$$

We now substitute (4.134) together with the wing surface equation (4.2) into the transformation of $\hat{v}$ in (4.132). We have

$$\hat{v}_{\text{new}} = U_\infty \varepsilon Re^{1/4} \left[\frac{\partial f}{\partial t}\big(t - M_\infty y, \breve{x}'\big) - \frac{\partial f}{\partial t}\big(t, \breve{x}'\big)\right]. \tag{4.135}$$

The coordinates (4.22), (4.63) used in the piston theory (§2) are related to the coordinates (4.133) of region 3 as

$$LRe^{-1/8}\breve{x}' = \hat{x}_0 + LRe^{-3/8}\breve{x}_*, \tag{4.136a}$$

$$LRe^{-1/4}y = L\varepsilon f(t,\breve{x}') + LRe^{-3/8}\tilde{y}_*. \tag{4.136b}$$

This gives

$$\breve{x}' = \breve{x}_0' + Re^{-1/4}\breve{x}_*, \qquad y = Re^{-1/8}\big[\tilde{y}_* + \varepsilon Re^{3/8} f(t,\breve{x}_0')\big], \tag{4.137a,b}$$

where x_0' gives the position of the wall roughness in the piston theory variables.

It remains to substitute (4.137) into (4.135) and Taylor expand the resulting equation assuming that $\varepsilon Re^{3/8} \ll 1$. We find that the "inner expansion of the outer solution" is

$$\hat{v}_{new} = U_\infty \bigg\{ \varepsilon Re^{1/8}\Big[-M_\infty \frac{\partial^2 f}{\partial t^2}(t,\breve{x}_0')\,\tilde{y}_*\Big] + \cdots \bigg\}. \tag{4.138a}$$

Similarly, it may be deduced that the rest of the fluid dynamics functions are expanded as

$$\hat{u}_{new} = U_\infty \bigg\{ 1 + \varepsilon Re^{1/8}\Big[-\frac{1}{M_\infty}\frac{\partial f}{\partial \breve{x}'}(t,\breve{x}_0')\Big] + \cdots \bigg\}, \tag{4.138b}$$

$$\hat{p}_{new} = p_\infty + \rho_\infty U_\infty^2 \bigg\{ \varepsilon Re^{1/4}\Big[\frac{1}{M_\infty}\frac{\partial f}{\partial t}(t,\breve{x}_0')\Big] + \cdots \bigg\}, \tag{4.138c}$$

$$\hat{h}_{new} = h_\infty + U_\infty^2 \bigg\{ \varepsilon Re^{1/4}\Big[\frac{1}{M_\infty}\frac{\partial f}{\partial t}(t,\breve{x}_0')\Big] + \cdots \bigg\}, \tag{4.138d}$$

$$\hat{\rho}_{new} = \rho_\infty \bigg\{ 1 + \varepsilon Re^{1/4}\Big[M_\infty \frac{\partial f}{\partial t}(t,\breve{x}_0')\Big] + \cdots \bigg\}. \tag{4.138e}$$

In order to evaluate the perturbations induced in region 3 by the displacement effect of the boundary layer we need to calculate the streamline slope at the outer edge of region 2. Substituting (4.117) into the first of equations (4.126) we find

$$\widetilde{\vartheta}_r = -\frac{1}{\tau_w}\frac{d\breve{A}_r}{d\breve{x}_*}. \tag{4.139}$$

If we now substitute (4.139) together with (4.131) into (4.125), then we will find that in region 2

$$\frac{\hat{v}}{\hat{u}} = Re^{-1/4}\sigma\frac{V_1}{U_{00}} + Re^{-1/4}\delta\left\{-\frac{1}{\tau_w}\frac{d\breve{A}_r}{d\breve{x}_*}\right\} + \\ + Re^{-1/4}\sigma\delta\left\{-\frac{1}{\tau_w}\frac{\partial\breve{A}_*}{\partial\breve{x}_*} + \frac{1}{\tau_w}\frac{d\breve{A}_r}{d\breve{x}_*}M_\infty\frac{\partial f}{\partial t}\right\} + \cdots. \tag{4.140}$$

This equation is written in the body-fitted coordinates with $\hat{x}$ lying on the roughness surface. We shall perform the flow analysis in the upper tier (region 3) in the coordinates with $\hat{x}$-axis following the body contour without roughness. Consequently, when performing the matching of the streamline slope in regions 2 and 3 we need to add to (4.140) the slope of the body roughness. Differentiating (4.91) we have

$$\frac{d\hat{y}}{d\hat{x}} = Re^{-1/4}\delta\frac{d\breve{G}}{d\breve{x}_*}. \tag{4.141}$$

We add this to (4.140) and use for V_1 an explicit expression; see (4.111). This results in

$$\frac{\hat{v}}{\hat{u}} = Re^{-1/4}\sigma\left\{-M_\infty\frac{Y}{U_{00}(Y)}\frac{\partial^2 f}{\partial t^2}\right\} + Re^{-1/4}\delta\left\{\frac{d\breve{G}}{d\breve{x}_*} - \frac{1}{\tau_w}\frac{d\breve{A}_r}{d\breve{x}_*}\right\} + \\ + Re^{-1/4}\sigma\delta\left\{-\frac{1}{\tau_w}\frac{\partial\breve{A}_*}{\partial\breve{x}_*} + \frac{1}{\tau_w}\frac{d\breve{A}_r}{d\breve{x}_*}M_\infty\frac{\partial f}{\partial t}\right\} + \cdots. \tag{4.142}$$

This suggest that the solution in the upper tier (region 3 in Figure 4.2) should be sought in the form

$$\hat{u} = U_\infty\left\{1 + \sigma Re^{-1/8}\left[-\frac{1}{M_\infty}\frac{\partial f}{\partial\breve{x}'}(t,\breve{x}'_0)\right] + \cdots \right. \\ \left. + Re^{-1/4}\delta\tilde{u}_r(\breve{x}_*,\tilde{y}_*) + Re^{-1/4}\delta\sigma\tilde{u}_*(t,\breve{x}_*,\tilde{y}_*) + \cdots\right\}, \tag{4.143a}$$

$$\hat{v} = U_\infty\left\{\sigma Re^{-1/8}\left[-M_\infty\frac{\partial^2 f}{\partial t^2}(t,\breve{x}'_0)\,\tilde{y}_*\right] + \cdots \right. \\ \left. + Re^{-1/4}\delta\tilde{v}_r(\breve{x}_*,\tilde{y}_*) + Re^{-1/4}\delta\sigma\tilde{v}_*(t,\breve{x}_*,\tilde{y}_*) + \cdots\right\}, \tag{4.143b}$$

$$\hat{p} = p_\infty + \rho_\infty U_\infty^2\left\{\sigma\left[\frac{1}{M_\infty}\frac{\partial f}{\partial t}(t,\breve{x}'_0)\right] + \cdots \right. \\ \left. + Re^{-1/4}\delta\tilde{p}_r(\breve{x}_*,\tilde{y}_*) + Re^{-1/4}\delta\sigma\tilde{p}_*(t,\breve{x}_*,\tilde{y}_*) + \cdots\right\}, \tag{4.143c}$$

$$\hat{h} = h_\infty + U_\infty^2 \Big\{ \sigma \Big[\frac{1}{M_\infty} \frac{\partial f}{\partial t}(t, \breve{x}_0') \Big] + \cdots$$
$$+ Re^{-1/4} \delta \tilde{h}_r(\breve{x}_*, \tilde{y}_*) + Re^{-1/4} \delta \sigma \tilde{h}_*(t, \breve{x}_*, \tilde{y}_*) + \cdots \Big], \tag{4.143d}$$
$$\hat{\rho} = \rho_\infty \Big\{ 1 + \sigma \Big[M_\infty \frac{\partial f}{\partial t}(t, \breve{x}_0') \Big] + \cdots$$
$$+ Re^{-1/4} \delta \tilde{\rho}_r(\breve{x}_*, \tilde{y}_*) + Re^{-1/4} \delta \sigma \tilde{\rho}_*(t, \breve{x}_*, \tilde{y}_*) + \cdots \Big\}, \tag{4.143e}$$

with the independent variables defined by

$$\hat{t} = \frac{L}{U_\infty} Re^{-1/4} t, \qquad \hat{x} = \hat{x}_0 + L Re^{-3/8} \breve{x}_*, \qquad \hat{y} = L Re^{-3/8} \tilde{y}_*. \tag{4.144a-c}$$

Substitution of (4.143) into the Navier-Stokes equations results in the following set of equations for the steady perturbations in region 3,

$$\frac{\partial \tilde{u}_r}{\partial \breve{x}_*} = -\frac{\partial \tilde{p}_r}{\partial \breve{x}_*}, \tag{4.145a}$$
$$\frac{\partial \tilde{v}_r}{\partial \breve{x}_*} = -\frac{\partial \tilde{p}_r}{\partial \tilde{y}_*}, \tag{4.145b}$$
$$\frac{\partial \tilde{h}_r}{\partial \breve{x}_*} = \frac{\partial \tilde{p}_r}{\partial \breve{x}_*}, \tag{4.145c}$$
$$\frac{\partial \tilde{\rho}_r}{\partial \breve{x}_*} + \frac{\partial \tilde{u}_r}{\partial \breve{x}_*} + \frac{\partial \tilde{v}_r}{\partial \tilde{y}_*} = 0, \tag{4.145d}$$
$$\tilde{h}_r + \frac{\tilde{\rho}_r}{(\gamma - 1) M_\infty^2} = \frac{\gamma}{\gamma - 1} \tilde{p}_r. \tag{4.145e}$$

In the next order approximation we have

$$\frac{\partial \tilde{u}_*}{\partial \breve{x}_*} + M_\infty \frac{\partial f}{\partial t}(t, \breve{x}_0') \frac{\partial \tilde{u}_r}{\partial \breve{x}_*} = -\frac{\partial \tilde{p}_*}{\partial \breve{x}_*}, \tag{4.146a}$$
$$\frac{\partial \tilde{v}_*}{\partial \breve{x}_*} + M_\infty \frac{\partial f}{\partial t}(t, \breve{x}_0') \frac{\partial \tilde{v}_r}{\partial \breve{x}_*} = -\frac{\partial \tilde{p}_*}{\partial \tilde{y}_*}, \tag{4.146b}$$
$$\frac{\partial \tilde{h}_*}{\partial \breve{x}_*} + M_\infty \frac{\partial f}{\partial t}(t, \breve{x}_0') \frac{\partial \tilde{h}_r}{\partial \breve{x}_*} = \frac{\partial \tilde{p}_*}{\partial \breve{x}_*}, \tag{4.146c}$$
$$\frac{\partial \tilde{\rho}_*}{\partial \breve{x}_*} + \frac{\partial \tilde{u}_*}{\partial \breve{x}_*} + \frac{\partial \tilde{v}_*}{\partial \tilde{y}_*} = -M_\infty \frac{\partial f}{\partial t}(t, \breve{x}_0') \Big(\frac{\partial \tilde{u}_r}{\partial \breve{x}_*} + \frac{\partial \tilde{v}_r}{\partial \tilde{y}_*} \Big), \tag{4.146d}$$
$$\tilde{h}_* + \frac{\tilde{\rho}_*}{(\gamma - 1) M_\infty^2} + \frac{\partial f}{\partial t}(t, \breve{x}_0') \Big(M_\infty \tilde{h}_r + \frac{1}{M_\infty} \tilde{\rho}_r \Big) = \frac{\gamma}{\gamma - 1} \tilde{p}_*. \tag{4.146e}$$

The streamline slope in region 2 is given by the equation (4.142). In order to deduce the corresponding equation in region 3 we need to use the asymptotic expansions for $\hat{u}$ and $\hat{v}$ in (4.143). We find that

$$\frac{\hat{v}}{\hat{u}} = Re^{-1/8}\sigma\left\{ - M_\infty \frac{\partial^2 f}{\partial t^2}\tilde{y}_*\right\} + Re^{-1/4}\delta\tilde{v}_r + Re^{-1/4}\sigma\delta\tilde{v}_* + \cdots . \tag{4.147}$$

Setting $\tilde{y}_* \to 0$ in (4.147) and comparing the result with (4.142), we can conclude that

$$\tilde{v}_r\Big|_{\tilde{y}_*=0} = \frac{d\breve{G}}{d\breve{x}_*} - \frac{1}{\tau_w}\frac{d\breve{A}_r}{d\breve{x}_*}, \tag{4.148a}$$

$$\tilde{v}_*\Big|_{\tilde{y}_*=0} = -\frac{1}{\tau_w}\frac{\partial\breve{A}_*}{\partial\breve{x}_*} + \frac{1}{\tau_w}\frac{d\breve{A}_r}{d\breve{x}_*}M_\infty\frac{\partial f}{\partial t}. \tag{4.148b}$$

The set of equations (4.145) may be reduced to a single equation for the pressure, $\tilde{p}_r$. Indeed, solving the state equation (4.145e) for $\tilde{h}_r$ and substituting the result into the energy equation (4.145c) results in

$$\frac{\partial\tilde{\rho}_r}{\partial\tilde{x}_*} = M_\infty^2\frac{\partial\tilde{p}_r}{\partial\tilde{x}_*}. \tag{4.149}$$

Now we substitute (4.149) and the $\hat{x}$-momentum equation (4.145a) into the continuity equation (4.145d). We find that

$$(M_\infty^2 - 1)\frac{\partial\tilde{p}_r}{\partial\tilde{x}_*} + \frac{\partial\tilde{v}_r}{\partial\tilde{y}_*} = 0. \tag{4.150}$$

It remains to cross-differentiate (4.150) with the $\hat{y}$-momentum equation (4.145b), and we will have

$$(1 - M_\infty^2)\frac{\partial^2\tilde{p}_r}{\partial\breve{x}_*^2} + \frac{\partial^2\tilde{p}_r}{\partial\tilde{y}_*^2} = 0, \tag{4.151}$$

The boundary condition for this equation is obtained by setting $\tilde{y}_* = 0$ in (4.145b) and using the matching condition (4.148a). This shows that

$$\frac{\partial\tilde{p}_r}{\partial\tilde{y}_*}\Big|_{\tilde{y}_*=0} = \frac{1}{\tau_w}\frac{d^2\breve{A}_r}{d\breve{x}_*^2} - \frac{d^2\breve{G}}{d\breve{x}_*^2}. \tag{4.152}$$

In order to close the boundary-value problem (4.151), (4.152) we shall also impose the attenuation condition

$$\tilde{p}_r \to 0 \quad \text{as} \quad \breve{x}_*^2 + \tilde{y}_*^2 \to \infty. \tag{4.153}$$

Similarly, the set of equations (4.146) may be reduced to the following equation for

$\tilde{p}_*$,

$$(1-M_\infty^2)\frac{\partial^2\tilde{p}_*}{\partial\breve{x}_*^2}+\frac{\partial^2\tilde{p}_*}{\partial\tilde{y}_*^2}=-(\gamma-1)M_\infty^3\frac{\partial f}{\partial t}(t,\breve{x}_0')\frac{\partial^2\tilde{p}_r}{\partial\breve{x}_*^2}. \tag{4.154a}$$

It should be solved with

$$\left.\frac{\partial\tilde{p}_*}{\partial\tilde{y}_*}\right|_{\tilde{y}_*=0}=\frac{1}{\tau_w}\frac{\partial^2\tilde{A}_*}{\partial\breve{x}_*^2}-\left\{i\breve{\omega}M_\infty\breve{F}(\breve{x}_0')\frac{d^2\breve{G}}{d\breve{x}_*^2}e^{i\breve{\omega}t}+c.c.\right\}, \tag{4.154b}$$

and

$$\tilde{p}_*\to 0\quad\text{as}\quad\breve{x}_*^2+\tilde{y}_*^2\to\infty. \tag{4.154c}$$

4.4.4 Viscous-inviscid interaction problem

We have found that in order to describe the steady flow past a wall roughness one has to solve the equations (4.104), (4.105) governing the flow in viscous sublayer (region 1) coupled with the equations (4.151) governing the flow in upper tier (region 3). We shall now write both sets of equations in canonical form. We apply the following affine transformations to the variables in the viscous sublayer,

$$\breve{U}_r=\frac{\mu_w^{1/4}\rho_w^{-1/2}}{\tau_w^{-1/4}\beta^{1/4}}U_r,\qquad\breve{V}_r=\frac{\mu_w^{3/4}\rho_w^{-1/2}}{\tau_w^{-3/4}\beta^{-1/4}}V_r,\qquad\breve{P}_r=\frac{\mu_w^{1/2}}{\tau_w^{-1/2}\beta^{1/2}}P_r, \tag{4.155a-c}$$

$$\breve{A}_r=\frac{\mu_w^{1/4}\rho_w^{-1/2}}{\tau_w^{-1/4}\beta^{1/4}}A_r,\qquad\breve{x}_*=\frac{\mu_w^{-1/4}\rho_w^{-1/2}}{\tau_w^{5/4}\beta^{3/4}}x_*,\qquad\breve{Y}_*=\frac{\mu_w^{1/4}\rho_w^{-1/2}}{\tau_w^{3/4}\beta^{1/4}}Y_*, \tag{4.155d-f}$$

where $\beta=\sqrt{1-M_\infty^2}$. We also transform the upper tier variables as

$$\tilde{p}_r=\frac{\mu_w^{1/2}}{\tau_w^{-1/2}\beta^{1/2}}p_r,\qquad\tilde{y}_*=\frac{\mu_w^{-1/4}\rho_w^{-1/2}}{\tau_w^{5/4}\beta^{7/4}}y_*,\qquad\breve{G}=\frac{\mu_w^{1/4}\rho_w^{-1/2}}{\tau_w^{3/4}\beta^{1/4}}G, \tag{4.156a-c}$$

As a result the viscous sublayer problem assumes the form

$$Y_*\frac{\partial U_r}{\partial x_*}+V_r=-\frac{dP_r}{dx_*}+\frac{\partial^2U_r}{\partial Y_*^2}, \tag{4.157a}$$

$$\frac{\partial U_r}{\partial x_*}+\frac{\partial V_r}{\partial Y_*}=0, \tag{4.157b}$$

and

$$U_r = V_r = 0 \quad \text{at} \quad Y_* = 0, \tag{4.157c}$$

$$U_r = A_r(x_*) \quad \text{at} \quad Y_* = \infty, \tag{4.157d}$$

$$U_r = 0 \quad \text{at} \quad x_* = -\infty, \tag{4.157e}$$

and the upper tier problem turns into

$$\frac{\partial^2 p_r}{\partial x_*^2} + \frac{\partial^2 p_r}{\partial y_*^2} = 0, \tag{4.158a}$$

$$p_r = P_r \quad \text{at} \quad y_* = 0, \tag{4.158b}$$

$$\left.\frac{\partial p_r}{\partial y_*}\right|_{y_*=0} = \frac{d^2 A_r}{dx_*^2} - \frac{d^2 G}{dx_*^2}, \tag{4.158c}$$

$$p_r \to 0 \quad \text{as} \quad x_*^2 + y_*^2 \to \infty. \tag{4.158d}$$

Here function A_r is still unknown but G is the shape of the roughness on the airfoil. Similarly, we shall apply the affine transformations

$$\breve{U}_* = \frac{\mu_w^{1/4}\rho_w^{-1/2}}{\tau_w^{-1/4}\beta^{1/4}} U_*, \qquad \breve{V}_* = \frac{\mu_w^{3/4}\rho_w^{-1/2}}{\tau_w^{-3/4}\beta^{-1/4}} V_*, \qquad \breve{P}_* = \frac{\mu_w^{1/2}}{\tau_w^{-1/2}\beta^{1/2}} P_*, \tag{4.159a-c}$$

$$\breve{A}_* = \frac{\mu_w^{1/4}\rho_w^{-1/2}}{\tau_w^{-1/4}\beta^{1/4}} A_*, \qquad t = \frac{\mu_w^{-1/2}}{\tau_w^{3/2}\beta^{1/2}} t_*, \qquad \breve{\omega} = \frac{\mu_w^{1/2}}{\tau_w^{-3/2}\beta^{-1/2}} \omega, \tag{4.159d-f}$$

$$\breve{F} = \frac{\mu_w^{-1/2}}{\tau_w^{3/2}\beta^{1/2}} F, \qquad \breve{x}' = \frac{\mu_w^{-3/4}\rho_w^{-1/2}}{\tau_w^{7/4}\beta^{1/4}} x' \tag{4.159g,h}$$

to the unsteady viscous sublayer problem (4.106), and

$$\tilde{p}_* = \frac{\mu_w^{1/2}}{\tau_w^{-1/2}\beta^{1/2}} p_*. \tag{4.160}$$

to the unsteady pressure perturbations in the upper tier, governed by (4.154).

This turns the viscous sublayer equations into

$$\frac{\partial U_*}{\partial t_*} + Y_* \frac{\partial U_*}{\partial x_*} + V_* = -\frac{\partial P_*}{\partial x_*} + \frac{\partial^2 U_*}{\partial Y_*^2} + \\ + \frac{1}{M_\infty}\frac{dF}{dx'}(x'_0) Q_1 e^{i\omega t_*} + M_\infty F(x'_0) Q_2 e^{i\omega t_*} + c.c., \tag{4.161a}$$

$$\frac{\partial U_*}{\partial x_*} + \frac{\partial V_*}{\partial Y_*} = 0, \tag{4.161b}$$

with

$$Q_1(x_*, Y_*) = (1+i)\sqrt{\frac{\omega}{2}} V_r e^{-(1+i)\sqrt{\frac{\omega}{2}}Y_*} - \left[e^{-(1+i)\sqrt{\frac{\omega}{2}}Y_*} - 1\right]\frac{\partial U_r}{\partial x_*},$$
$$Q_2(x_*, Y_*) = i\omega\left[2\frac{dP_r}{dx_*} + i\omega Y_* \frac{\partial U_r}{\partial Y_*} + \left[n(\gamma-1) - 2\right]\frac{\partial^2 U_r}{\partial Y_*^2}\right].$$

The boundary conditions for these equations assume the form

$$U_* = V_* = 0 \quad \text{at} \quad Y_* = 0, \tag{4.161c}$$
$$U_* = A_*(t_*, x_*) \quad \text{at} \quad Y_* = \infty, \tag{4.161d}$$
$$U_* = 0 \quad \text{at} \quad x_* = -\infty. \tag{4.161e}$$

The corresponding upper tier problem now has the form

$$\frac{\partial^2 p_*}{\partial x_*^2} + \frac{\partial^2 p_*}{\partial y_*^2} = -(\gamma - 1)\frac{M_\infty^3}{1 - M_\infty^2}\frac{\partial^2 p_r}{\partial x_*^2}\left\{i\omega F(x'_0) e^{i\omega t_*} + c.c.\right\}, \tag{4.162a}$$
$$\left.\frac{\partial p_*}{\partial y_*}\right|_{y_*=0} = \frac{\partial^2 A_*}{\partial x_*^2} - \left\{i\omega M_\infty F(x'_0)\frac{d^2 G}{dx_*^2} e^{i\omega t_*} + c.c.\right\}, \tag{4.162b}$$
$$p_* \to 0 \quad \text{as} \quad x_*^2 + y_*^2 \to \infty. \tag{4.162c}$$

4.5 Solution of the viscous-inviscid interaction problem

In solving the viscous-inviscid interaction problem we will use the Fourier Transform technique. As in Chapter 2 the interaction problem consists of two problems the steady (4.157), (4.158) and the unsteady (4.161), (4.162) problems. The first problem determines steady perturbations generated by the roughness, which is achieved by finding a displacement function A_r as a function of the prescribed shape of the roughness G. The second problem will look at two mechanisms which generate Tollman-Schlichting waves in the flow. Similarly as for the steady case it is achieved by finding a displacement function A_*, which now expected to be a function of the shape of the roughness, Mach number and surface vibrations F.

4.5.1 Steady problem

It is convenient to start with the inviscid equation (4.158a). We introduce the Fourier Transform of the pressure, p_r, as follows

$$\bar{p}_r(k, y_*) = \int_{-\infty}^{\infty} p_r(x_*, y_*) e^{-ikx_*} dx_*, \tag{4.163}$$

which reduces (4.158a) to the following ordinary differential equation,

$$-k^2 \bar{p}_r + \frac{d^2 \bar{p}_r}{dy_*^2} = 0, \tag{4.164a}$$

The Fourier Transforms of the boundary conditions (4.158) are written as

$$\bar{p}_r = 0 \qquad \text{at} \quad y_* = \infty, \tag{4.164b}$$

$$\frac{d\bar{p}_r}{dy_*} = k^2 \big[\bar{G}(k) - \bar{A}_r(k)\big] \quad \text{at} \quad y_* = 0, \tag{4.164c}$$

where $\bar{G}(k)$ and $\bar{A}_r(k)$ are the Fourier Transforms of the roughness shape function, $G(x_*)$ and the displacement function, $A_r(x_*)$, respectively.

The solution to (4.164) is written as

$$\bar{p}_r = |k| \big[\bar{A}_r(k) - \bar{G}(k)\big] e^{-|k| y_*}. \tag{4.165}$$

Setting $y_* = 0$ in the above equation gives the Fourier Transform of the pressure in the viscous sublayer,

$$\bar{P}_r = |k| \big[\bar{A}_r - \bar{G}(k)\big]. \tag{4.166}$$

Now we turn to the viscous problem (4.157). Applying the Fourier Transform to (4.157a) and (4.157b) we have

$$ikY_* \bar{U}_r + \bar{V}_r = -ik\bar{P}_r + \frac{d^2 \bar{U}_r}{dY_*^2}, \tag{4.167a}$$

$$ik\bar{U}_r + \frac{d\bar{V}_r}{dY_*} = 0, \tag{4.167b}$$

while the boundary conditions (4.157c)–(4.157e) assume the form

$$\bar{U}_r = \bar{V}_r = 0 \quad \text{at} \quad Y_* = 0, \tag{4.167c}$$
$$\bar{U}_r = \bar{A}_r \quad \text{at} \quad Y_* = \infty. \tag{4.167d}$$

If we set $Y_* = 0$ in (4.167a) and use the solution for the pressure (4.166), then we will find that

$$\left.\frac{d^2\bar{U}_r}{dY_*^2}\right|_{Y_*=0} = ik\bar{P}_r = ik|k|\big[\bar{A}_r - \bar{G}(k)\big]. \tag{4.168}$$

Now we differentiate (4.167a) with respect to Y_* and use the continuity equation (4.167b) to eliminate $\bar{V}_r$. This leads to the following equation for $\bar{U}_r$,

$$ikY_*\frac{d\bar{U}_r}{dY_*} = \frac{d^3\bar{U}_r}{dY_*^3}. \tag{4.169a}$$

It should be solved with the boundary conditions

$$\bar{U}_r = 0 \quad \text{at} \quad Y_* = 0, \tag{4.169b}$$
$$\frac{d^2\bar{U}_r}{dY_*^2} = ik|k|\big[\bar{A}_r - \bar{G}(k)\big] \quad \text{at} \quad Y_* = 0, \tag{4.169c}$$
$$\bar{U}_r = \bar{A}_r \quad \text{at} \quad Y_* = \infty. \tag{4.169d}$$

The transformation of the independent variable

$$\zeta = \theta Y_*, \tag{4.170}$$

with $\theta = (ik)^{1/3}$, turns (4.169a) into the Airy equation for the derivative $d\bar{U}_r/d\zeta$,

$$\frac{d^3\bar{U}_r}{d\zeta^3} - \zeta\frac{d\bar{U}_r}{d\zeta} = 0. \tag{4.171a}$$

In the new variables the boundary conditions (4.169b)–(4.169d) assume the form

$$\bar{U}_r = 0 \quad \text{at} \quad \zeta = 0, \tag{4.171b}$$
$$\frac{d^2\bar{U}_r}{d\zeta^2} = (ik)^{1/3}|k|\big[\bar{A}_r - \bar{G}(k)\big] \quad \text{at} \quad \zeta = 0, \tag{4.171c}$$
$$\bar{U}_r = \bar{A}_r \quad \text{at} \quad \zeta = \infty. \tag{4.171d}$$

which, following the same argument as in subsection 2.5.1, reduces to

$$\frac{d\bar{U}_r}{d\zeta} = C_1 Ai(\zeta). \tag{4.172}$$

Substitution of (4.172) into (4.171*c*) yields

$$C_1 Ai'(0) = (ik)^{1/3}|k|\big[\bar{A}_r - \bar{G}(k)\big]. \tag{4.173}$$

In order to deduce the second equation relating the two unknown constants, C_1 and $\bar{A}_r$, we integrate (4.172) with the initial condition (4.171*b*),

$$\bar{U}_r = C_1 \int\limits_0^\zeta Ai(s)ds, \tag{4.174}$$

and, after setting $\zeta = \infty$ in (4.174), use the boundary condition (4.171*d*). This gives

$$\bar{A}_r = \tfrac{1}{3}C_1. \tag{4.175}$$

It remains to solve the pair of equations (4.173) and (4.175) for C_1 and $\bar{A}_r$. We find that

$$C_1 = \frac{3(ik)^{1/3}|k|}{(ik)^{1/3}|k| - 3Ai'(0)}\bar{G}(k), \tag{4.176}$$

$$\bar{A}_r = \frac{(ik)^{1/3}|k|}{(ik)^{1/3}|k| - 3Ai'(0)}\bar{G}(k). \tag{4.177}$$

With known C_1 the Fourier Transform, $\bar{U}_r$, of the longitudinal velocity can be calculated with the help of equation (4.174). In order to find the Fourier Transform of the lateral velocity, $\bar{V}_r$ one needs to integrate the equation (4.167*b*). Using (4.170) this equation is written as

$$\frac{d\bar{V}_r}{d\zeta} = -(ik)^{2/3}\bar{U}_r. \tag{4.178}$$

Taking into account that $\bar{V}_r = 0$ at $\zeta = 0$, we have

$$\bar{V}_r = -(ik)^{2/3} \int\limits_0^\zeta \bar{U}_r(\zeta')d\zeta'. \tag{4.179}$$

Summarising, it follows from (4.174), (4.176) and (4.179) that

$$\bar{U}_r = \bar{G}(k)\Phi(\zeta;k), \qquad \bar{V}_r = \bar{G}(k)\Psi(\zeta;k), \tag{4.180}$$

where

$$\Phi(\zeta;k) = \frac{3(ik)^{1/3}|k|}{(ik)^{1/3}|k| - 3Ai'(0)} \int_0^\zeta Ai(s)ds, \tag{4.181}$$

$$\Psi(\zeta;k) = -(ik)^{2/3} \int_0^\zeta \Phi(\zeta';k)d\zeta'. \tag{4.182}$$

4.5.2 Unsteady problem

Now our task will be to solve the unsteady viscous-inviscid interaction problem (4.161), (4.162). Being guided by the form of the forcing terms in (4.161 a), (4.162 a) and (4.162 b) we represent the solution in the form

$$U_* = \left\{ \frac{1}{M_\infty} \frac{dF}{dx'}(x_0')U_1(x_*, Y_*) + M_\infty F(x_0')U_2(x_*, Y_*) \right\} e^{i\omega t_*} + c.c., \tag{4.183a}$$

$$V_* = \left\{ \frac{1}{M_\infty} \frac{dF}{dx'}(x_0')V_1(x_*, Y_*) + M_\infty F(x_0')V_2(x_*, Y_*) \right\} e^{i\omega t_*} + c.c., \tag{4.183b}$$

$$P_* = \left\{ \frac{1}{M_\infty} \frac{dF}{dx'}(x_0')P_1(x_*) + M_\infty F(x_0')P_2(x_*) \right\} e^{i\omega t_*} + c.c., \tag{4.183c}$$

$$A_* = \left\{ \frac{1}{M_\infty} \frac{dF}{dx'}(x_0')A_1(x_*) + M_\infty F(x_0')A_2(x_*) \right\} e^{i\omega t_*} + c.c., \tag{4.183d}$$

$$p_* = \left\{ \frac{1}{M_\infty} \frac{dF}{dx'}(x_0')p_1(x_*, y_*) + M_\infty F(x_0')p_2(x_*, y_*) \right\} e^{i\omega t_*} + c.c.. \tag{4.183e}$$

This splits the flow perturbations into two parts. Both are linked to the pressure perturbations (4.35) produced by the wing surface vibrations. However, in the first part are the flow perturbations due to the pressure along the boundary layer, and the second are the flow perturbations due to the pressure variations with time. The former are found by solving the following boundary-value problem in region 1,

$$i\omega U_1 + Y_* \frac{\partial U_1}{\partial x_*} + V_1 = -\frac{dP_1}{dx_*} + \frac{\partial^2 U_1}{\partial Y_*^2} + Q_1, \tag{4.184a}$$

$$\frac{\partial U_1}{\partial x_*} + \frac{\partial V_1}{\partial Y_*} = 0, \tag{4.184b}$$

and

$$U_1 = V_1 = 0 \quad \text{at} \quad Y_* = 0, \tag{4.184c}$$
$$U_1 = A_1(x_*) \quad \text{at} \quad Y_* = \infty, \tag{4.184d}$$
$$U_1 = 0 \quad \text{at} \quad x_* = -\infty. \tag{4.184e}$$

The pressure P_1 in (4.184a) is not known in advance; it should be found by solving the boundary-value problem,

$$\frac{\partial^2 p_1}{\partial x_*^2} + \frac{\partial^2 p_1}{\partial y_*^2} = 0, \tag{4.185a}$$

$$p_1 = P_1 \quad \text{and} \quad \frac{\partial p_1}{\partial y_*} = \frac{\partial^2 A_1}{\partial x_*^2} \quad \text{at} \quad y_* = 0, \tag{4.185b}$$
$$p_1 \to 0 \quad \text{as} \quad x_*^2 + y_*^2 \to \infty. \tag{4.185c}$$

for region 3.

The inviscid problem (4.185) is dealt with in the same way as the corresponding steady problem (4.158). It yields the following equation for the Fourier Transform of the pressure in region 1,

$$\bar{P}_1 = |k|\bar{A}_1. \tag{4.186}$$

The viscous problem (4.184) is written in terms of the Fourier Transforms as

$$i(\omega + kY_*)\bar{U}_1 + \bar{V}_1 = -ik\bar{P}_1 + \frac{d^2\bar{U}_1}{dY_*^2} + \bar{Q}_1, \tag{4.187a}$$
$$ik\bar{U}_1 + \frac{d\bar{V}_1}{dY_*} = 0, \tag{4.187b}$$

$$\bar{U}_1 = \bar{V}_1 = 0 \quad \text{at} \quad Y_* = 0, \tag{4.187c}$$
$$\bar{U}_1 = \bar{A}_1(k) \quad \text{at} \quad Y_* = \infty. \tag{4.187d}$$

Here

$$\bar{Q}_1 = (1+i)\sqrt{\frac{\omega}{2}}e^{-(1+i)\sqrt{\frac{\omega}{2}}Y_*}\bar{V}_r - ik\Big[e^{-(1+i)\sqrt{\frac{\omega}{2}}Y_*} - 1\Big]\bar{U}_r. \tag{4.188}$$

The equations (4.187a), (4.187b) may be manipulated in the same way as the corresponding steady flow equations (4.167a), (4.167b). We start by eliminating $\bar{V}_1$ which is achieved through differentiation of (4.187a) with respect to Y_*. This leads to the equation

$$i(\omega + kY_*)\frac{d\bar{U}_1}{dY_*} = \frac{d^3\bar{U}_1}{dY_*^3} + \frac{d\bar{Q}_1}{dY_*}. \tag{4.189}$$

Since we are dealing now with the third order differential equation, an additional boundary condition for $\bar{U}_1$ is required. It is obtained by setting $Y_* = 0$ in (4.187a). Since $\bar{U}_1$, $\bar{V}_1$, $\bar{U}_r$ and $\bar{V}_r$ are all zero at $Y_* = 0$, we will have

$$\left.\frac{d^2\bar{U}_1}{dY_*^2}\right|_{Y_*=0} = ik\bar{P}_1 = ik|k|\bar{A}_1. \tag{4.190}$$

If we now introduce a new independent variable

$$z = z_0 + \theta Y_*, \tag{4.191}$$

with

$$z_0 = \frac{i\omega}{(ik)^{2/3}}, \qquad \theta = (ik)^{1/3}, \tag{4.192}$$

then the equation (4.189) and the boundary conditions (4.187c), (4.187d) and (4.190) assume the form

$$\frac{d^3\bar{U}_1}{dz^3} - z\frac{d\bar{U}_1}{dz} = \bar{G}(k)H_1(Y_*;k), \tag{4.193a}$$

$$\bar{U}_1 = 0 \qquad \text{at} \quad z = z_0, \tag{4.193b}$$

$$\frac{d^2\bar{U}_1}{dz^2} = (ik)^{1/3}|k|\bar{A}_1 \quad \text{at} \quad z = z_0, \tag{4.193c}$$

$$\bar{U}_1 = \bar{A}_1 \qquad \text{at} \quad z = \infty. \tag{4.193d}$$

Here

$$H_1 = \frac{\omega}{k}e^{-(1+i)\sqrt{\frac{\omega}{2}}Y_*}\Psi(\zeta;k) + (ik)^{1/3}\Big[e^{-(1+i)\sqrt{\frac{\omega}{2}}Y_*} - 1\Big]\frac{d\Phi}{d\zeta}, \tag{4.194}$$

with functions $\Phi(\zeta;k)$ and $\Psi(\zeta;k)$ given by (4.181) and (4.182), respectively.

The general solution of equation (4.193a) may be written as

$$\frac{d\bar{U}_1}{dz} = \bar{G}(k)\,\varphi_1(z) + C_1 Ai(z) + C_2 Bi(z), \tag{4.195}$$

where $\varphi_1(z)$ is the solution of the boundary-value problem

$$\begin{gathered} \varphi_1'' - z\varphi_1 = H_1, \\ \varphi_1'(z_0) = 0, \quad \varphi_1(\infty) = 0. \end{gathered} \tag{4.196}$$

Notice that we have chosen φ_1 to be zero at $z = \infty$. Notice further that the boundary condition (4.193d) requires $d\bar{U}_1/dz$ to tend to zero as $z \to \infty$. This is only possible if $C_2 = 0$. Hence,

$$\frac{d\bar{U}_1}{dz} = \bar{G}(k)\,\varphi_1(z) + C_1 Ai(z). \tag{4.197}$$

Substitution of (4.197) into (4.193c) yields the first equation relating the two unknown constants, C_1 and $\bar{A}_1$,

$$C_1 Ai'(z_0) = (ik)^{1/3}|k|\bar{A}_1. \tag{4.198}$$

In order to deduce the second equation for C_1 and $\bar{A}_1$ we integrate (4.197) with the initial condition (4.193b),

$$\bar{U}_1 = \bar{G}(k)\int_{z_0}^{z} \varphi_1(z')dz' + C_1\int_{z_0}^{z} Ai(z')dz', \tag{4.199}$$

then set $z = \infty$ in (4.199), and use the boundary condition (4.193d). This gives

$$\bar{A}_1 = \bar{G}(k)\int_{z_0}^{\infty} \varphi_1(z)dz + C_1\int_{z_0}^{\infty} Ai(z)dz. \tag{4.200}$$

Eliminating C_1 from (4.198) and (4.200), we find that

$$\bar{A}_1 = \frac{Ai'(z_0)\int\limits_{z_0}^{\infty}\varphi_1(z)dz}{Ai'(z_0) - (ik)^{1/3}|k|\int\limits_{z_0}^{\infty} Ai(z)dz}\,\bar{G}(k). \tag{4.201}$$

It remains to substitute the above equation into (4.186), which yields

$$\bar{P}_1(k) = \frac{Ai'(z_0)|k|\int\limits_{z_0}^{\infty}\varphi_1(z)dz}{Ai'(z_0) - (ik)^{1/3}|k|\int\limits_{z_0}^{\infty} Ai(z)dz}\,\bar{G}(k). \tag{4.202}$$

In order to return back from the Fourier to physical variables one needs to apply the inverse Fourier integral to (4.202). Before doing this we shall repeat the analysis for the second part of the solution decomposition in (4.183).

To perform this task we need to solve the following boundary-value problem in the viscous sublayer (region 1)

$$i\omega U_2 + Y_* \frac{\partial U_2}{\partial x_*} + V_2 = -\frac{dP_2}{dx_*} + \frac{\partial^2 U_2}{\partial Y_*^2} + Q_2, \tag{4.203a}$$

$$\frac{\partial U_2}{\partial x_*} + \frac{\partial V_2}{\partial Y_*} = 0, \tag{4.203b}$$

$$U_2 = V_2 = 0 \quad \text{at} \quad Y_* = 0, \tag{4.203c}$$

$$U_2 = A_2(x_*) \quad \text{at} \quad Y_* = \infty, \tag{4.203d}$$

$$U_2 = 0 \quad \text{at} \quad x_* = -\infty, \tag{4.203e}$$

together with the boundary-value problem,

$$\frac{\partial^2 p_2}{\partial x_*^2} + \frac{\partial^2 p_2}{\partial y_*^2} = -i\omega(\gamma - 1)\frac{M_\infty^2}{1 - M_\infty^2}\frac{\partial^2 p_r}{\partial x_*^2}, \tag{4.204a}$$

$$\frac{\partial p_2}{\partial y_*} = \frac{\partial^2 A_2}{\partial x_*^2} - i\omega \frac{d^2 G}{dx_*^2} \quad \text{at} \quad y_* = 0, \tag{4.204b}$$

$$p_2 \to 0 \quad \text{as} \quad x_*^2 + y_*^2 \to \infty. \tag{4.204c}$$

for region 3.

The inviscid flow problem (4.204) is written in terms of the Fourier Transforms as

$$\frac{d^2 \bar{p}_2}{dy_*^2} - k^2 \bar{p}_2 = \Lambda(k,\omega)\bar{G}(k)e^{-|k|y_*}, \tag{4.205a}$$

$$\frac{d\bar{p}_2}{dy_*} = -k^2 \bar{A}_2 + i\omega k^2 \bar{G}, \quad \text{at} \quad y_* = 0, \tag{4.205b}$$

$$\bar{p}_2 \to 0 \quad \text{as} \quad y_* = \infty. \tag{4.205c}$$

The constant, $\Lambda(k,\omega)$, on the right hand side of (4.205a) is calculated using the solution (4.165), (4.177) for the steady pressure, p_r,

$$\Lambda(k,\omega) = (\gamma - 1)\frac{M_\infty^2}{1 - M_\infty^2}\frac{3i\omega k^2|k|Ai'(0)}{(ik)^{1/3}|k| - 3Ai'(0)}. \tag{4.206}$$

The solution of the boundary-value problem (4.205) is written as

$$\bar{p}_2 = -\frac{\Lambda}{2|k|}\bar{G}(k)y_* e^{-|k|y_*} + \left[|k|\bar{A}_2 - \left(i\omega|k| + \frac{\Lambda}{2k^2}\right)\bar{G}(k)\right]e^{-|k|y_*}. \tag{4.207}$$

Setting $y_* = 0$ in (4.207) gives the Fourier Transform $\bar{P}_2(k)$, of the pressure, $P_2(x_*)$, in the viscous sublayer,

$$\bar{P}_2(k) = |k|\bar{A}_2 - \left(i\omega|k| + \frac{\Lambda}{2k^2}\right)\bar{G}(k). \tag{4.208}$$

The viscous sublayer problem (4.203) is written in terms of the Fourier Transforms as

$$i(\omega + kY_*)\bar{U}_2 + \bar{V}_2 = -ik\bar{P}_2 + \frac{d^2\bar{U}_2}{dY_*^2} + \bar{Q}_2, \tag{4.209a}$$

$$ik\bar{U}_2 + \frac{d\bar{V}_2}{dY_*} = 0, \tag{4.209b}$$

$$\bar{U}_2 = \bar{V}_2 = 0 \quad \text{at} \quad Y_* = 0, \tag{4.209c}$$

$$\bar{U}_2 = \bar{A}_2(k) \quad \text{at} \quad Y_* = \infty. \tag{4.209d}$$

Here

$$\bar{Q}_2 = -2k\omega\bar{P}_r - \omega^2 Y_* \frac{d\bar{U}_r}{dY_*} + i\omega\big[n(\gamma-1) - 2\big]\frac{d^2\bar{U}_r}{dY_*^2}. \tag{4.210}$$

As usual we start the solution of this problem with setting $Y_* = 0$ in (4.209a). We find that

$$\left.\frac{d^2\bar{U}_2}{dY_*^2}\right|_{Y_*=0} = ik\bar{P}_2 + n(\gamma-1)k\omega\bar{P}_r. \tag{4.211}$$

If we now use equation (4.208) for $\bar{P}_2$ and equations (4.166) and (4.177) for $\bar{P}_r$, then we will have

$$\left.\frac{d^2\bar{U}_2}{dY_*^2}\right|_{Y_*=0} = ik|k|\bar{A}_2 + (ik)^{2/3}R(k;\omega)\bar{G}(k), \tag{4.212}$$

where

$$R(k,\omega) = \frac{\Lambda(k,\omega)}{2(ik)^{5/3}} - i\omega(ik)^{1/3}|k|\left[1 + \frac{3n(\gamma-1)Ai'(0)}{(ik)^{1/3}|k| - 3Ai'(0)}\right]. \tag{4.213}$$

Now we differentiate (4.209a) with respect to Y_* and introduce a new independent variable

$$z = z_0 + (ik)^{1/3}Y_*, \qquad z_0 = \frac{i\omega}{(ik)^{2/3}}. \tag{4.214}$$

This leads to the following equation for $\bar{U}_2$,

$$\frac{d^3\bar{U}_2}{dz^3} - z\frac{d\bar{U}_2}{dz} = \bar{G}(k)H_2(Y_*;k), \tag{4.215a}$$

with

$$H_2 = \frac{3(ik)^{1/3}|k|}{(ik)^{1/3}|k| - 3Ai'(0)}\left\{\left[\frac{\omega^2}{(ik)^{2/3}} - i\omega\big[n(\gamma-1)-2\big]\zeta\right]Ai(\zeta) + \frac{\omega^2}{(ik)^{2/3}}\zeta Ai'(\zeta)\right\}. \tag{4.215b}$$

The boundary conditions (4.209c), (4.209d), (4.212) are written in terms of the new independent variable, z, as

$$\begin{aligned}
\bar{U}_2 &= 0 && \text{at} \quad z = z_0, && (4.215c)\\
\frac{d^2\bar{U}_2}{dz^2} &= (ik)^{1/3}|k|\bar{A}_2 + \bar{G}(k)R(k,\omega) && \text{at} \quad z = z_0, && (4.215d)\\
\bar{U}_2 &= \bar{A}_2(k) && \text{at} \quad z = \infty. && (4.215e)
\end{aligned}$$

The solution of the boundary-value problem (4.215) may be constructed in the same way as it was done with the problem (4.193). We find that

$$\bar{P}_2(k) = \left\{\frac{Ai'(z_0)\int\limits_{z_0}^{\infty}\varphi_2(z)dz + R(k,\omega)\int\limits_{z_0}^{\infty}Ai(z)dz}{Ai'(z_0) - (ik)^{1/3}|k|\int\limits_{z_0}^{\infty}Ai(z)dz}|k| - i\omega|k| - \frac{\Lambda(k,\omega)}{2k^2}\right\}\bar{G}(k), \tag{4.216}$$

where $\varphi_2(z)$ is the solution of the boundary-value problem

$$\varphi_2'' - z\varphi_2 = H_2,$$
$$\varphi_2'(z_0) = 0, \qquad \varphi_2(\infty) = 0.$$

4.5.3 Calculation of the receptivity coefficients

We shall now apply the inverse Fourier transformation to $\bar{P}_1(k)$ and $\bar{P}_2(k)$. The first of these is given by (4.202), whence

$$P_1(x_*) = \frac{1}{2\pi}\int\limits_{-\infty}^{\infty}\frac{Ai'(z_0)|k|\int\limits_{z_0}^{\infty}\varphi_1(z)dz}{Ai'(z_0) - (ik)^{1/3}|k|\int\limits_{z_0}^{\infty}Ai(z)dz}\bar{G}(k)e^{ikx_*}dk. \tag{4.217}$$

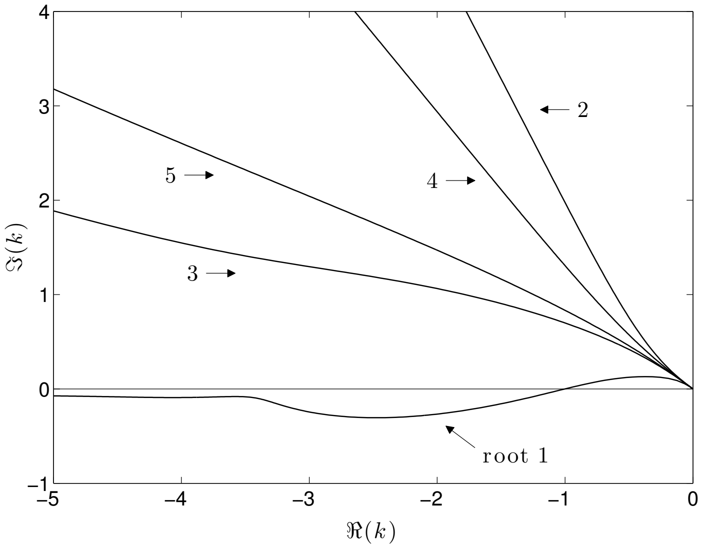

Figure 4.3: The first five roots of the dispersion equation in the complex k-plane.

The integration in (4.217) is performed along the real axis. Our main interest is in the behaviour of the perturbations downstream of the roughness. For $x_* > 0$ it is convenient to consider an analytical extension of the integrand into the upper half plane and change the contour of integration as will be explained later. When deforming the contour of integration we need to identify the poles of the integrand. These are given by the dispersion equation

$$Ai'(z_0) - (ik)^{1/3}|k| \int_{z_0}^{\infty} Ai(z)dz = 0. \tag{4.218}$$

This equation has been studied by various authors, and it is known that there are infinite (countable) number of roots of (4.218). The position of each root depends on the frequency ω. The trajectories of the first five roots, as ω changes from zero to infinity, are shown in Figure 4.3. All the roots originate at $\omega = 0$ from the coordinate origin, and all of them, except the first one, remain in the second quadrant for all $\omega \in (0, \infty]$, indicating that the corresponding perturbations in the boundary layer decay with x. The behaviour of the first root is different. It stays in the second quadrant until the frequency reaches its critical value, $\omega_* = 2.29797$, and then it crosses the real axis at the point $k_* = 1.00049$ and remains in the third quadrant for all $\omega \in (\omega_*, \infty)$. This root represents the Tollmien-Schlichting wave; our task is to determine its amplitude.

Let us consider a value of the frequency, ω, which is smaller than the critical

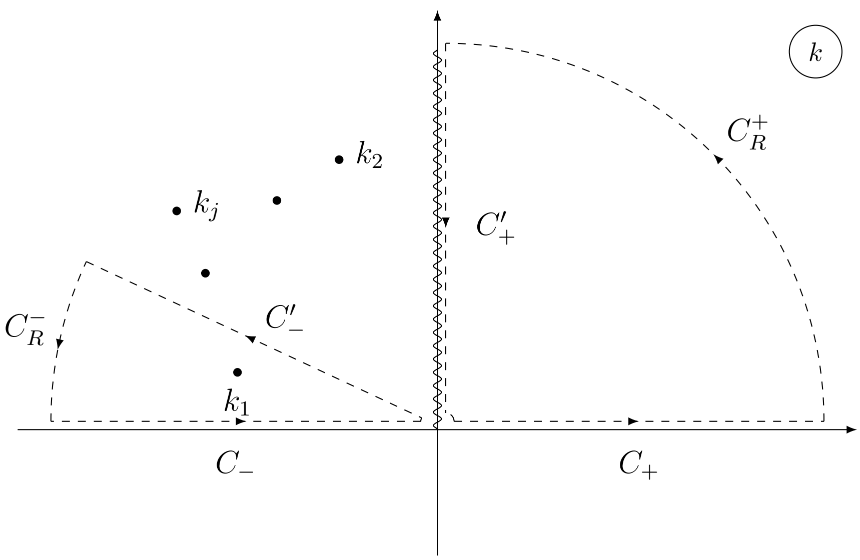

Figure 4.4: Deformation of the contour of integration.

frequency, ω_*. For such ω all the roots of (4.218) are represented by points which lie in the second quadrant of the complex k-plane, as shown in Figure 4.4. Remember that when introducing an analytical branch of the function $(ik)^{1/3}$ we had to make a branch cut along the positive imaginary axis in the k-plane. Also, the analytical extension of $|k|$ in the integrand in (4.217) requires the branch cut to be extended to the entire imaginary axis. Therefore, we shall split the integration interval into two parts, the negative real semi-axis and positive real semi-axis, shown in Figure 4.4 as C_- and C_+, respectively,

$$P_1(x_*) = \frac{1}{2\pi}\int\limits_{-\infty}^{0} \mathcal{M}(k;\omega,x_*)dk + \frac{1}{2\pi}\int\limits_{0}^{\infty} \mathcal{N}(k;\omega,x_*)dk. \tag{4.219}$$

Here

$$\mathcal{M}(k;\omega,x_*) = -\frac{Ai'(z_0)k\int\limits_{z_0}^{\infty}\varphi_1(z)dz}{Ai'(z_0) - i(ik)^{4/3}\int\limits_{z_0}^{\infty}Ai(z)dz}\bar{G}(k)e^{ikx_*}, \tag{4.220}$$

and

$$\mathcal{N}(k;\omega,x_*) = \frac{Ai'(z_0)k\int\limits_{z_0}^{\infty}\varphi_1(z)dz}{Ai'(z_0) + i(ik)^{4/3}\int\limits_{z_0}^{\infty}Ai(z)dz}\bar{G}(k)e^{ikx_*}. \tag{4.221}$$

When calculating the first integral in (4.219) we shall close the contour of integration by adding to C_- a ray, C'_-, and a circular arc, C_R^-, of large radius R. We shall choose the angle between the ray C'_- and the negative real semi-axis such that only one root, k_1, finds itself inside the combined contour. Using the Residue theorem we find

$$\int\limits_{C_-} \mathcal{M} dk = -2\pi i \frac{Ai'(z_0) k \int\limits_{z_0}^{\infty} \varphi_1(z) dz}{\frac{4}{3}(ik)^{1/3} \int\limits_{z_0}^{\infty} Ai(z) dz - \frac{2}{3}\frac{z_0}{k}\big[z_0 + i(ik)^{4/3}\big] Ai(z_0)}\Bigg|_{k=k_1} \bar{G}(k_1) e^{ik_1 x_*}$$
$$- \int\limits_{C'_-} \mathcal{M}(k;\omega,x_*)dk - \int\limits_{C_R^-} \mathcal{M}(k;\omega,x_*)dk. \qquad (4.222)$$

We shall show that the integral along the arc C_R^- tends to zero as the arc radius, R, tends to infinity. In order to perform this task we need to return to the boundary-value problem (4.196) and study the asymptotic behaviour of its solution in the limit

$$k \to \infty, \qquad \omega = O(1). \qquad (4.223)$$

Setting $k \to \infty$ in (4.181), (4.182) yields

$$\Phi = 3 \int\limits_0^{\zeta} Ai(\zeta') d\zeta', \qquad \Psi = -3(ik)^{2/3} \int\limits_0^{\zeta} d\zeta' \int\limits_0^{\zeta'} Ai(\zeta'') d\zeta''. \qquad (4.224)$$

With ζ being an order one quantity, $Y_* = (ik)^{-1/3}\zeta$ is small, and therefore, the function (4.194) may be approximated as

$$H_1 = -3(1+i)\sqrt{\frac{\omega}{2}}\,\zeta Ai(\zeta) + O\big[(ik)^{-1/3}\big]. \qquad (4.225)$$

It remains to notice that $z_0 = i\omega/(ik)^{1/3}$ tend to zero in the limit (4.223), which reduces the boundary-value problem (4.196) to

$$\frac{d^2\varphi_1}{dz^2} - z\varphi_1 = -3(1+i)\sqrt{\frac{\omega}{2}}\,\zeta Ai(\zeta),$$
$$\frac{d\varphi_1}{dz}(0) = 0, \qquad \varphi_1(\infty) = 0.$$

Clearly, the solution to this problem, φ_1, is an order one quantity, and so is the integral

$$\int_0^\infty \varphi_1(z)dz = O(1). \tag{4.226}$$

If we assume that the function $f(x)$ representing the wall roughness shape is integrable on the interval $x \in (-\infty, \infty)$ together with its modulus, i.e. there exists a positive constant B such that

$$|\bar{G}(k)| = \left| \int_{-\infty}^{\infty} G(x)e^{-ikx}dx \right| \leq \int_{-\infty}^{\infty} |G(x)|dx < B. \tag{4.227}$$

then it is easily deduced from (4.220) that

$$\mathcal{M} = O(k^{-1/3}) \quad \text{as} \quad k \to \infty. \tag{4.228}$$

This proves that the function $\mathcal{M}(k;\omega,x_*)$ satisfies the conditions of Jordan's lemma, which allows to conclude that for all $x > 0$ the integral along C_R^- in (4.222) tends to zero as the arc radius $R \to \infty$.

The two remaining terms on the right hand side of (4.222) represent the generated Tollmien-Schlichting wave and the continuous spectrum of the perturbation field around the roughness. We shall show that the continuous spectrum integral,

$$\int_{C'_-} \mathcal{M}(k;\omega,x_*)dk, \tag{4.229}$$

dies away further downstream, and the Tollmien-Schlichting wave alone will remain in the boundary layer behind the roughness. The integral (4.229) is a Laplace type integral. Its asymptotic behaviour may be determined with the help of Watson's lemma. When employing the lemma one needs to know the behaviour of the integrand, $\mathcal{M}(k;\omega,x_*)$, at small values of k. Keeping this in mind we return to the boundary-value problem (4.196), and this time assume that

$$k \to 0, \qquad \omega = O(1). \tag{4.230}$$

It is convenient to recast the boundary-value problem (4.196) using $\zeta = z - z_0$ as the independent variable. We have

$$\frac{d^2\varphi_1}{d\zeta^2} - (z_0 + \zeta)\varphi_1 = H_1(\zeta), \tag{4.231a}$$

$$\frac{d\varphi_1}{d\zeta}(0) = 0, \quad \varphi_1(\infty) = 0. \tag{4.231b}$$

With ζ being an order one quantity, $Y_* = \zeta/(ik)^{1/3}$ appears to be large, and it follows from (4.194) and (4.181) that

$$H_1 = -\frac{(ik)^{2/3}k}{Ai'(0)}Ai(\zeta) + \cdots \quad \text{as} \quad k \to 0. \tag{4.232}$$

We further notice that in the limit (4.230), $z_0 = i\omega/(ik)^{2/3}$ tends to infinity. Hence, the leading order solution of the equation (4.231a) is obtained by balancing the second term on the left hand side with the forcing term on the right hand side. We find

$$\varphi_1 = -\frac{H_1}{z_0} = -\frac{(ik)^{7/3}}{\omega Ai'(0)}Ai(\zeta) + \cdots . \tag{4.233}$$

Consequently,

$$\int_{z_0}^{\infty} \varphi_1(z)dz = \int_0^{\infty} \varphi_1 d\zeta = -\frac{(ik)^{7/3}}{3\omega Ai'(0)} + \cdots . \tag{4.234}$$

We are ready now to analyse the equation (4.220) for the function $\mathcal{M}(k;\omega,x_*)$. Since $z_0 = i\omega/(ik)^{1/3}$ tends to infinity in the limit (4.230), the well known asymptotic formulae for the derivative and integral of the Airy function,

$$Ai'(z_0) = -\frac{z_0^{1/4}}{2\sqrt{\pi}}\, e^{-\frac{2}{3}z_0^{3/2}} + \cdots, \qquad \int_{z_0}^{\infty} Ai(\zeta)\, d\zeta = \frac{z_0^{-3/4}}{2\sqrt{\pi}}\, e^{-\frac{2}{3}z_0^{3/2}} + \cdots \tag{4.235a,b}$$

may be used. It follows from (4.235) that the two terms in the denominator in (4.220) are related to one another as

$$\frac{Ai'(z_0)}{i(ik)^{4/3}\int_{z_0}^{\infty} Ai(z)dz} = -\frac{z_0}{i(ik)^{4/3}} = \frac{\omega}{k^2} \gg 1. \tag{4.236}$$

Keeping this in mind and using (4.234) in (4.220) we find that

$$\mathcal{M}(k;\omega,x_*) = \frac{(ik)^{10/3}}{3i\omega Ai'(0)}\bar{G}(0)e^{ikx_*} + \cdots . \tag{4.237}$$

Watson's lemma converts (4.237) into the following asymptotic representation of the continuous spectrum integral (4.229)

$$\int_{C'_-} \mathcal{M}(k;\omega,x_*)dk = -\frac{1-i\sqrt{3}}{6\omega Ai'(0)}\Gamma\left(\frac{13}{3}\right)\bar{G}(0)\frac{1}{x_*^{13/3}} + \cdots \quad \text{as} \quad x_* \to \infty. \tag{4.238}$$

The second integral in (4.219) may be treated in a similar way. We close the contour of integration as shown in Figure 4.4. Since there are no roots of the dispersion equation in the first quadrant of the complex k-plane and given that contribution of the integral along arc C_R^+ tends to zero as $R \to \infty$, the integral along the real positive semi-axis, C_+ may be substituted with the integral along imaginary semi-axis, C'_+. The latter is easily evaluated with the help of the Watson lemma as it was done with the integral (4.238) along C'_-. We find

$$\int_{C_+} \mathcal{N}(k;\omega,x_*)dk = -\int_{C'_+} \mathcal{N}(k;\omega,x_*)dk =$$
$$= -\frac{1+i\sqrt{3}}{6\omega Ai'(0)}\Gamma\left(\frac{13}{3}\right)\bar{G}(0)\frac{1}{x_*^{13/3}} + \cdots \quad \text{as} \quad x_* \to \infty. \tag{4.239}$$

It remains to substitute (4.238) back into (4.222) and combine with (4.239) using the equation (4.219). This results in

$$P_1(x_*) = \tfrac{1}{2}\mathcal{K}_1(\omega)\bar{G}(k_1)e^{ik_1x_*} - \frac{i\Gamma(13/3)}{2\pi\sqrt{3}\,\omega Ai'(0)}\bar{G}(0)\frac{1}{x_*^{13/3}} + \cdots. \tag{4.240}$$

Here

$$\mathcal{K}_1(\omega) = -i\left.\frac{2Ai'(z_0)k\int\limits_{z_0}^{\infty}\varphi_1(z)dz}{\frac{4}{3}(ik)^{1/3}\int\limits_{z_0}^{\infty}Ai(z)dz - \frac{2}{3}\frac{z_0}{k}\left[z_0 + i(ik)^{4/3}\right]Ai(z_0)}\right|_{k=k_1}. \tag{4.241}$$

is a universal function of the frequency, ω. It neither depends on the wing surface vibration function (4.2) nor it depends on the wall roughness shape (4.91). We shall call $\mathcal{K}_1(\omega)$ the first receptivity coefficient. The results of a numerical calculation of $\mathcal{K}_1(\omega)$ are displayed in Figure 4.5.

These calculations were performed in the same way as it is described at the end of Chapter 2. We start by choosing a real value of the frequency, ω. The corresponding values of k and z_0 are found from the solution of the dispersion equation (4.218); we

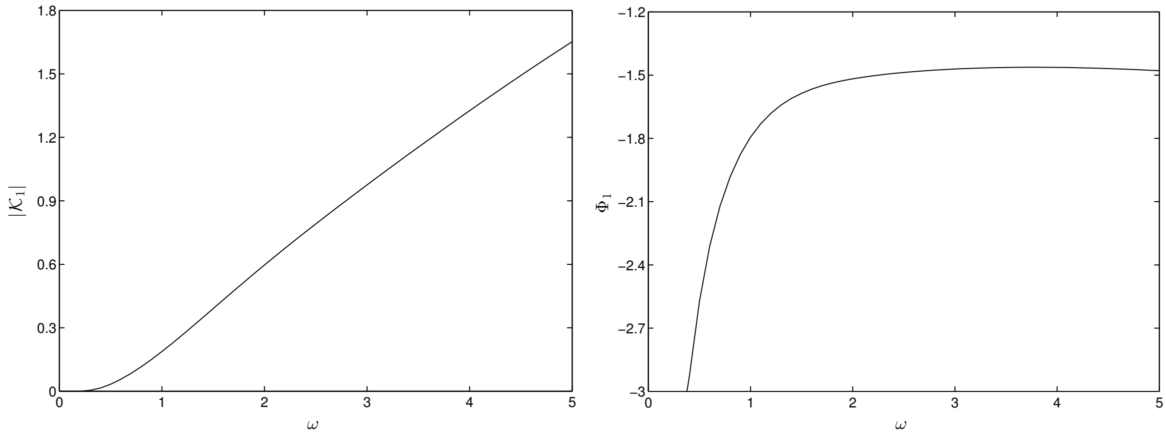

(a) Modulus of the receptivity coefficient

(b) Argument of the receptivity coefficient

Figure 4.5: The first receptivity coefficient dependence on frequency.

are interested here in the first root (see Figure 4.3). This is followed by calculations of the function φ_1, which is found by solving the boundary-value problem (4.196).

The receptivity coefficient, $\mathcal{K}_1(\omega)$ is represented in the exponential form, $\mathcal{K}_1 = |\mathcal{K}_1|e^{i\Phi_1}$. Figure 4.5(a) shows the modulus of the receptivity coefficient, and its argument is shown in Figure 4.5(b).

Now we have to repeat the analysis for the second part of the solution in (4.183). Through solving the boundary-value problems (4.203), (4.204) in the Fourier space we have found that the Fourier Transform of the pressure, $P_2(x_*)$, is given by (4.216). Applying the Inverse Fourier Transform to (4.216) and closing again the integration contour as shown in Figure 4.4 we find that downstream of the roughness

$$P_2(x_*) = \tfrac{1}{2}\mathcal{K}_2(\omega)\bar{G}(k_1)e^{ik_1x_*} + O(x_*^{-2}), \tag{4.242}$$

where

$$\mathcal{K}_2(\omega) = -2ik\frac{Ai'(z_0)\int\limits_{z_0}^{\infty}\varphi_2(z)dz + R(k,\omega)\int\limits_{z_0}^{\infty}Ai(z)dz}{\tfrac{4}{3}(ik)^{1/3}\int\limits_{z_0}^{\infty}Ai(z)dz - \tfrac{2}{3}\tfrac{z_0}{k}\left[z_0 + i(ik)^{4/3}\right]Ai(z_0)}\Bigg|_{k=k_1} \tag{4.243}$$

is the second receptivity coefficient. Notice that unlike $\mathcal{K}_1$ the second receptivity coefficient, $\mathcal{K}_2$, depends on the viscosity parameter, n, the specific heats ratio, γ, and on the Mach number, M_∞. Figure 4.6 shows the results of calculations of the equation (4.243) obtained with $n = 1/2$ and $\gamma = 7/5$.

Let us now substitute (4.241) and (4.243) into the equation for the pressure in (4.183). Disregarding the continuous spectrum contributions, we find that the pressure

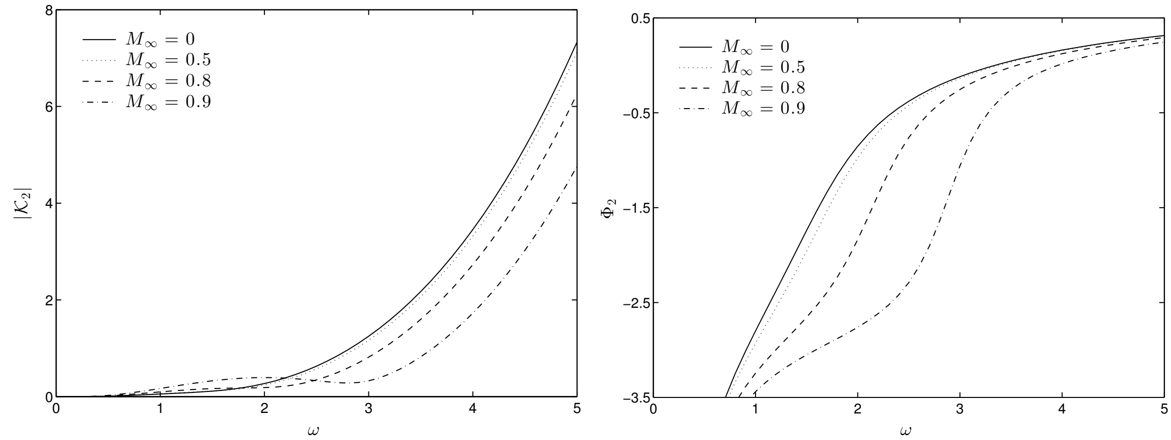

(a) Modulus of the receptivity coefficient (b) Argument of the receptivity coefficient

Figure 4.6: The second receptivity coefficient dependence on frequency and Mach number.

oscillations in the boundary layer downstream of the roughness

$$P_*(t_*, x_*) = \bar{G}(k_1)\frac{1}{M_\infty}\frac{dF}{dx'}(x_0')\tfrac{1}{2}\big|\mathcal{K}_1(\omega)\big|e^{i(\omega t_* + k_1 x_* + \Phi_1)} + \\ + \bar{G}(k_1)M_\infty F(x_0')\tfrac{1}{2}\big|\mathcal{K}_2(\omega)\big|e^{i(\omega t_* + k_1 x_* + \Phi_2)} + c.c.. \tag{4.244}$$

This shows that the harmonic oscillations of the wing surface produce two Tollmien-Schlichting waves in the boundary layer behind a wall roughness. Their amplitudes are

$$\left|\bar{G}(k_1)\frac{1}{M_\infty}\frac{dF}{dx'}(x_0')\mathcal{K}_1(\omega)\right| \quad \text{and} \quad \left|\bar{G}(k_1)M_\infty F(x_0')\mathcal{K}_2(\omega)\right|, \tag{4.245}$$

respectively.

4.6 Discussion of the results

This work shows that in the case of the elastic wing surface vibrations with the characteristic wave length of an order $LRe^{-1/8}$ two mechanisms prove to be equally important for the boundary layer receptivity. The first is due to gradient of the pressure in the near wall layer, which is caused by surface wavelike oscillations. The second is due to the roughness oscillations and compressibility of the fluid surrounding it. The analysis of these two mechanisms led us to an expression for the pressure (4.244) which contains two receptivity coefficients $\mathcal{K}_1$ and $\mathcal{K}_2$.

The first receptivity coefficient (4.241) is due to the first mechanism for which numerical calculations are presented in Figure 4.5. It can be observed that as the frequency of the wing surface oscillations increase the modulus of the receptivity coefficient increases.

The second receptivity coefficient (4.243) is not only a function of the frequency, as $\mathcal{K}_1$, but it also involves properties of the free stream. The calculations of $\mathcal{K}_2$ are presented in Figure 4.6 where $n = 1/2$ and $\gamma = 7/5$. Additional calculations with n being 1 and 3/4 showed that increasing the value of the viscosity parameter reduces the value of the modules of the receptivity coefficient by less than 1% but it does not alter the behaviour of the coefficient compared to the presented results.

It can be seen that the second receptivity coefficient remains almost unchanged when M_∞ increases from zero to 0.5, but then the effect of further Mach number increase becomes more noticeable. Similarly as in the case of the first receptivity coefficient we see that as the frequency of the wing surface oscillations increase the modulus of the receptivity coefficient increases. However the increase is more rapid and values of the modulus of the receptivity coefficient are much higher. This suggests that the compressibility effects in the receptivity problem of the elastic wing surface vibrations are more important than the pressure variations along the surface.

5 Conclusions

This research presents a theoretical analysis of the generation of Tollmien-Schlichting waves in a boundary layer on the wing surface due to external acoustic disturbances and elastic vibrations of the wing itself. As the Tollmien-Schlichting waves are observed at relatively large values of the Reynolds number, an asymptotic approach to the flow analysis is adopted.

It is assumed that in the spectrum of the acoustic disturbances and the wing vibrations there are harmonics which come in resonance with the Tollmien-Schlichting wave on the lower branch of the stability curve. When dealing with acoustic disturbances we assumed the flow outside the boundary layer to be transonic, in which case effective generation of the Tollmien-Schlichting waves takes place if the frequency of acoustic waves, ω, is chosen to be an order $Re^{2/9}$ quantity. The problem of wing oscillations was considered assuming that the flow is subsonic, in which case the frequency of order $Re^{1/4}$ was considered.

The analysis of the boundary layer receptivity to the acoustic disturbances problem started with the study of the potential flow far from the boundary layer, in addition, it is assumed that the free-stream Mach number, M_∞, is such that, $M_\infty^2 = 1 + O(Re^{-1/9})$. It was shown that in this regime there are two plane acoustic waves with distinctively different characteristics. One of these always travels downstream in the streamwise direction and has $O(1)$ phase velocity. This wave was chosen in the analysis presented in Chapter 2. The second wave, which phase velocity is an order $Re^{-1/9}$ quantity and direction of the propagation depends on the free-stream Mach number, is considered in Chapter 3.

The physical explanation of the receptivity mechanism described in Chapter 2 is as follows; as acoustic perturbations penetrate into the boundary layer, a Stokes layer forms on the surface of the plate. With the frequency being an $O(Re^{2/9})$ quantity, its thickness is estimated as an order $Re^{-11/18}$ quantity. The oscillatory motion of the fluid in the Stokes layer is excited by the pressure gradient, which is a periodic function of time. This process has been studied on numerous occasions for subsonic flows, including in receptivity theory (see, for example, Ruban, 1984; Goldstein, 1985). The Stokes layer on its own is incapable of producing the Tollmien-Schlichting waves. The reason is that the resonance conditions require the external perturbations to have not only the same frequency as the Tollmien-Schlichting waves, but also the same wave length. The characteristic wave length of the perturbation field in the Stokes layer is much longer than that of the Tollmien-Schlichting waves. However, the situation changes when the Stokes layer encounters a wall roughness, which are plentiful in real aerodynamic flows. If the longitudinal extent of the roughness is an order $Re^{-1/3}$ quantity, then efficient generation of Tollmien-Schlichting waves becomes possible.

This work is restricted to the case when the Stokes layer interacts with an isolated roughness. The flow near the roughness is described by triple-deck theory. The solution of the triple-deck problem was found in an analytic form and the main concern was with the flow behaviour downstream of the roughness. It was found that the Tollmien-Schlichting wave is forming behind the roughness in the boundary layer. Its amplitude has been expressed in terms of the receptivity coefficient, which represent the efficiency of generation process.

The analysis shows that in the transonic regime the receptivity coefficient depends not only on the initial frequency of the perturbations, as it was in the case of the subsonic flow (see Ruban, 1984), it also depends on the free-stream Mach number. Results are presented in Figures 2.9 and 2.10.

The second wave found from the analysis of the potential flow in Chapter 2 is considered in Chapter 3. For small values of the Mach number the wave travels upstream and as the velocity of the wave is increased and it surpasses the speed of sound, the wave turns and now propagates downstream. The analysis presented in this chapter adopts the former situation, the acoustic wave propagation upstream. It also may be shown that in order to satisfy the resonance conditions it is necessary to consider an oblique wave instead of the one-dimensional plane acoustic wave, as it was for the first problem. It is assumed that the characteristic wavenumber in the normal direction, β, is an order $Re^{5/18}$ quantity.

The study of the dispersion equation for the particular problem suggests that the characteristic wavenumber in the streamwise direction is in fact an order $Re^{1/3}$ quantity, but it does not produce the Tollmien-Schlichting wave as the wave propagates upstream. In order to achieve the efficient generation of the Tollmien-Schlichting waves it is necessary to introduce a roughness located upstream of the acoustic wave source, which longitudinal extent is $O(Re^{-1/3})$ quantity. The flow near the roughness is described by the triple-deck theory, where the interaction of the oblique acoustic wave and the steady disturbances caused by the isolated roughness is the main mechanism behind the generation of the the Tollmien-Schlichting waves. It was deduced that the receptivity coefficient now depends on the free-stream Mach number, the shape of the roughness and acoustic wave parameters. Results are presented in Figure 3.3, where the shape of the roughness is described by the Gaussian function.

Comparing the receptivity coefficients deduced in Chapter 2 and Chapter 3, for downstream and upstream propagating waves, respectively, the former increases until a certain value but the latter decreases with increasing frequency. It also may be noted that the receptivity process of the upstream propagating wave is much more effective as its modulus has larger value as compared to the receptivity coefficient for the downstream propagating wave, particularly for moderate values of the frequency, where the receptivity coefficient for the upstream propagating wave has a peak value. The behaviour of the receptivity coefficient for the downstream propagating wave is similar to the behaviour of the receptivity coefficient for the acoustic problem in the subsonic flow regime (see Ruban, 1984). It may be shown that for the positive values of the Kármán-Guderley parameter the modulus of the receptivity coefficient is smaller than the equivalent in the subsonic flow. Reducing the value of the Kármán-Guderley parameter increases the value of the modulus of the receptivity coefficient above the subsonic flow equivalent. This behaviour is observed for $O(1)$ values of the Kármán-Guderley parameter, but in the limit of large negative values of the Kármán-Guderley parameter the subsonic regime behaviour is recovered.

The third problem is concerned with receptivity of the boundary layer on the wing surface due to an elastic vibration of the wing itself. Similarly, as for the acoustic problems, the analysis started with the study of the flow outside the boundary layer. In this situation the free-stream Mach number was chosen to be $M_\infty \gg Re^{-1/4}$. It was found that, as the frequency of the wing surface vibrations is high, $\omega \sim Re^{1/4}$, the perturbations produced by wing surface vibrations can be described in the framework of the piston theory.

As the pressure perturbations penetrate into the boundary layer, a Stokes layer forms on the wing surface, with thickness estimated as an order $Re^{-5/8}$ quantity. In the flow considered there are two physical mechanisms through which an oscillatory motion of the fluid in the Stokes layer is excited. The first one is the same as for the acoustic problem where the pressure gradient forces the fluid to oscillate in the direction along the wing surface. The second mechanism can only be observed in compressible flows. Here the pressure itself is responsible for the Stokes layer. This involves the following chain of events. The pressure pulsations at the outer edge of the boundary layer cause periodic compression and expansion of the boundary layer. As a result the fluid particles find themselves in an oscillatory motion in the direction normal to the wall. In this motion the fluid particles migrate from a region with lower velocity, close to the wall, into a region with higher velocity, further away from the wall, and then return back. As they do so an exchange between the instantaneous acceleration of the fluid and the convective acceleration takes place, which creates periodic time oscillations of the longitudinal velocity.

The two mechanisms prove to be equally important if the characteristic wave length of the elastic vibrations of the wing surface, ℓ, is an order $O(LRe^{-1/8})$ quantity, with L being the wing cord. If $\ell \ll LRe^{-1/8}$, then the first mechanism defines the flow behaviour in the Stokes layer. If, on the other hand, $\ell \gg Re^{-1/8}$, then the second mechanism is dominant. Interestingly enough, in the second case the velocity oscillations are not confined to the Stokes layer itself, but also persist in the rest of the boundary layer.

In this situation the Stokes layer on its own is incapable of producing the Tollmien-Schlichting waves, and as before, for that reason the localised wall roughness with the longitudinal extent of an order $Re^{-3/8}$ quantity has to be introduced. The flow near the roughness is described by the triple-deck theory, where the flow appears to be compressible in all three tiers of the triple-deck structure.

It was found that there are two Tollmien-Schlichting waves forming in the boundary layer behind the roughness; these are produced by the two physical mechanisms of excitation of the flow oscillations in the Stokes layer. The first receptivity process is similar to the one studied earlier, see Chapter 2, with difference that now flow is considered to be in the subsonic regime. In fact, if the "acoustic" receptivity coefficient in the subsonic regime is denoted as $\mathcal{K}_\mathrm{a}$, then

$$\mathcal{K}_1 = -2\omega\mathcal{K}_\mathrm{a}$$

The second receptivity process does not have an analogue in the literature, and it was found that the second receptivity coefficient, $\mathcal{K}_2$, is rather large, see figure 4.6(a), as compared with the first receptivity coefficient, $\mathcal{K}_1$, see figure 4.5(a). The latter in its turn is larger than the acoustic receptivity coefficient, $\mathcal{K}_\mathrm{a}$ for all $\omega > \frac{1}{2}$. This suggests that the receptivity to the wing surface vibrations has to play a major role in the laminar-turbulent transition in the boundary layer.

In order to compare the effectiveness of the receptivity process in the vibrating wing problem in subsonic flow with its equivalent in transonic flow, it is necessary to perform additional analysis. In transonic regime flow is more sensitive to the compressibility of the gas as it is in subsonic regime. It is also expected that in transonic regime the problem will have a distinguished limit as it is in this situation, but that it will be larger than $LRe^{-1/8}$.

References

ABRAMOWITZ, M. & STEGUN, I. A. 1965 *Handbook of mathematical functions: with formulas, graphs and mathematical tables*. Dover Publications, Inc.

ADAMSON, JR., T. C. 1974 Shock wave boundary-layer interactions in laminar transonic flow. *AIAA J.* .

BENDIKSEN, O. O. 2011 Review of unsteady transonic aerodynamics: Theory and applications. *Progr. Aero. Sci.* .

BERTOLOTTI, F. P., HERBERT, T. & SPALART, P. R. 1992 Linear and nonlinear stability of the Blasius boundary layer. *J. Fluid Mech.* .

BODONYI, R. J. & KLUWICK, A. 1982 Supercritical transonic trailing-edge flow. *Quart. Appl. Math.* .

BODONYI, R. J. & KLUWICK, A. 1998 Transonic trailing-edge flow. *Quart. Appl. Math.* .

BODONYI, R. J. & SMITH, F. T. 1981 The upper branch stability of the blasius boundary-layer, including non-parallel flow effects. *Proc. R. Soc. Lond. A* .

BOGDANOV, A. N., DIESPEROV, V. N., ZHUK, V. I. & CHERNYSHEV, A. V. 2010 Triple-deck theory in transonic flows and boundary layer stability. *Comput. Math. Math. Phys* .

BOUTHIER, M. 1972 Stabilité linéaire des écoulements presque parallèles, I. *Journal de Mecanique* .

BOWLES, R. I. & SMITH, F. T. 1993 On boundary-layer transition in transonic flow. *J Eng Math* .

BULDAKOV, E. V. & RUBAN, A. I. 2002 On transonic viscous–inviscid interaction. *J. Fluid Mech.* .

CHOUDHARI, M. & STREETT, C. L. 1992 A finite Reynolds-number approach for the prediction of boundary-layer receptivity in localized regions. *Phys. Fluids* .

COLE, J. D. & COOK, P. L. 1986 *Transonic Aerodynamics: problems in asymptotic theory*. Elsevier Science Publishers B. V.

DIETZ, A. J. 1999 Local boundary-layer receptivity to a convected free-stream disturbance. *J. Fluid Mech.* .

DRAZIN, P. G. & REID, W. H. 2004 *Hydrodynamic stability*. Cambridge University Press.

DUCK, P. W., RUBAN, A. I. & ZHIKHAREV, C. N. 1996 The generation of Tollmien-Schlichting waves by free-stream turbulence. *J. Fluid Mech.* .

FEDOROV, A. V. 2011 Transition and stability of high-speed boundary layers. *Annual Rev. Fluid Mech.* .

GASTER, M. 1974 On the effects of boundary-layer growth on flow stability. *J. Fluid Mech.* .

GOLDSTEIN, M. E. 1983 The evolution of Tollmien-Schlichting waves near a leading edge. *J. Fluid Mech.* .

GOLDSTEIN, M. E. 1985 Scattering of acoustic-waves into Tollmien-Schlichting waves by small streamwise variations in surface geometry. *J. Fluid Mech.* .

HERBERT, T. 1997 Parabolized Stability Equations. *Annual Rev. Fluid Mech.* .

HERBERT, T. & BERTOLOTTI, F. P. 1987 Stability analysis of nonparallel boundary layers. *Bull. Am. Phys. Soc.* .

KERIMBEKOV, R. M. & RUBAN, A. I. 2005 Receptivity of boundary layers to distributed wall vibrations. *Proc. R. Soc. Lond. A* .

KLEBANOFF, P. S., TIDSTROM, K. D. & SARGENT, L. M. 1962 The three-dimensional nature of boundary-layer instability. *J. Fluid Mech.* .

LANDAU, L. D. & LIFSHITZ, E. M. 1987 *Fluid Mechanics*. Elsevier Science.

LIEPMANN, H. W. & ROSHKO, A. 1957 *Elements of gasdynamics*. John Wiley & Sons.

LIGHTHILL, J. M. 1953 On boundary layers and upstream Influence. II. Supersonic flows without separation. In *Proceedings of the Royal Society of London. Series A*.

Lin, C. C. 1944 On the stability of two-dimensional parallel flows. *Proc. Natl. Acad. Sci. USA* .

Messiter, A. F. 1970 Boundary-layer flow near the trailing edge of a flat plate. *SIAM J. Appl. Math.* .

Messiter, A. F., Feo, A. & Melnik, R. E. 1971 Shock-wave strength for separation of a laminar boundary layer at transonic speeds. *AIAA J.* .

Neiland, V. Y. 1969 Theory of laminar boundary layer separation in supersonic flow. *Fluid Dynamics* .

Orr, W. M. 1907 The stability or instability of the steady motions of a perfect liquid and of a viscous liquid. *Proceedings of the Royal Irish Academy. Section A: Mathematical and Physical Sciences* .

Prandtl, L. 1921 Bemerkungen über die Entstehung der Turbulenz. *Z. angew. Math. Mech.* .

Rayleigh, L. 1880 On the Stability, or Instability, of certain Fluid Motions. *Proceedings of the London Mathematical Society* .

Reynolds, O. 1883 An experimental investigation of the circumstances which determine whether the motion of water shall be direct or sinuous, and of the law of resistance in parallel channels. *Philosophical Transactions of the Royal Society of London* .

Rogers, D. F. 1992 *Laminar flow analysis*. Cambridge University Press.

Ruban, A. I. 1984 On the generation of Tollmien-Schlichting waves by sound. *Fluid Dynamics* .

Ruban, A. I., Bernots, T. & Pryce, D. 2013 Receptivity of the boundary layer to vibrations of the wing surface. *J. Fluid Mech.* .

Ruban, A. I. & Türkylmaz, İ. 2000 On laminar separation at a corner point in transonic flow. *J. Fluid Mech.* .

Ruban, A. I., Wu, X. & Pereira, R. M. S. 2006 Viscous–inviscid interaction in transonic Prandtl–Meyer flow. *J. Fluid Mech.* .

Saric, W. S. & Nayfeh, A. H. 1975 Nonparallel stability of boundary-layer flows. *Phys. Fluids* .

SARIC, W. S., REED, H. L. & KERSCHEN, E. J. 2002 Boundary-layer receptivity to freestream disturbances. *Annual Rev. Fluid Mech.* .

SCHMID, P. J. & HENNINGSON, D. S. 2001 *Stability and Transition in Shear Flows*. Springer.

SCHUBAUER, G. B. & KLEBANOFF, P. S. 1956 Contributions on the mechanics of boundary layer transition. *Tech. Rep.*.

SCHUBAUER, G. B. & SKRAMSTAD, H. K. 1948 Laminar-boundary-layer oscillations and transition on a flat plate. *Tech. Rep.*.

SMITH, F. T. 1979*a* Nonlinear stability of boundary layers for disturbances of various sizes. *Proc. R. Soc. Lond. A* .

SMITH, F. T. 1979*b* On the non-parallel flow stability of the Blasius boundary layer. *Proc. R. Soc. Lond. A* .

SOMMERFELD, A. 1908 Ein Beitrag zur hydrodynamischen Erklärung der turbulenten Flüssigkeitsbewegungen. In *Proc. 4th Int. Cong. Math.*.

SQUIRE, H. B. 1933 On the stability for three-dimensional disturbances of viscous fluid flow between parallel walls. *Proc. R. Soc. Lond. A* .

STEWARTSON, K. 1964 *The theory of laminar boundary layer in compressible fluids*. Clarendon Press.

STEWARTSON, K. & WILLIAMS, P. G. 1969 Self-induced separation. *Proceedings of the Royal Society of London. Series A* .

SYCHEV, V. V., RUBAN, A. I., SYCHEV, V. V. & KOROLEV, G. L. 1998 *Asymptotic theory of separation flows*. Cambridge University Press.

TERENT'EV, E. D. 1981 The linear problem of a vibrator in a subsonic boundary layer. *J. Appl. Math. Mech.* .

TIMOSHIN, S. N. 1990 Asymptotic form of the lower branch of the neutral curve in transonic boundary layer. *Uch. zap. TsAGI* .

WU, X. 1999 Generation of Tollmien-Schlichting waves by convecting gusts interacting with sound. *J. Fluid Mech.* .

WU, X. 2001 Receptivity of boundary layers with distributed roughness to vortical and acoustic disturbances: a second-order asymptotic theory and comparison with experiments. *J. Fluid Mech.* .

A Appendix

A.1 Nondimensionalization of the Navier-Stokes equations

In the two-dimensional Cartesian coordinate system, where the system is defined by $(\hat{x}, \hat{y})$ with $\hat{x}$ measured along the plate surface from its leading edge, and $\hat{y}$ in the perpendicular direction, the compressible Navier-Stokes equations (Landau & Lifshitz, 1987) may written as

$$\hat{\rho}\left(\frac{\partial \hat{u}}{\partial \hat{t}} + \hat{u}\frac{\partial \hat{u}}{\partial \hat{x}} + \hat{v}\frac{\partial \hat{u}}{\partial \hat{y}}\right) = -\frac{\partial \hat{p}}{\partial \hat{x}} + \frac{\partial}{\partial \hat{x}}\left[\hat{\mu}\left(\frac{4}{3}\frac{\partial \hat{u}}{\partial \hat{x}} - \frac{2}{3}\frac{\partial \hat{v}}{\partial \hat{y}}\right)\right] + \frac{\partial}{\partial \hat{y}}\left[\hat{\mu}\left(\frac{\partial \hat{u}}{\partial \hat{y}} + \frac{\partial \hat{v}}{\partial \hat{x}}\right)\right], \tag{A.1a}$$

$$\hat{\rho}\left(\frac{\partial \hat{v}}{\partial \hat{t}} + \hat{u}\frac{\partial \hat{v}}{\partial \hat{x}} + \hat{v}\frac{\partial \hat{v}}{\partial \hat{y}}\right) = -\frac{\partial \hat{p}}{\partial \hat{y}} + \frac{\partial}{\partial \hat{y}}\left[\hat{\mu}\left(\frac{4}{3}\frac{\partial \hat{v}}{\partial \hat{y}} - \frac{2}{3}\frac{\partial \hat{u}}{\partial \hat{x}}\right)\right] + \frac{\partial}{\partial \hat{x}}\left[\hat{\mu}\left(\frac{\partial \hat{u}}{\partial \hat{y}} + \frac{\partial \hat{v}}{\partial \hat{x}}\right)\right], \tag{A.1b}$$

$$\begin{aligned}\hat{\rho}\left(\frac{\partial \hat{h}}{\partial \hat{t}} + \hat{u}\frac{\partial \hat{h}}{\partial \hat{x}} + \hat{v}\frac{\partial \hat{h}}{\partial \hat{y}}\right) = {}& \frac{\partial \hat{p}}{\partial \hat{t}} + \hat{u}\frac{\partial \hat{p}}{\partial \hat{x}} + \hat{v}\frac{\partial \hat{p}}{\partial \hat{y}} + \hat{\mu}\left(\frac{\partial \hat{u}}{\partial \hat{y}} + \frac{\partial \hat{v}}{\partial \hat{x}}\right)^2 \\ & + \hat{\mu}\left(\frac{4}{3}\frac{\partial \hat{u}}{\partial \hat{x}} - \frac{2}{3}\frac{\partial \hat{v}}{\partial \hat{y}}\right)\frac{\partial \hat{u}}{\partial \hat{x}} + \hat{\mu}\left(\frac{4}{3}\frac{\partial \hat{v}}{\partial \hat{y}} - \frac{2}{3}\frac{\partial \hat{u}}{\partial \hat{x}}\right)\frac{\partial \hat{v}}{\partial \hat{y}} \\ & + \frac{1}{Pr}\left[\frac{\partial}{\partial \hat{x}}\left(\hat{\mu}\frac{\partial \hat{h}}{\partial \hat{x}}\right) + \frac{\partial}{\partial \hat{y}}\left(\hat{\mu}\frac{\partial \hat{h}}{\partial \hat{y}}\right)\right],\end{aligned} \tag{A.1c}$$

$$\frac{\partial \hat{\rho}}{\partial \hat{t}} + \frac{\partial (\hat{\rho}\hat{u})}{\partial \hat{x}} + \frac{\partial (\hat{\rho}\hat{v})}{\partial \hat{y}} = 0, \tag{A.1d}$$

$$\hat{h} = \frac{\gamma}{\gamma - 1}\frac{\hat{p}}{\hat{\rho}}. \tag{A.1e}$$

Here Pr is the Prandtl number, which is the ratio of momentum to thermal diffusivity and γ is the specific heat ratio. The dimensional velocity components are denoted as $(\hat{u}, \hat{v})$ and time by $\hat{t}$. The gas density is $\hat{\rho}$, the pressure $\hat{p}$, the enthalpy $\hat{h}$ and the dynamic viscosity coefficient $\hat{\mu}$.

In order to introduce non-dimensional variables, we denote the distance from the leading edge of the plate to the roughness by L. The velocity, density, pressure and viscosity in the unperturbed flow upstream of the plate are U_∞, ρ_∞, p_∞ and μ_∞, respectively. Then setting

$$\hat{t} = \frac{L}{U_\infty} t_*, \qquad \hat{x} = L x_*, \qquad \hat{y} = L y_*, \qquad \hat{p} = p_\infty + \rho_\infty U_\infty^2 p_*, \tag{A.2a-d}$$

$$\hat{u} = U_\infty u_*, \qquad \hat{v} = U_\infty v_*, \qquad \hat{\rho} = \rho_\infty \rho_*, \qquad \hat{h} = U_\infty^2 h_*, \qquad \hat{\mu} = \mu_\infty \mu_*, \tag{A.2e-i}$$

which turns (A.1) into

$$\begin{aligned}
\rho_* \left(\frac{\partial u_*}{\partial t_*} + u_* \frac{\partial u_*}{\partial x_*} + v_* \frac{\partial u_*}{\partial y_*} \right) = -\frac{\partial p_*}{\partial x_*} + \frac{1}{Re} \Bigg\{ & \frac{\partial}{\partial x_*} \left[\mu_* \left(\frac{4}{3} \frac{\partial u_*}{\partial x_*} - \frac{2}{3} \frac{\partial v_*}{\partial y_*} \right) \right] \\
& + \frac{\partial}{\partial y_*} \left[\mu_* \left(\frac{\partial u_*}{\partial y_*} + \frac{\partial v_*}{\partial x_*} \right) \right] \Bigg\},
\end{aligned} \tag{A.3a}$$

$$\begin{aligned}
\rho_* \left(\frac{\partial v_*}{\partial t_*} + u_* \frac{\partial v_*}{\partial x_*} + v_* \frac{\partial v_*}{\partial y_*} \right) = -\frac{\partial p_*}{\partial y_*} + \frac{1}{Re} \Bigg\{ & \frac{\partial}{\partial y_*} \left[\mu_* \left(\frac{4}{3} \frac{\partial v_*}{\partial y_*} - \frac{2}{3} \frac{\partial u_*}{\partial x_*} \right) \right] \\
& + \frac{\partial}{\partial x_*} \left[\mu_* \left(\frac{\partial u_*}{\partial y_*} + \frac{\partial v_*}{\partial x_*} \right) \right] \Bigg\},
\end{aligned} \tag{A.3b}$$

$$\begin{aligned}
\rho_* \left(\frac{\partial h_*}{\partial t_*} + u_* \frac{\partial h_*}{\partial x_*} + v_* \frac{\partial h_*}{\partial y_*} \right) = {} & \frac{\partial p_*}{\partial t_*} + u_* \frac{\partial p_*}{\partial x_*} + v_* \frac{\partial p_*}{\partial y_*} \\
& + \frac{1}{Re} \Bigg\{ \frac{1}{Pr} \left[\frac{\partial}{\partial x_*} \left(\mu_* \frac{\partial h_*}{\partial x_*} \right) + \frac{\partial}{\partial y_*} \left(\mu_* \frac{\partial h_*}{\partial y_*} \right) \right] \\
& + \mu_* \left(\frac{4}{3} \frac{\partial u_*}{\partial x_*} - \frac{2}{3} \frac{\partial v_*}{\partial y_*} \right) \frac{\partial u_*}{\partial x_*} + \mu_* \left(\frac{4}{3} \frac{\partial v_*}{\partial y_*} - \frac{2}{3} \frac{\partial u_*}{\partial x_*} \right) \frac{\partial v_*}{\partial y_*} \\
& + \mu_* \left(\frac{\partial u_*}{\partial y_*} + \frac{\partial v_*}{\partial x_*} \right)^2 \Bigg\},
\end{aligned} \tag{A.3c}$$

$$\frac{\partial \rho_*}{\partial t_*} + \frac{\partial (\rho_* u_*)}{\partial x_*} + \frac{\partial (\rho_* v_*)}{\partial y_*} = 0, \tag{A.3d}$$

$$h_* = \frac{\gamma}{\gamma - 1} \frac{p_*}{\rho_*} + \frac{1}{(\gamma - 1) M_\infty^2 \rho_*}. \tag{A.3e}$$

Here M_∞ is the free-stream Mach number and Re is the Reynolds number, which are defined as

$$M_\infty = \frac{U_\infty}{a_\infty}, \qquad a_\infty = \sqrt{\gamma \frac{p_\infty}{\rho_\infty}}, \qquad Re = \frac{\rho_\infty U_\infty L}{\mu_\infty}. \tag{A.4a-c}$$

In the body-fitted coordinates the Navier-Stokes equations are written as

$$\hat{\rho}\left(\frac{\partial \hat{u}}{\partial \hat{t}} + \frac{\hat{u}}{1+\kappa\hat{y}}\frac{\partial \hat{u}}{\partial \hat{x}} + \hat{v}\frac{\partial \hat{u}}{\partial \hat{y}} + \frac{\kappa\hat{u}\hat{v}}{1+\kappa\hat{y}}\right) = -\frac{\partial \hat{p}}{\partial \hat{x}} + \frac{\partial}{\partial \hat{y}}\left(\hat{\mu}\frac{\partial \hat{u}}{\partial \hat{y}}\right) + \cdots, \tag{A.5a}$$

$$\hat{\rho}\left(\frac{\partial \hat{v}}{\partial \hat{t}} + \frac{\hat{u}}{1+\kappa\hat{y}}\frac{\partial \hat{v}}{\partial \hat{x}} + \hat{v}\frac{\partial \hat{v}}{\partial \hat{y}} - \frac{\kappa\hat{u}^2}{1+\kappa\hat{y}}\right) = -\frac{\partial \hat{p}}{\partial \hat{y}} + \frac{\partial}{\partial \hat{y}}\left(\hat{\mu}\frac{\partial \hat{v}}{\partial \hat{y}}\right) + \cdots, \tag{A.5b}$$

$$\begin{aligned}\hat{\rho}\left(\frac{\partial \hat{h}}{\partial \hat{t}} + \frac{\hat{u}}{1+\kappa\hat{y}}\frac{\partial \hat{h}}{\partial \hat{x}} + \hat{v}\frac{\partial \hat{h}}{\partial \hat{y}}\right) = \frac{\partial \hat{p}}{\partial \hat{t}} + \frac{\hat{u}}{1+\kappa\hat{y}}\frac{\partial \hat{p}}{\partial \hat{x}} + \hat{v}\frac{\partial \hat{p}}{\partial \hat{y}} + \\ + \frac{1}{Pr}\frac{\partial}{\partial \hat{y}}\left(\hat{\mu}\frac{\partial \hat{h}}{\partial \hat{y}}\right) + \hat{\mu}\left(\frac{\partial \hat{u}}{\partial \hat{y}}\right)^2 + \cdots,\end{aligned} \tag{A.5c}$$

$$\frac{\partial \hat{\rho}}{\partial \hat{t}} + \frac{1}{1+\kappa\hat{y}}\frac{\partial(\hat{\rho}\hat{u})}{\partial \hat{x}} + \frac{1}{1+\kappa\hat{y}}\frac{\partial}{\partial \hat{y}}\Big[\hat{\rho}\hat{v}(1+\kappa\hat{y})\Big] = 0, \tag{A.5d}$$

$$\hat{h} = \frac{\gamma}{\gamma-1}\frac{\hat{p}}{\hat{\rho}}. \tag{A.5e}$$

Here κ denotes the aerofoil contour curvature and for brevity we leave only main viscous terms in the momentum an energy equations. Using nondimensionalisation variables (A.2) these equations reduce to

$$\begin{aligned}\rho_*\left(\frac{\partial u_*}{\partial t_*} + \frac{u_*}{1+\kappa y_*}\frac{\partial u_*}{\partial x_*} + v_*\frac{\partial u_*}{\partial y_*} + \frac{\kappa u_* v_*}{1+\kappa y_*}\right) = -\frac{\partial p_*}{\partial x_*} + \\ + \frac{1}{Re}\frac{\partial}{\partial y_*}\left(\mu_*\frac{\partial u_*}{\partial y_*}\right) + \cdots,\end{aligned} \tag{A.6a}$$

$$\begin{aligned}\rho_*\left(\frac{\partial v_*}{\partial t_*} + \frac{u_*}{1+\kappa y_*}\frac{\partial v_*}{\partial x_*} + v_*\frac{\partial v_*}{\partial y_*} - \frac{\kappa {u_*}^2}{1+\kappa y_*}\right) = -\frac{\partial p_*}{\partial y_*} + \\ + \frac{1}{Re}\frac{\partial}{\partial y_*}\left(\mu_*\frac{\partial v_*}{\partial y_*}\right) + \cdots,\end{aligned} \tag{A.6b}$$

$$\begin{aligned}\rho_*\left(\frac{\partial h_*}{\partial t_*} + \frac{u_*}{1+\kappa y_*}\frac{\partial h_*}{\partial x_*} + v_*\frac{\partial h_*}{\partial y_*}\right) = \frac{\partial p_*}{\partial t_*} + \frac{u_*}{1+\kappa y_*}\frac{\partial p_*}{\partial x_*} + v_*\frac{\partial p_*}{\partial y_*} + \\ + \frac{1}{Re}\left[\frac{1}{Pr}\frac{\partial}{\partial y_*}\left(\mu_*\frac{\partial h_*}{\partial y_*}\right) + \mu_*\left(\frac{\partial u_*}{\partial y_*}\right)^2\right] + \cdots,\end{aligned} \tag{A.6c}$$

$$\frac{\partial \rho_*}{\partial t_*} + \frac{1}{1+\kappa y_*}\frac{\partial(\rho_* u_*)}{\partial x_*} + \frac{1}{1+\kappa y_*}\frac{\partial}{\partial y_*}\left[\rho_* v_*(1+\kappa y_*)\right] = 0, \tag{A.6d}$$

$$h_* = \frac{\gamma}{\gamma-1}\frac{p_*}{\rho_*} + \frac{1}{(\gamma-1)M_\infty^2\rho_*}. \tag{A.6e}$$

A.2 Steady Compressible Boundary Layer Flow

A flat plate placed in a uniform flow of gas disturbs the flow only in the immediate vicinity of the surface. Thus the steady flow past the plate is uniform with an exception of the wall boundary-layer. This layer thickness tends to zero as the Reynolds number increases in accordance with $y_* = O(Re^{-1/2})$. The solution of the steady Navier-Stokes equations in the boundary-layer on the surface of the plate is represented in the form of the following asymptotic expansions

$$u_* = U_0\,(x_*, Y) + \dots, \qquad \rho_* = R_0\,(x_*, Y) + \dots, \tag{A.7a,b}$$
$$v_* = Re^{-1/2} V_0\,(x_*, Y) + \dots, \qquad h_* = H_0\,(x_*, Y) + \dots, \tag{A.7c,d}$$
$$p_* = Re^{-1/2} \breve{p}_a\,(x_*, Y) + \dots, \qquad \mu_* = \mu_0\,(x_*, Y) + \dots. \tag{A.7e,f}$$

Substitution of (A.7) into the Navier-Stokes equations leads to the classical boundary-layer equations

$$R_0 U_0 \frac{\partial U_0}{\partial x_*} + R_0 V_0 \frac{\partial U_0}{\partial Y} = \frac{\partial}{\partial Y}\left(\mu_0 \frac{\partial U_0}{\partial Y}\right), \tag{A.8a}$$
$$R_0 U_0 \frac{\partial H_0}{\partial x_*} + R_0 V_0 \frac{\partial H_0}{\partial Y} = \frac{1}{Pr}\frac{\partial}{\partial Y}\left(\mu_0 \frac{\partial H_0}{\partial Y}\right) + \mu_0 \left(\frac{\partial U_0}{\partial Y}\right)^2, \tag{A.8b}$$
$$U_0 \frac{\partial R_0}{\partial x_*} + R_0 \frac{\partial V_0}{\partial Y} + R_0 \frac{\partial U_0}{\partial x_*} + V_0 \frac{\partial R_0}{\partial Y} = 0, \tag{A.8c}$$
$$H_0 = \frac{1}{(\gamma - 1) R_0}. \tag{A.8d}$$

Solving these equations we need to pose the following boundary conditions on the leading edge of the plate

$$U_0 = 0, \qquad H_0 = \frac{1}{(\gamma - 1)} \qquad \text{at} \qquad x = 0, \qquad Y \in [0, \infty). \tag{A.9a,b}$$

On the outer edge of the boundary layer conditions are

$$U_0 = 1, \qquad H_0 = \frac{1}{(\gamma - 1)} \qquad \text{at} \qquad Y = \infty, \qquad x \in [0, \infty). \tag{A.10a,b}$$

In addition, the solution also has to satisfy the no-slip condition on the surface of the plate

$$U_0 = V_0 = 0 \qquad \text{at} \qquad Y = 0, \qquad x \in [0, \infty), \tag{A.11a,b}$$

which has to be supplemented with an appropriate thermal condition. Here it will be assumed that the plate is thermally isolated, therefore

$$\frac{\partial H_0}{\partial Y} = 0 \qquad \text{at} \qquad Y = 0, \qquad x \in [0, \infty)\,. \tag{A.11c}$$

The boundary-value problem (A.7)-(A.11) admits a self-similar solution in the form

$$U_0(x_*, Y) = U(\eta), \qquad V_0(x_*, Y) = \frac{1}{\sqrt{x_*}} V(\eta), \qquad R_0(x_*, Y) = \rho(\eta), \tag{A.12a-c}$$

$$H_0(x_*, Y) = H(\eta), \qquad \mu_0(x_*, Y) = \mu(\eta), \tag{A.12d,e}$$

where

$$\eta = \frac{Y}{\sqrt{x_*}} \tag{A.13}$$

Substitution of (A.12) into the equations (A.7), reduces it to

$$-\frac{1}{2}\eta\rho U U' + \rho V U' = \left(\mu U'\right)', \tag{A.14a}$$

$$-\frac{1}{2}\eta\rho U H' + \rho V H' = \frac{1}{Pr}\left(\mu H'\right)' + \mu\left(U'\right)^2, \tag{A.14b}$$

$$-\frac{1}{2}\eta\left(\rho U'\right) + \left(\rho V'\right) = 0, \tag{A.14c}$$

$$H = \frac{1}{(\gamma - 1)\rho}. \tag{A.14d}$$

Here apostrophe denotes derivation with respect to η. These equations are supplemented with linear equation relating the viscosity coefficient and the enthalpy

$$\hat{\mu} = \chi\hat{h}. \tag{A.15}$$

In dimensionless form the equation above is written as

$$\mu = (\gamma - 1)\, M_\infty^2 H, \tag{A.16}$$

which in transonic flow reduces to

$$\mu = (\gamma - 1)\, H. \tag{A.17}$$

Combined the state equation (A.14d) and (A.17) we deduce that

$$\rho\mu = 1 \tag{A.18}$$

Substituting (A.12) into the boundary conditions (A.9)-(A.11), we find

$$U = V = H' = 0 \qquad \text{at} \qquad \eta = 0, \tag{A.19a-c}$$

$$U = 1, \qquad H = \frac{1}{\gamma - 1} \qquad \text{at} \qquad \eta = \infty. \tag{A.19d,e}$$

Equations (A.14) may be simplified introducing a new function, $f(\eta)$, such that

$$f'(\eta) = \rho U \qquad \text{and} \qquad f(0) = 0. \tag{A.20a,b}$$

Rearranging and substituting the new function into the continuity equation (A.14c) we obtain

$$-\frac{1}{2}(\eta\rho U)' + (\rho V)' = -\frac{1}{2}f'. \tag{A.21}$$

Integrating the equation above and using the fact that $V(0) = f(0) = 0$, we deduce that

$$-\frac{1}{2}\eta\rho U + \rho V = -\frac{1}{2}f. \tag{A.22}$$

Substituting the expression (A.22) into the remaining equations (A.14a) and (A.14b) we write

$$-\frac{1}{2}fU' = (\mu U')', \tag{A.23a}$$

$$-\frac{1}{2}fH' = \frac{1}{Pr}(\mu H')' + \mu(U')^2. \tag{A.23b}$$

Further simplification is achieved by introducing the Dorodnitsyn-Howarth transformation (Stewartson, 1964)

$$\xi = \int_0^\eta \rho(s)\, ds, \tag{A.24}$$

which together with (A.18) turns equations (A.20) and (A.23) into

$$\frac{d^3 f}{d\xi^3} + \frac{1}{2}f\frac{d^2 f}{d\xi^2} = 0, \tag{A.25a}$$

$$\frac{1}{2}f\frac{dH}{d\xi} + \frac{1}{Pr}\frac{d^2 H}{d\xi^2} + \left(\frac{d^2 f}{d\xi^2}\right)^2 = 0, \tag{A.25b}$$

$$\frac{df}{d\xi} = U. \tag{A.25c}$$

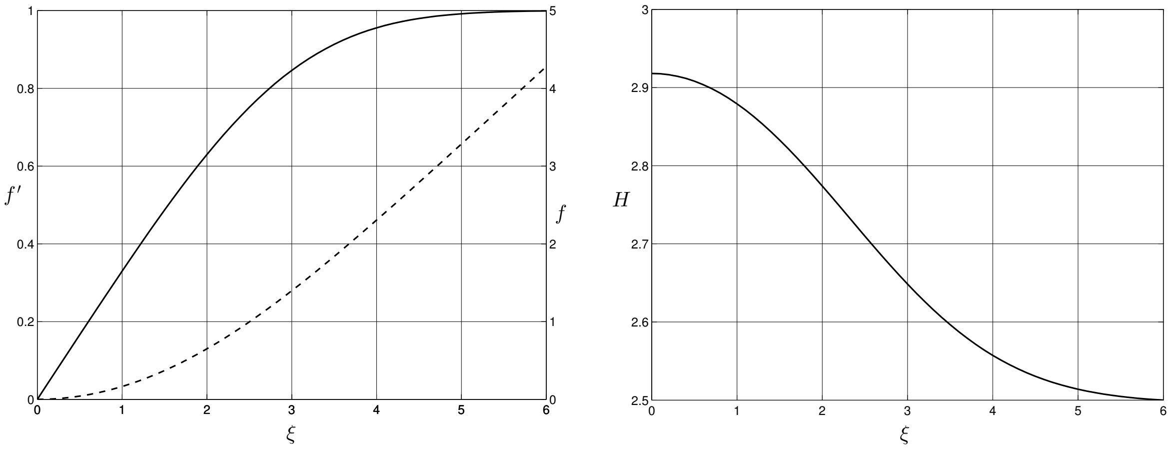

(a) Solid line corresponds to the profile of the streamwise velocity profile $f'(\xi)$, and the dashed line shows the function $f(\xi)$.

(b) Distribution of the enthalpy across the boundary layer

Figure A.1: Solution for the compressible Blasius boundary layer.

It can be seen that the state equation (A.25a) coincides with the classical Blasius equation for incompressible boundary layer. The boundary conditions for this equation may be deduced from (A.20) and the fact that $\rho = 1$ at the the outer edge of the boundary layer, thus

$$f(0) = \frac{df}{d\xi}(0) = 0 \qquad \text{and} \qquad \frac{df}{d\xi}(\infty) = 1, \tag{A.26a-c}$$

The boundary conditions for (A.25b) may be written as

$$\frac{dH}{d\xi}(0) = 0 \qquad \text{and} \qquad H(\infty) = \frac{1}{\gamma - 1}. \tag{A.27a-c}$$

The equation (A.25a) can be solve using the classical Runge-Kutta method after which we can obtain solution to the equation (A.25b). The results of calculation are displayed in Figure A.1. The particular interest is the behaviour of the solution near the plates surface, where point $\xi = 0$ is a regular point for both equations. Therefore, functions $f(\xi)$ and $H(\xi)$ can be represented by Taylor expansion

$$\begin{cases} f(\xi) = \dfrac{\lambda}{2}\xi^2 + O(\xi^5) \\ H(\xi) = h_w + O(\xi^2) \end{cases} \qquad \text{as} \qquad \xi \to 0. \tag{A.28a,b}$$

From the numerical solution the values of constants λ and h_w are found to be

$$\lambda = 0.3321, \qquad h_w = 2.9180. \tag{A.29a,b}$$

Together with (A.14d) and (A.17), this leads to

$$\begin{cases} \rho(\xi) = \rho_w + O(\xi^2) \\ \mu(\xi) = \mu_w + O(\xi^2) \end{cases} \quad \text{as} \quad \xi \to 0, \tag{A.30a,b}$$

where

$$\rho_w = \frac{1}{(\gamma-1)h_w}, \qquad \mu_w = (\gamma-1)h_w. \tag{A.31a,b}$$

Substituting (A.30) back into (A.24), and using (A.28) in (A.25c) we find that the streamwise velocity component may be represented near the wall as

$$U = \lambda\rho_w\eta + O(\eta^4). \tag{A.32}$$

Returning back to equations in (A.12) we conclude that near the surface of the plate we have

$$\begin{cases} U_0(x_*, Y) = \tau\left(x_*\right)Y + O\left(Y^4\right) \\ R_0(x_*, Y) = \rho_w + O\left(Y^2\right) \\ H_0(x_*, Y) = h_w + O\left(Y^2\right) \\ \mu_0(x_*, Y) = \mu_w + O\left(Y^2\right) \end{cases} \quad \text{as} \quad Y \to 0, \tag{A.33a-d}$$

where

$$\tau\left(x_*\right) = \frac{\lambda\rho_w}{\sqrt{x_*}} \tag{A.34}$$